Integrated Cavity Output Spectroscopy And Its Non-Invasive Applications In Biomedical Diagnosis

Thesis submitted for the degree of

Doctor of Philosophy (Science)

in

Chemistry (Experimental)

By

Suman Som

Department of Chemistry

University of Calcutta

2017

Dedicated to my

Parents, Supervisor and Teachers

Acknowledgements

Completion of this doctoral dissertation would never have been completed without the immense support, help and guidance of several important people. Now the time has come to express my gratitude in words to all of those people who had played a catalytic role to complete my 5 years long journey.

First and foremost, I would like to express my sincere gratitude to my supervisor Dr. Manik Pradhan for his valuable guidance, scholarly inputs and continuous encouragement which I have received throughout my research work. A person with an amicable and positive disposition, Sir has always made himself available for innumerous helpful scientific discussion to clarify my doubts. I consider it as a great opportunity to do my doctoral programme under his guidance and to learn from his instrumental expertise, insight into various experimental problems, wisdom and inspiration. He has also provided me a wonderful scientific environment to work and gain scientific experience. Thank you Sir, for all your kind help and support for me.

I would also like to express my gratitude to our collaborators Dr. Sujit Chaudhuri, AMRI Hospitals, Salt Lake, Kolkata and Dr. Sunil B. Daschakraborty, Ruby General Hospital for their support and help during the biomedical studies.

I would like to thank all of my lab mates Abhijit, Gourab, Chiranjit, Mithun, Santanu, Sanchi, Akash, Iqbal and Sasthi for providing the friendly environment in our lab. I would like to specially mention my first three lab mates Abhijit, Gourab and Chiranjit for immense unconditional help and support from the early days. I would like to express my heartily gratitude to Gourab for sharing a glorious moment over long period of time and unconditional help.

I am extremely grateful to all of my teachers throughout my life. First I would like express my gratitude to my first chemistry teacher Mr. Sukriti Samanta who had made me enthusiastic toward chemistry by his unique and sensible style. Beside that I would also like to convey my sincere gratitude to Dr. Ramesh L. Gardas (IIT Madras) and Dr. Deepak Chopra (IISER Bhopal) for their motivation in doing research during my post graduate studies.

I would like to thank my childhood friends Janmenjay, Shimul and Toton (four musketeers including me!) for sharing evergreen moments in my village life. My special thank goes out for my college friends mainly, Souvik, Tamal, Shilaj, Tirthaprasad, Siladitya, Amit, Sanjoy, Sisir for giving me some long-lasting moments and friendship. I would also like to thank Susobhan for giving me the taste of friendship in SN Bose days.

Last but not least, I would like to pay high regards to my beloved parents for their devotions, sincere encouragement, support and inspiration throughout my research work that have made me more courageous, dedicated and patient. I owe everything to them and they are the reasons for what I am today. I feel myself very fortunate to have them as parents, Swati as sister and Vidyasagar as brother-in-law. It is their unconditional love, well wishes and confidence on me that have made this thesis a success.

Dated: (Suman Som)

Department of Chemical, Biological and Macro-Molecular Sciences,

S. N. Bose Centre for Basic Sciences

Salt lake, Kolkata-700106

India

Contents

Abstract

In this thesis, we have investigated the applicability of high-resolution laser-based integrated cavity output spectroscopy (ICOS) technique in biomedical diagnostics. ICOS is one of the most advanced cavity-enhanced absorption techniques and consists of high-finesse optical cavity coupled with two ultra-high reflectivity mirrors which gives rise to the effective optical pathlength of several kilometres. One of the major advantages of ICOS is the ultra-sensitive detection of trace molecular species that can be achieved in parts-per-billion (ppb) to parts-per-trillion (ppt) levels. Here, we have exploited the high-sensitivity of ICOS technique for the measurements of trace volatile organic compounds (VOCs) in human breath for non-invasive diagnosis of the gastric pathogen *Helicobacter pylori* (*H. pylori*) infection, the most common causative agent for gastrointestinal disorders. First, we have investigated the clinical feasibility of the measurements of the major metabolite of human breath, carbon dioxide (CO_2) and its two major isotopolouges, carbon-13 and oxygen-18 (^{13}C and ^{18}O) for non-invasive diagnosis of *H. pylori* infection by incorporating the ^{13}C-enriched urea breath test. We determined several optimal diagnostic cut-off values of ^{13}C and ^{18}O isotopes for the detection of *H. pylori* infection.

Next, we have investigated the potential role glucose metabolism in the pathogenesis of *H. pylori* infection in human stomach by means of time-dependent excretion kinetics of $^{13}CO_2$ by ICOS methodology. Several lines of evidence suggest that ^{18}O isotope of body water (H_2O^{18}) and ^{16}O isotope of $^{12}C^{16}O_2$ are rapidly interchanged due to the enzymatic activity of carbonic anhydrase (CA) during CO_2 transportation. We have demonstrated that in response to CA activity the ^{18}O-isotopic fractionations of breath CO_2 are potentially linked with the pathogenesis of *H. pylori* infection. The time-dependent excretion kinetics of $^{18}O/^{16}O$ isotope ratios in exhaled breath CO_2 in response of ^{13}C-tagged glucose metabolism were performed in order to establish the previous hypothesis.

Next, we have explored the potential role of *H. pylori* infection in the development of type 2 diabetes (T2D), the most common metabolic disorder in humans. By glucose breath test (GBT) with high-precision measurements of $^{13}CO_2/^{12}CO_2$ isotope ratios by ICOS technique, we have established a missing link between *H. pylori* infection and

T2D, which has never been explored before. Moreover, by utilizing the high-resolution cavity ring-down spectroscopy (CRDS) technique, we have investigated that nitric oxide (NO) in human breath is potentially linked in the pathogenesis of peptic ulcer disease and non-ulcer dyspepsia. Our findings suggest that NO could be used as a potential biomarker for the detection of *H. pylori*-induced peptic ulcer disease and thus may open a new non-invasive strategy for precise evolution of the actual disease state in a more better and robust way without any endoscopic biopsy tests.

Finally, we developed a model-based breath analysis method utilizing the different biological pathways of glucose metabolism for monitoring of blood glucose profile. The model-based method provides a person's blood glucose profile with time. The person's physical parameters and $^{13}CO_2/^{12}CO_2$ isotope ratios in exhaled breath are used for the quantitative estimation of blood glucose profile and subsequently identifies the actual metabolic state of a person and thus it offers a novel strategy into the accurate and fast diagnosis of diabetes mellitus.

List of Publications

List of publications related to Thesis work:

[1] **Suman Som**, Abhijit Maity, Gourab Dutta Banik, Chiranjit Ghosh, Sujit Chaudhuri, Sunil Baran Daschakraborty, Shibendu Ghosh and Manik Pradhan, "*Excretion kinetics of ^{13}C-urea breath test: influences of endogenous CO_2 production and dose recovery on the diagnostic accuracy of Helicobacter pylori infection"*. ***Analytical and Bioanalytical Chemistry***, 406(22), 5405-5412, (**2014).**

[2] **Suman Som**, Anulekha De, Gourab Dutta Banik, Abhijit Maity, Chiranjit Ghosh, Mithun Pal, Sunil B Daschakraborty, Sujit Chaudhuri, Subhra Jana and Manik Pradhan, "*Mechanisms linking metabolism of Helicobacter pylori to ^{18}O and ^{13}C-isotopes of human breath CO_2"*. ***Scientific Reports (Nature Publishing Group)***, 5, 10936, (**2015).**

[3] **Suman Som**, Gourab Dutta Banik, Sujit Chaudhuri and Manik Pradhan, "*^{13}C and ^{18}O isotopes of breath CO_2 as markers for detection of Helicobacter pylori infection in type 2 diabetes"* (Under Review, **2017**).

[4] **Suman Som**, Gourab Dutta Banik, Abhijit Maity, Sujit Chaudhuri and Manik Pradhan, "*Exhaled nitric oxide as a potential marker for detecting non-ulcer dyspepsia and peptic ulcer disease"* (Under Review, **2017**).

[5] **Suman Som**, Chiranjit Ghosh and Manik Pradhan, *"A model-based breath analysis method for the estimation of blood glucose profile"* (to be submitted, **2017**).

List of publications as co-author apart from Thesis work:

[1] Gourab Dutta Banik, **Suman Som**, Abhijit Maity, Mithun Pal, Sanchi Maithani, Santanu Mandal and Manik Pradhan, "*An EC-QCL based N_2O sensor at 5.2 μm using cavity ring-down spectroscopy for environmental applications"*. ***Analytical Methods***, 9, 2315-2320, (**2017)**.

[2] Abhijit Maity, Mithun Pal, **Suman Som**, Sanchi Maithani, Sujit Chaudhuri and Manik Pradhan, "*Natural ^{18}O and ^{13}C-urea in gastric juice: a new route for non-invasive detection of ulcers"*. ***Analytical and Bioanalytical Chemistry***, 409, 193-200, (**2017)**.

[3] Chiranjit Ghosh, Gourab Dutta Banik, Abhijit Maity, **Suman Som**, Arpita Chakraborty, Chitra Selvan, Shibendu Ghosh, Subhankar Chowdhury and Manik Pradhan, "*Oxygen-18 isotope of breath CO_2 linking to erythrocytes carbonic anhydrase activity: a biomarker for pre-diabetes and type 2 diabetes"*. ***Scientific Reports (Nature Publishing Group)***, 5, 8137, (**2015)**.

[4] Abhijit Maity, **Suman Som**, Chiranjit Ghosh, Gourab Dutta Banik, Sunil B Daschakraborty, Shibendu Ghosh, Sujit Chaudhuri and Manik Pradhan, "*Oxygen-18 stable isotope of exhaled breath CO_2 as a non-invasive marker of Helicobacter pylori infection"*. ***Journal of Analytical Atomic Spectrometry***, 29 (12), 2251-2255, (**2014)**.

[5] Abhijit Maity, Gourab Dutta Banik ,Chiranjit Ghosh, **Suman Som**, Sujit Chaudhuri, Sunil B Daschakraborty, Shibendu Ghosh, Barnali Ghosh, Arup K Raychaudhuri and Manik Pradhan, "*Residual gas analyzer mass spectrometry for human breath analysis: a new tool for the non-invasive diagnosis of Helicobacter pylori infection"*. ***Journal of Breath Research***, 8(1), 016005, (**2014)**.

Chapter 1

1.1 Introduction

The most ubiquitous and precise method available for the study of the interaction of light and matter is spectroscopy. Among various spectroscopic techniques, laser-based direct absorption spectroscopy has widely been used to study the precise wavelength dependent molecular property in gas phase. Recent advancements of the optical laser-based cavity-enhanced spectroscopy (CES) techniques with high-sensitivity and molecular selectivity make it possible to measure the ultra-low concentration of various trace molecular species in gaseous phase [1-4]. Integrated cavity output spectroscopy (ICOS) a variant of CES is the major advanced technique which exploits the high-finesse optical cavities comprised of high-reflective mirrors to enhance the optical pathlength. The main advantage of ICOS is that it offers enormous sensitivity based on the properties of the passive optical resonator to enhance the optical pathlength for which it has widespread applicability in life sciences, in particular in the field of biomedical research and clinical diagnostics [5-11]. Due to high effective optical pathlength (few kilometre) the detection limit goes down to parts-per-billion (ppb) to parts-per-trillion (ppt) levels. The optical cavity-based ICOS technique offers a real-time measurement of the trace volatile molecular species from both environment and human breath with high specificity. Now-a-days several sophisticated analytical tools are available for the measurement of the trace molecular species in human breath such as mass spectrometry based gas chromatography mass-spectrometry (GC-MS), isotope ratio mass-spectrometry (IRMS), proton transfer reaction mass-spectrometry (PTR-MS) and selected ion flow tube mass-spectrometry (SIFT-MS) [12-15]. However, the extensive applications of these methodologies are limited for laboratory research. One of the main drawbacks of these methodologies is that real-time on-line measurement is not possible and there are several intrinsic operational complicacies of these kinds of systems. But the advances in diode and quantum cascade laser (QCL) technology and ICOS-based analytical methods may open up a new platform for quantitative estimation of trace gases in ultra-low concentration in human breath which subsequently give raise to a

number of interesting applications in biomedical research and non-invasive diagnostics.

Breath analysis has recently gained a considerable attention due to its potential applicability of monitoring biochemical processes occurring inside our body. Over the past decades breath analysis has become an important non-invasive diagnostic tool for selective and early-stage diagnosis of various diseases. The quantitative analysis of exhaled breath can provide important information about the physiological and health status of a living subject. The physiological basis of breath analysis is the exchange of gas between air and blood. The main advantage of breath analysis compared to other diagnostic methodologies (including blood, urine and endoscopy based biopsy tests) that it is completely non-invasive method and it implies virtually repeatability with respect to frequency, access and cost. Breath sample collections are somewhat easier than the collection of biogenic fluid such as blood, urine and biopsy samples [16-19].

Human breath consists of more than 3000 different molecular species. The bulk matrix of breath is a mixture of few atmospheric molecules, e.g., nitrogen (N_2), oxygen (O_2), carbon dioxide (CO_2) and water vapour (H_2O) in relatively high concentrations, with several volatile organic compounds (VOCs) concentrations ranging from parts-per-million (ppm) to parts-per-trillion (ppt). The specific component of complex matrix of exhaled breath is termed as molecular "breath-print". In terms of origin, these volatile substances may be generated through endogenous or exogenous pathways and potentially linked with some specific diseases or metabolic disorders in human and can be considered as possible biomarkers [20-22]. This detection knowledge suggests that breath analysis is a useful tool for real-time disease detection or metabolic status monitoring. Therefore, detection of trace VOCs in exhaled breath can lead us to early-stage diagnosis of several diseases such as diabetes mellitus, *Helicobacter pylori* infection, asthma, chronic obstructive pulmonary disease (COPD), inflammatory bowel disease (IBD) and small intestinal bacterial overgrowth (SIBO).

However, many volatile metabolites carried by the bloodstream pass the alveolar-capillary interface and can be found in exhaled breath. The major metabolite in breath is carbon dioxide (CO_2), which is exhaled in volume fractions of about 4%. [23, 24] Though CO_2 itself is not a marker of disease but it can play a significant role in breath

testing when ^{13}C-labelled substrates are applied. A prominent example of isotopic breath test is the non-invasive diagnosis of *Helicobacter pylori* infection in the gastrointestinal tract by means of $^{13}CO_2$ breath test. The basic principle of ^{13}C-breath test is that after administration of a ^{13}C-labelled substrate, the carbon is converted to $^{13}CO_2$ in course of enzymatic reactions like oxidation, hydrolysis, decarboxylation and comes out through exhaled breath [25, 26]. If the elimination of $^{13}CO_2$ in breath is the rate determining step of the metabolic reaction then the rate of $^{13}CO_2$ elimination reflects the actual metabolic situation. Therefore by applying the ^{13}C-tracer substrate we can monitor the metabolic state and defects of human body. However for ^{13}C-breath test, an artificially enriched substrate is normally used because there are naturally occurring differences in the δ^{13}C values in breath of the different human populations because of the physiological differences in the C3 and C4 plants [27-29]. Currently, there are several types of ^{13}C-breath test available such as ^{13}C-mixed triglyceride (MTG) breath test for fat digestion and cystic fibrosis (CF), ^{13}C-methacetin breath test (MBT) for liver function test, ^{13}C-xylose breath test for small intestinal bacterial overgrowth (SIBO), sodium bicarbonate ^{13}C-breath test (SBT) for atrophic gastritis, uracil-2-^{13}C-breath test (UBT) for pyrimidine metabolic disorder, ^{13}C-glucose breath test (^{13}C-GBT) for type 2 diabetes, ^{13}C-urea breath test (^{13}C-UBT) for *Helicobacter pylori* infection [30-36]. In this thesis, we have utilized a high-resolution laser-based integrated cavity output spectroscopy (ICOS) technique for trace molecular species along with their isotopes in human breath for non-invasive diagnosis of *Helicobacter pylori* infection in human stomach.

Helicobacter pylori (*H. pylori*) is a ubiquitous gram-negative micro-organism found on the luminal surface of the gastric epithelium. It was first isolated by Warren and Marshall in 1983 [37]. Now-a-days half of the world population is infected by the gastric pathogen *H. pylori* and the prevalence of this infection in developing country is ~70-80% [38, 39]. *H. pylori* is a human specific gastric pathogen and often it is acquired in childhood from family members but the exact path of person to person transmission is still not fully understood. The prevalence of the infection increases with older age and with lower socio-economic status during childhood and thus varies markedly around the world [40-43]. During colonization *H. pylori* induces local chronic inflammation in the gastric mucosa. Although the full spectrum of pathogenesis is currently unknown, but *H. pylori* is linked with several upper-

gastrointestinal diseases such as epigastric pain, functional dyspepsia, bloating, nausea, and vomiting, along with delayed gastric emptying. *H. pylori* plays a causative role for the development of three important upper gastrointestinal diseases i.e. duodenal or gastric ulcer, gastric cancer and gastric mucosa-associated lymphoid-tissue (MALT) lymphoma. Epidemiological studies showed that *H. pylori* is responsible for about 75% of all gastric cancers and 63% of all stomach cancers worldwide [44-50]. The great majority of patients with *H. pylori* infection will not have significant clinical complications therefore early diagnosis of the infection is very much essential.

Several diagnostic methods are currently available to detect the *H. pylori* infection and all are diverse in nature depending on the choice of the methods or protocols. Each method has its own advantages, disadvantages and limitations. Depending on the use of endoscopy, methods are categorized as invasive procedure which included biopsy-based histological evaluation, culture, polymerase chain reaction (PCR) and rapid urease test (RUT). Alternatively, urea breath test (UBT), serology and stool antigen test (SAT) are performed which are categorized as non-invasive procedure. But the main limitation of invasive procedure is that due to patchy distribution of *H. pylori* in the gastric mucosa multiple tissue samples are collected from the different areas of the stomach which further leads to less sensitivity and specificity to diagnose the presence of *H. pylori*. Again in case of RUT the most conventional method to detect the *H. pylori* infection, sensitivity largely depends on the amount of bacteria in the biopsy samples; at least 10^5 cells are required for positive test and also the use of antibiotic suppress the urease activity which further leads to the false-negative results. Among the non-invasive test, urea breath test (UBT) is the one of the most accurate to determine the presence of *H. pylori* infection with more than 97% sensitivity and specificity [51-54]. The underlying principle of UBT relies on the hydrolyzing capability of urease enzyme secreted from *H. pylori*. To survive in the hostile condition of stomach, *H. pylori* secretes urease enzyme which hydrolyzes urea into ammonia (NH_3) and carbon dioxide (CO_2). *H. pylori* is a neutralophilic organism which survive in an environmental pH 6.0 to 8.0 with optimal growth close to pH 7.0. Normally the pH of the stomach is ~2.0, therefore *H. pylori* cannot survive in this high acidic condition. To overcome this adverse effect, *H. pylori* hydrolyzes the urea to produce the alkaline ammonia to maintain the pH of its neighbouring environment.

Although these non-invasive methods have few limitations, but due to use of proton pump inhibitor therapy or antibiotic therapy, the sensitivity of these methods is severely decreased. Therefore the aim of our study is to propose an alternative non-invasive methodology by exploiting the laser-based technique with high diagnostic sensitivity and specificity.

In the recent times the ^{13}C-urea breath test (^{13}C-UBT) has become a non-invasive gold-standard methodology to detect the *H. pylori* infection and particularly to understand the effect of eradication therapy like antibiotic therapy. The ^{13}C-UBT is based on the principle that when a dose of ^{13}C-tagged urea [$^{13}CO(NH_2)_2$] is orally administered, *H. pylori* hydrolyze it in ammonia (NH_3) and isotopically labelled $^{13}CO_2$ [55-57]. $^{13}CO_2$ diffuses into the blood and then it is excreted in exhaled breath. Normally, the human body does not oxidize urea and if ^{13}C is recovered in the breath following ingestion of ^{13}C-urea it proved that the patient is infected. Now, the postulate is that *H. pylori* infected subjects will exhale more $^{13}CO_2$ compared to healthy controls (*H. pylori* negative subjects) upon the ingestion of ^{13}C-enriched urea. As the diagnostic sensitivity of ^{13}C-UBT is not upto the marked so there is a pressing need to develop a better diagnostic methodology with high sensitivity and specificity for early detection of *H. pylori* infection. To overcome this problem, we have proposed the percentage dose of ^{13}C-recovered per hour (^{13}C-PDR) in ^{13}C-UBT in order to account the amount of ^{13}C-enriched substrate metabolised at any given time [58, 59]. Therefore the aim of this study was to check the clinical feasibility of ^{13}C-PDR methodology in accurate detection of *H. pylori* infection by monitoring the $^{13}CO_2/^{12}CO_2$ stable isotope ratios in exhaled breath using the high-precision ICOS technique.

Glucose is the most common simple form of carbohydrate. The gastric pathogen *H. pylori* utilises it as a primary source of energy substrate, although the overall metabolism of *H. pylori* yet remains inadequately understood. *H. pylori* can metabolize glucose by both oxidative and fermentative pathways through a glucokinase activity and enzymes of the pentose phosphate and glycolysis pathway [60-62]. CO_2 and its isotopes are major metabolite of glucose metabolism which are then transported to the lungs through the bloodstream, and finally excreted in human breath. *H. pylori* uptake the glucose from its environment using a specific D-glucose transporter and this transporter is sodium-linked [63]. However, the precise role of

glucose metabolism, especially in the pathogenesis of the *H. pylori* infection is not currently known. Therefore another aim of our study is to explore the potential link between isotopes of breath CO_2 and *H. pylori* infection in response to ^{13}C-enriched glucose metabolism and to check the feasibility of the method for diagnostic purposes.

Moreover, several lines of evidence suggest that *H. pylori* has two distinct form of carbonic anhydrase (CA) (α-CA and β-CA), which plays an important role in acid acclimation during the gastric colonization. It also catalyzes the reversible interconversion between CO_2 and HCO_3^- ($CO_2 + H_2O \leftrightarrow H^+ + HCO_3^-$) [64-67]. On the other hand, recent evidences implicate that due to enzymatic activity of CA, there have been a rapid interchange between ^{18}O isotope of body water (H_2O^{18}) and ^{16}O-isotope of $^{12}C^{16}O_2$ during CO_2 transportation ($^{12}C^{16}O_2 + H_2O^{18} \leftrightarrow H_2{}^{12}C^{18}O^{16}O_2 \leftrightarrow {}^{12}C^{18}O^{16}O + H_2O^{16}$) [68, 69]. Therefore these activities suggest that exchange of oxygen-18 isotope of breath CO_2 may be linked with the pathogenesis of *H. pylori* infection. To address this issue, we have investigated the time-dependent excretion kinetics of $^{18}O/^{16}O$ isotope ratios in exhaled breath CO_2 in response to ^{13}C-tagged glucose metabolism. In extent of this work, we have explored the possible role of ^{18}O isotope of breath CO_2 in response on normal glucose (unlabelled) in pathogenesis of *H. pylori* infection.

Furthermore, there are several lines of evidence which revealed that the effects of *H. pylori* infection not are only confined to gastrointestinal tract but are also associated with other extragastric diseases such as idiopathic thrombocytophenic purpurae (ITP), cardiovascular diseases, anemia and type 2 diabetes (T2D) [70-72]. Currently, T2D is the most common metabolic disorder worldwide which is characterized by high levels of blood glucose mediated from insulin resistance and pancreatic β-cell dysfunction. A growing body of evidence suggested that there is a potential link between *H. pylori* infection and T2D but it still remains controversial. Some epidemiological studies implicated that individual with T2D have higher risk of *H. pylori* infection than non-diabetic individuals. In contrast, other studies have also found that there is no such association between *H. pylori* infection and T2D, even sometimes reverse relation between them also observed. Emerging data indicates that the infection is potentially linked with T2D in many aspects but the underlying mechanisms is very complex, involving chronic inflammation, insulin resistance, glucotoxicity, lipotoxicity,

pancreatic β-cell dysfunction, oxidative stress, and gastric hormones. Pathogenesis of T2D is complex and multifactorial [73-75]. Accumulating evidences indicate that *H. pylori* induced gastrointestinal inflammation alter the metabolism of glucose, which are also normal in T2D. Thus this finding suggests that *H. pylori* may play a pathological factor in development of T2D. On the other hand, carbonic anhydrase (CA) plays an important role in cellular metabolism and the alteration of glucose metabolism is associated with changes in CA activity in T2D [76]. *H. pylori* also linked with CA activity through pH regulation. All these past studies suggest that exchange of oxygen-18 isotope in breath CO_2 is pathologically linked with both *H. pylori* infection and T2D and thus might be a marker for non-invasive assessment of *H. pylori* infection in complication with T2D. Therefore we elucidated the potential role of *H. pylori* infection in pathogenesis of T2D by simultaneous monitoring of $^{13}C/^{12}C$ and $^{18}O/^{16}O$ isotope ratios of breath CO_2 in response to glucose metabolism using the laser-based high-precision integrated cavity output spectroscopy (ICOS) technique.

As mentioned previously, that the some specific molecules in exhaled may be used as "breath-prints" to selectively diagnose the several complex and long-lasting diseases. It is noteworthy to mention that nitric oxide (NO) has gained immense interest in both basic and applied research in medical diagnosis. The typical concentration range of NO in exhaled breath is 20 to 50 ppb. NO is generated by the oxidative conversion of L-arginine to L-citrulline via three isoforms of nitric oxide synthase (NOS). However, among all the isoforms of NOS, inducible nitric oxide synthase (iNOS) produces the largest amount of NO in gastrointestinal tract compared to endothelial NOS (eNOS) and neuronal NOS (nNOS) [77-79]. NO is normally considered as a biomarker for the respiratory disease such as asthma, chronic obstructive pulmonary disease (COPD). NO is also a biologically active signalling molecule that plays an important role in inflammatory process in the gastric environment. It is also well known that persistent infection with *H. pylori* in the gastric mucosa induces the chronic local inflammation. A growing body of evidences suggest that the concentration of exhaled breath NO was altered in *H. pylori* assisted peptic ulcer disease (PUD) due to the enhanced iNOS activity. These activities suggest that iNOS plays a significant role in the pathogenesis of gastroduodenal disorders and consequently promotes the development of peptic ulcer. Again, it is found that urease enzyme can also able to stimulate the macrophage

iNOS expression which also further enhanced the NO production [80]. Therefore another aim of our present study was to elucidate the role of breath NO for precise evaluation of non-ulcerous state prior to the onset of ulceration in gastric niche utilizing a lab-based high-resolution cavity ring-down spectroscopic (CRDS) method.

Breath analysis is a non-invasive method for the clinical application and by analyzing the concentration of the biomarkers, we can able to detect the disease or monitor the disease progression. Breath components (VOCs) are normally generated by the metabolic procedure in human body and carried through blood stream. Now glucose is the central molecule of the metabolism and CO_2 is the major metabolite. So, there should be relationships between blood glucose and breath CO_2. Now the current techniques for blood glucose monitoring are normally invasive methods and not a real-time. On contrary breath analysis is a real-time procedure. Therefore, the aim of our study is to explore the role of $^{13}CO_2/^{12}CO_2$ isotope ratios in exhaled breath for non-invasive monitoring of the metabolic procedure and subsequently development of a theoretical model based on the glucose metabolism for real-time non-invasive monitoring of blood glucose profile.

1.2 References

[1] van Hekden J H *et al.*, Sensitive trace gas detection with cavity enhanced absorption spectroscopy using a continuous wave external-cavity quantum cascade laser. *Appl. Phys. Lett.* **103,** 131114 (2013).

[2] Moser H *et al.*, Implementation of a quantum cascade laser-based gas sensor prototype for sub-ppmv H_2S measurements in a petrochemical process gas stream. *Anal. Bioanal. Chem.* **409,** 729-739 (2017).

[3] Kosterev A *et al.*, Application of quantum cascade lasers to trace gas analysis. *Appl. Phys. B* **90,** 165-176 (2008).

[4] Menzel A *et al.*, Spectroscopic detection of biological NO with a quantum cascade laser. *Appl. Phys. B* **72,** 859-863 (2001).

[5] Parameswaran K R *et al.*, Off-axis integrated cavity output spectroscopy with a mid-infrared interband cascade laser for real-time breath ethane measurements. *Appl. Opt.* **48,** 73-79 (2009).

[6] Wang C and Sahay P, Breath analysis using laser spectroscopic techniques: breath biomarkers, spectral fingerprints, and detection limits. *Sensors* **9,** 8230-8262 (2009).

[7] Wojtas J, Mikolajczyk J and Bielecki Z, Aspects of the application of cavity enhanced spectroscopy to nitrogen oxides detection. *Sensors* **13,** 7570-7598 (2013).

[8] Thorpe M J *et al.*, Cavity-enhanced optical frequency comb spectroscopy: application to human breath analysis. *Opt. Exp.* **16,** 2387-2397 (2008).

[9] Baer D S *et al.*, Sensitive absorption measurements in the near-infrared region using off-axis integrated-cavity-output spectroscopy. *Appl. Phys. B* **75,** 261-265 (2002).

[10] Cristescu S M *et al.*, Laser-based systems for trace gas detection in life sciences. *Appl. Phys. B* **92,** 343-349 (2008).

[11] Engel G S *et al.*, Ultrasensitive near-infrared integrated cavity output spectroscopy technique for detection of CO at 1.57 μm: new sensitivity limits for absorption measurements in passive optical cavities. *Appl. Opt.* **45,** 9221-9229 (2006).

[12] Stellard F and Elzinga H, Analytical techniques in biomedical stable isotope applications: (isotope ratio) mass spectrometry or infrared spectrometry? *Isotopes Environ. Health Stud.* **41,** 345-361 (2005).

[13] Blake R S *et al.*, Proton-Transfer Reaction Mass Spectrometry. *Chem. Rev.* **109,** 861-896 (2009).

[14] Kumar S *et al.*, Selected ion flow tube mass spectrometry analysis of exhaled breath for volatile organic compound profiling of esophago-gastric cancer. *Anal. Chem.* **85,** 6121-6128 (2013).

[15] Smith D and Spanel P, Selected ion flow tube mass spectrometry (SIFT-MS) for on-line trace gas analysis. *Mass. Spectrom. Rev.* **24,** 661-700 (2005).

[16] Lourenco C and Turner C, Breath analysis in disease diagnosis: methodological considerations and applications. *Metabolites.* **4,** 465-498 (2014).

[17] Miekisch W, Schubert J K and Noeldge-Schomburg G F, Diagnostic potential of breath analysis-focus on volatile organic compounds. *Clin. Chim. Acta.* **347,** 25-39 (2004).

[18] Amann A *et al.*, Applications of breath gas analysis in medicine. *Int. J. Mass Spec.* **239,** 227-233 (2004).

[19] Cao W and Duan Y, Breath analysis: potential for clinical diagnosis and exposure assessment. *Clin. Chem.* **52,** 800-811 (2006).

[20] Sethi S, Nand R and Chakrabortya T, Clinical application of volatile organic compound analysis for detecting infectious diseases. *Clin. Microbiol. Rev.* **26,** 462-475 (2013).

[21] Schmidt K and Podmore I, Current challenges in volatile organic compounds analysis as potential biomarkers of cancer. *J. Biomarkers* **981458,** 1-16 (2015).

[22] Amann A *et al.*, The human volatilome: volatile organic compounds (VOCs) in exhaled breath, skin emanations, urine, feces and saliva. *J. Breath Res.* **8,** 034001, (2014).

[23] Smith D, Pysanenko A and Spanel P, The quantification of carbon dioxide in humid air and exhaled breath by selected ion flow tube mass spectrometry. *Rapid Commun. Mass Spectrom.* **23,** 1419-1425 (2009).

[24] Kope K A *et al.*, Effects of ventilation on the collection of exhaled breath in humans. *J. Appl. Physiol.* **96,** 1371-1379 (2004).

[25] Goddard A F, Logan R P H, Review article: urea breath tests for detecting *Helicobacter pylori*. *Aliment. Pharmacol. Ther.* **11,** 641-649 (1997).

[26] Machado R S, Patrício F R and Kawakami E, ^{13}C-urea breath test to diagnose *Helicobacter pylori* infection in children aged up to 6 years. *Helicobacter* **9,** 39-45 (2004).

[27] McCue M D and Welch Jr K C, ^{13}C‐Breath testing in animals: theory, applications, and future directions. *J. Comp. Physiol. B* **186,** 265-285 (2016).

[28] Kohn M W, Carbon isotope compositions of terrestrial C3 plants as indicators of (paleo)ecology and (paleo)climate. *Proc. Natl. Acad. Sci. USA* **107,** 19691-19695 (2010).

[29] Boutton T W, Lynott M J and Bumsted M P, Stable carbon isotopes and the study of prehistoric human diet. *Crit. Rev. Food Sci. Nutr.* **30,** 373-385 (1991).

[30] Giannini A *et al.*, ^{13}C-Aminopyrine breath test to evaluate severity of disease in patients with chronic hepatitis C virus infection. *Aliment. Pharmacol. Ther.* **16,** 717-25. (2002).

[31] Herzog D C *et al.*,^{13}C-labeled mixed triglyceride breath test (^{13}C MTG-BT) in healthy children and children with cystic fibrosis (CF) under pancreatic enzyme

replacement therapy (PERT): A pilot study. *Clin. Biochem.* **41,** 1489-1492 (2008).

[32] Braden B *et al.*, ^{13}C-methacetin breath test as liver function test in patients with chronic hepatitis C virus infection. *Aliment, Pharmacol, Ther.* **21,** 179-185. (2005).

[33] Susan D F *et al.*, The ^{13}C-xylose breath test for the diagnosis of small bowel bacterial overgrowth in children. *J. Ped. Gastro. Nutr.* **25,** 153-158 (1997).

[34] Mattison L K *et al.*,The uracil breath test in the assessment of dihydropyrimidine dehydrogenase activity: pharmacokinetic relationship between expired $^{13}CO_2$ and plasma [2-^{13}C] dihydrouracil. *Clin. Cancer Res.* **12,** 549-555 (2006).

[35] Hussain M *et al.*, ^{13}C-Glucose breath testing provides a noninvasive measure of insulin resistance: calibration analyses against clamp studies. *Diabetes Technol. Ther.* **16,** 102-112 (2014).

[36] Ghosh C *et al.*,Oxygen-18 isotope of breath CO_2 linking to erythrocytes carbonic anhydrase activity: a biomarker for pre-diabetes and type 2 diabetes. *Sci. Rep.* **5,** 8137, (2015).

[37] Marshall B J and Warren J R, Unidentified curved bacilli in the stomach of patients with gastritis and peptic ulceration. *The Lancet* **323,** 1311-1315 (1984).

[38] Goh K L *et al.*, Epidemiology of *Helicobacter pylori* infection and public health implications. *Helicobacter* **16,** 1-9 (2011).

[39] Eusebi L H, Zagari R M and Bazzoli F, Epidemiology of *Helicobacter pylori* infection. *Helicobacter* **19,** S1:1-5 (2014).

[40] Cave D R, How is *Helicobacter pylori* transmitted? *Gastroenterology* **113,** S9-14 (1997).

[41] Mégraud F, Transmission of *Helicobacter pylori*: faecal-oral versus oral-oral route. *Aliment. Pharmacol. Ther.* **9,** 2:85-91 (1995).

[42] Chen S *et al.*,The prevalence of *Helicobacter pylori* infection decreases with older age in atrophic gastritis. *Gastroenterol. Res. Pract.* **2013,** 1-7, (2013).

[43] Moayyedi P *et al.*, Relation of adult lifestyle and socioeconomic factors to the prevalence of *Helicobacter pylori* infection. *Int. J. Epidemiol.* **31,** 624-631 (2002).

[44] De Luca A and Iaquinto G, *Helicobacter pylori* and gastric diseases: a dangerous association. *Cancer Lett.* **213,** 1-10 (2004).

[45] Testerman T L and Morris J, Beyond the stomach: an updated view of *Helicobacter pylori* pathogenesis, diagnosis, and treatment. *World J. Gastroenterol.* **20,** 12781-12808 (2014).

[46] Wroblewski L E, Peek R M and Wilson K T, *Helicobacter pylori* and gastric cancer: factors that modulate disease risk. *Clin. Microbiol. Rev.* **23,** 713-739 (2010).

[47] Polk D B and Peek R M, *Helicobacter pylori*: gastric cancer and beyond. *Nat. Rev. Cancer* **10,** 403-414 (2010).

[48] Kusters J G, van Vliet A H M and Kuipers E J, Pathogenesis of *Helicobacter pylori* Infection. *Clin. Microbiol. Rev.***19,** 449-490 (2006).

[49] Peterson W L, *Helicobacter pylori* and peptic ulcer disease. *N. Engl. J. Med.* **324,** 1043-1048 (1991).

[50] Hagymási K and Tulassay Z, *Helicobacter pylori* infection: new pathogenetic and clinical aspects. *World J. Gastroenterol.* **20,** 6386-6399 (2014).

[51] Graham D Y *et al.*,Campylobacter pylori detected noninvasively by the ^{13}C-urea breath test. *The Lancet* **329,** 1174-1177 (1987).

[52] Miftahussurur M and Yamaoka Y, Diagnostic methods of *Helicobacter pylori* infection for epidemiological Studies: critical importance of indirect test validation. *Biomed. Res. Int.* **2016,** 1-14 (2016).

[53] Goddard A F and Logan R P H, Diagnostic methods for *Helicobacter pylori* detection and eradication. *Br. J. Clin. Pharmacol.* **56,** 273-283 (2003).

[54] Uotani T and Graham D Y, Diagnosis of *Helicobacter pylori* using the rapid urease test. *Ann. Transl. Med.* **3,** 9 (2015).

[55] Gisbert J P and Pajares J M, Review article: ^{13}C-urea breath test in the diagnosis of *Helicobacter pylori* infection -a critical review. *Aliment. Pharmacol. Ther.* 20, 1001-1017 (2004).

[56] Savarino V, Vigneri S and Celle G, The ^{13}C urea breath test in the diagnosis of *Helicobacter pylori* infection. *Gut* **45,** SI18-22 (1999).

[57] Mauro M *et al.*, ^{13}C urea breath test for *Helicobacter pylori*: determination of the optimal cut-off point in a Canadian community population. *Can. J. Gastroenterol.* **20,** 770-774 (2006).

[58] Pantoflickova D *et al.*, ^{13}C urea breath test (UBT) in the diagnosis of *Helicobacter pylori*; why does it work better with acid test meals? *Gut* **52,** 933-937 (2003).

[59] Som S *et al.*, Excretion kinetics of ^{13}C-urea breath test: influences of endogenous CO_2 production and dose recovery on the diagnostic accuracy of *Helicobacter pylori* infection. *Anal. Bioanal. Chem.* **406,** 5405-5412 (2014).

[60] Tomb J F *et al.*, The complete genome sequence of the gastric pathogen *Helicobacter pylori*. *Nature* **388,** 539-547 (1997).

[61] Hazell S L and Mendz G L, How *Helicobacter pylori* works: an Overview of the metabolism of *Helicobacter pylori*. *Helicobacter* **2,** 1-12, (1997).

[62] Chalk P A, Roberts A D and Blows W M, Metabolism of pyruvate and glucose by intact cells of *Helicobacter pylori* studied by ^{13}C NMR spectroscopy. *Microbiology* **140,** 2085-2092 (1994).

[63] Psakis G *et al.*, The sodium-dependent D-glucose transport protein of Helicobacter pylori. *Mol. Microb.* **71,** 391-403 (2009).

[64] Bury-Moné S *et al.*, Roles of α and β carbonic anhydrases of *Helicobacter pylori* in the urease-dependent response to acidity and in colonization of the murine gastric mucosa. *Infect. Immun.* **76,** 497-509 (2008).

[65] Marcus E A *et al.*, The Periplasmic α-carbonic anhydrase activity of *Helicobacter pylori* is essential for acid acclimation. *J. Bacteriol.* **187,** 729-738 (2005).

[67] Nishimori I *et al.*,Carbonic anhydrase inhibitors: the β-carbonic anhydrase from *Helicobacter pylori* is a new target for sulfonamide and sulfamate inhibitors. *Bioorg. Med. Chem. Lett.* **17,** 3585-3594 (2007).

[68] Epstein S and Zeiri L, Oxygen and carbon isotopic compositions of gases respired by humans, *Proc. Natl. Acad. Sci. USA*. **85,** 1727-1731 (1988).

[69] Som S *et al.*, Mechanisms linking metabolism of *Helicobacter pylori* to ^{18}O and ^{13}C-isotopes of human breath CO_2. *Sci. Rep.* **5,** 10936 (2015).

[70] Franceschi F *et al.*, *Helicobacter pylori* and extragastric diseases. *Helicobacter* **19,** 52-58 (2014).

[71] Franceschi F *et al.*, Clinical effects of *Helicobacter pylori* outside the stomach. *Nat. Rev. Gastroenterol. Hepatol.* **11,** 234-42 (2014).

[72] Suzuki H, Marshall B J and Hibi T, Overview: *Helicobacter pylori* and extragastric disease. *Int. J. Hematol.* **84,** 291-300 (2006).

[73] He C, Yang Z, Lu N H, *Helicobacter pylori* infection and diabetes: is it a myth or fact? *World J. Gastroenterol.* **20,** 4607-4617 (2014).

[74] Jeon C Y *et al.*, *Helicobacter pylori* infection is associated with an increased rate of diabetes. *Diabetes Care* **35,** 520-525 (2012).

[75] Yang Z *et al.*, Potential effect of chronic *Helicobacter pylori* infection on glucose metabolism of Mongolian gerbils. *World J. Gastroenterol.* **21,** 12593-12604 (2015).

[76] Effects of glycation on erythrocyte carbonic anhydrase-I and II in patients with diabetes mellitus. *Turk. J. Med. Sci.* **30,** 135-141 (2000).

[77] Forstermann U and Sessa W C, Nitric oxide synthases: regulation and function. *Eur. Heart J.* **33,** 829-837 (2012).

[78] Obonyo M *et al.*, Interactions between inducible nitric oxide and other inflammatory mediators during *Helicobacter pylori* infection. *Helicobacter* **8,** 495-502 (2003).

[79] Wilson K T *et al.*, Helicobacter pylori stimulates inducible nitric oxide synthase expression and activity in a murine macrophage cell line. *Gastroenterology* **111,** 1524-1533 (1996).

[80] Gobert A P *et al.*, Cutting edge: urease release by *Helicobacter pylori* stimulates macrophage inducible nitric oxide synthase. *J. Immunol.* **168,** 6002-6006 (2002).

Chapter 2

Materials and Methods

An overview of experimental techniques

In order to investigate the various biochemical and biophysical processes of *Helicobacter pylori* and its related diseases, different experimental tools have been employed. These mainly included the integrated cavity output spectroscopy (ICOS) and cavity ring down spectroscopy (CRDS) techniques. In this chapter, brief discussions of these tools have been discussed with various systems which have been used in our studies.

2.1 Integrated Cavity Output Spectroscopy (ICOS)

The integrated cavity output spectroscopy (ICOS) is a high-sensitive cavity enhanced laser absorption spectroscopy. It was first reported by Anthony O'Keefe in 1988 [1, 2]. The technique is based upon the excitation of a dense spectrum of transverse cavity mode and detecting the leaking light intensity from a high-finesse optical cavity [3-6]. In ICOS, the absorption signal is obtained by integrating the total transmitted light signal leaking through the optical cavity.

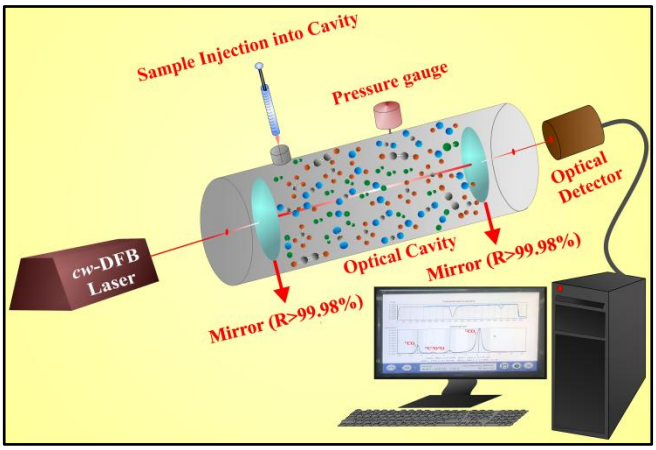

Figure 1. *Schematic diagram of Integrated Cavity Output Spectroscopy (ICOS)*

The measured absorption is thus a function of the different intensities passing through the cavity with and without an absorbing medium. In ICOS technique, the pathlength becomes effectively infinite as the light retraces the same path in each cycle [7-9]. In

this technique, we will be able to measure the very weak absorption band of a molecular species because in every pass the absorptions are added in time which cumulatively gives us a large integrated output. Therefore, by utilizing the ICOS methodology it will be possible to measure the trace molecular species with ultra-low concentration in the level of ppb to ppt. As the off-axis alignment of ICOS is more insensitive to the vibrations and misalignments than the on-axis ICOS, so more precisely our technique is off-axis integrated cavity output spectroscopy (OA-ICOS) [5, 10-12] method. For our study, we have utilized a high-resolution carbon dioxide (CO_2) isotope analyzer (CCIA 36-EP, Los Gatos Research, USA) to measure the isotopes of CO_2 i.e. $^{12}C^{16}O^{16}O$, $^{13}C^{16}O^{16}O$ and $^{12}C^{18}O^{16}O$ for non-invasive tracing of *Helicobacter pylori* in gastrointestinal tract. The high-resolution CO_2 analyzer exploits the off axis ICOS technology and comprised of a high-finesse cylindrical optical cavity (~ 59 cm) coupled with two high-reflective (R ~ 99.98%) mirrors at the both end of the cavity [13-17]. This optical arrangement provides an effective optical pathlength ~ 3 km through the gas sample, which further allows to high-precision measurement of the isotopes of CO_2 in breath sample.

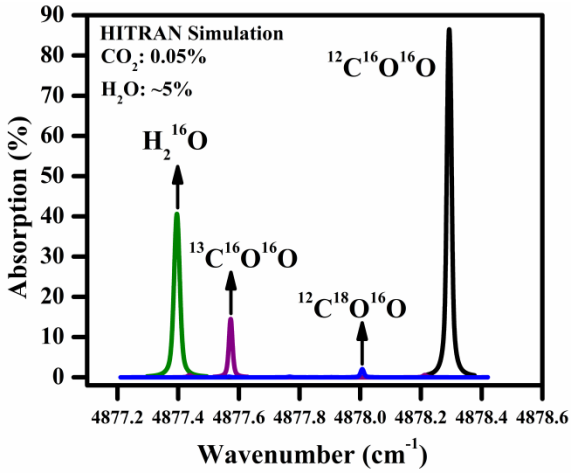

Figure 2. *HITRAN simulation of CO_2 isotopes i.e. $^{12}C^{16}O^{16}O$, $^{12}C^{18}O^{16}O$ and $^{13}C^{16}O^{16}O$ corresponding to R (34), P (32) and P (12) rotational lines of ($2\nu_1+\nu_3$) combinational band with peak centre at 4878.292 cm^{-1}, 4878.006 cm^{-1} and 4877.572 cm^{-},^{1} respectively*

A continuous wave distributed feedback (*cw*-DFB) diode laser operating at ~2.05 μm is repeatedly tuned over 20 GHz to scan the absorption features of $^{12}C^{16}O^{16}O$,

$^{12}C^{18}O^{16}O$ and $^{13}C^{16}O^{16}O$ at the wavenumbers of 4878.292 cm^{-1}, 4878.006 cm^{-1} and 4877.572 cm^{-1}, respectively. The cavity temperature of the ICOS is regulated at 46 $^{\circ}C$ by a resistive heater and feedback control system. The pressure of the inside cavity maintained at 30 Torr through a diaphragm pump. A solenoid valve along with mass flow controllers are used to control the flow of samples inside the cavity of ICOS. The absorption features of $^{12}C^{16}O^{16}O$, $^{12}C^{18}O^{16}O$ and $^{13}C^{16}O^{16}O$ corresponding to the R (34), P (32) and P (12) rotational lines, respectively in the $(2\nu_1+\nu_3)$ $[(0,0^0,0)\rightarrow(2,0^0,1)]$ vibrational combinational band of CO_2, have been utilized to measure the $^{13}C/^{12}C$ and $^{18}O/^{16}O$ isotope ratios simultaneously from exhaled breath samples. The data were captured at a rate of 1 Hz. The transmitted laser intensities were recorded by exploiting a photodetector after passing through a breath sample of interest. Absorption was determined from the measurement of voltage from the photodetector. Beer-Lambert law was utilized to calculate the concentration after integrating the absorption spectrum.

The isotopic enrichments of $^{13}C^{16}O^{16}O$ and $^{12}C^{18}O^{16}O$ in breath sample are usually expressed by the conventional notation, $\delta^{13}C$ and $\delta^{18}O$ in per mil (‰) with respect to the international standard Pee Dee Belemnite (PDB). They are represented as $\delta^{13}C‰ = (R_{sample}/R_{standard} - 1) \times 1000$ and $\delta^{18}O‰ = (R_{sample}/R_{standard} - 1) \times 1000$, where, R_{Sample} is the $^{13}C/^{12}C$ and $^{18}O/^{16}O$ stable isotope ratios of the sample and $R_{Standard}$ is the international standard PDB values i.e. 0.0112372 and 0.0020672, respectively for $\delta^{13}C$ and $\delta^{18}O$ measurements. The accuracy and precision of ICOS method for the $\delta^{13}C‰$ measurements in breath samples were determined by measuring three calibration standards, containing 5% CO_2 in air analyzed by IRMS (Cambridge Isotope Laboratory, USA), with $\delta^{13}C$ values ranging from baseline-level (− 22.8‰) to high-level (− 7.33‰) including the mid-level (− 13.22‰) whereas a standard NOAA air tank with $\delta^{18}O$ = -1‰ was used for the calibration of $\delta^{18}O$ (‰) values measurements. The typical precision of the ICOS system for the measurement of $\delta^{13}C‰$ and $\delta^{18}O‰$ values in exhaled breath samples are ± 0.15‰ and ± 0.20‰, respectively. A 25 mL breath sample was injected into the ICOS cell with a syringe/stopcock for the measurements. High-purity dry nitrogen (HPNG10-1, F-DGSi SAS, France, purity > 99.99%), as the carrier gas, was used to purge the cavity and dilute the breath samples.

2.2 Cavity Ring-Down Spectroscopy (CRDS)

Cavity ring-down spectroscopy (CRDS) is a high-finesse stable optical cavity-based direct absorption spectroscopy technique. CRDS technique was first reported by O'Keefe and Deacon in 1988. CRDS has a significantly higher sensitivity than the conventional absorption spectroscopy techniques. In CRD spectroscopy, the gaseous sample is placed inside a high-finesse optical cavity consisting of two highly reflective mirrors at the both end of the cavity. When a fraction of laser light coupled into the cavity, the light suffers a back and forth reflection inside the cavity. In every reflection a small fraction of the laser light leaks out of the cavity and the transmitted light was measured by a photo-detector. In CRD spectroscopy, decay time was measured by measuring the time dependence leaking out light from the cavity, instead of measuring the total transmitted light from the cavity [3, 18-22]. Therefore the hypothesis is that more the sample is absorbed, the shorter will be the decay time. There are several advantages of CRDS technique compared to other conventional absorption techniques. Since the absorption is determined from the time behaviour of the signal, so it is independent of pulse to pulse fluctuations of the laser. The technique offers the sensitivity upto 10^{-8} to 10^{-10}cm^{-1} which in turn demonstrate the direct high-resolution measurement of the trace molecular species from parts-per-billion (ppb) to parts-per-trillion (ppt) levels. Moreover, the CRDS technique offers the measurement of the absorption in absolute scale, so it does not require any secondary calibration.

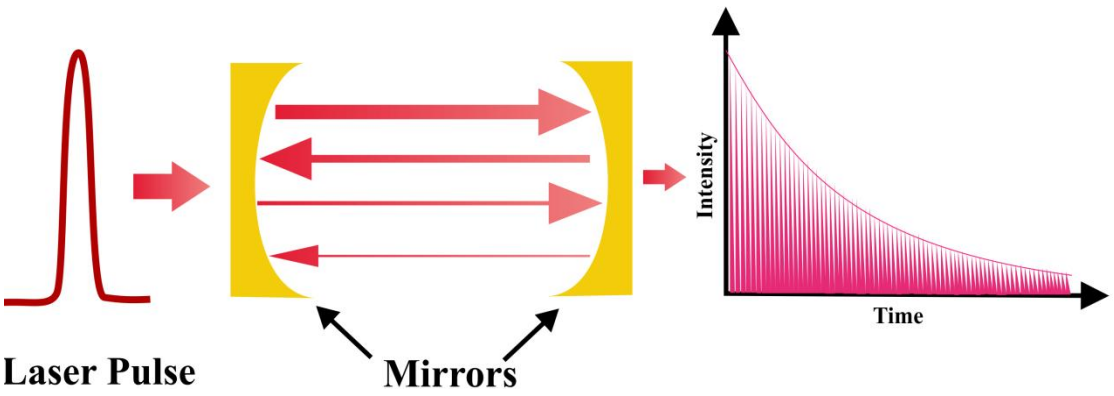

Figure 3. *Principle of cavity ring-down spectroscopy technique*

CRDS has widespread applications in life sciences, in particular in the field of biomedical research and clinical diagnosis. As CRDS has the ability to measure the

concentration in absolute scale, so it has immense potential in quantitative measurement of trace volatile molecules. One of the most important biogenic sources of trace gas is human breath. Several trace gases are formed endogenously such as nitric oxide (NO) and carbon monoxide (CO) with concentration typically in the low ppb region. NO is an important biomarker and known as central mediator in the biological systems [23]. It is well reported that NO has strong absorption bands around 5.2 μm. So to elucidate the potential role of breath NO in the pathogenesis of *Helicobacter pylori* infection, we have utilized a high-resolution cavity ring-down spectrometer (CRDS) coupled with a continuous wave external cavity quantum cascade laser (*cw*-EC-QCL) operating at the centre wavelength 5.2 μm was utilized to measure the concentration of NO in exhaled breath. The experimental arrangement of the cavity ring-down spectroscopy (CRDS) set-up has been demonstrated elsewhere in detail [24, 25]. In brief, a widely tunable room-temperature controlled EC-QCL (TLS-41053, Daylight Solutions, USA) was employed as a mid-IR excitation source for detection of NO in the mid-IR spectral region. The *cw*-EC-QCL has the specified tuning range of 1832-1965 cm^{-1} with mode-hop-free (MHF) tuning range of 1847-1965 cm^{-1} which allows the high-resolution ro-vibronic spectroscopic measurements of gaseous species. The laser has the extremely narrow linewidth of ~ 0.0001 cm^{-1} with output power > 80 mw throughout the tuning range. A high finesse optical cavity (~ 50 cm) comprised with two high reflectivity mirrors (R~ 99.97%) at both ends offers an effective path length of ~1.7 km, used as measurement cell. The QCL beam exiting from the cavity was focused on to a thermoelectrically cooled photovoltaic HgCdTe detector (VIGO, PVI-3TE-6) by an off axis parabolic mirror. The detector signal was then passed through several electronics and finally recorded by a high-speed data-acquisition card (PCI 5122, National Instruments) and analyzed using a custom written LabVIEW programs. To measure the NO concentration in exhaled breath, we have probed the R(12.5) rotational line in the fundamental vibrational band with center at 1912.071 cm^{-1} and 1912.081 cm^{-1} which have the equal line strength of 1.928×10^{-20} $cm^{2}mol^{-1}cm^{-1}$ at 296 K according to the HITRAN database.

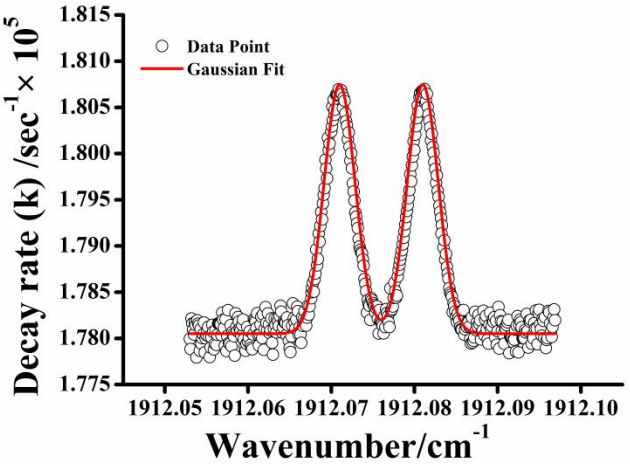

Figure 4. *Typical CRDS spectrum of NO molecule using a standard calibration gas of 60 ppb at 10 Torr pressure inside the cavity by probing the R(12.5) rotational line. The spectrum was fitted with a Gaussian distribution function of FWHM of 0.0044 cm^{-1} which lies in the Doppler broadening of NO at 296 K*

The region is free from overlapping absorption features of water, CO_2, CH_4 etc. which contributed as the major component in exhaled breath. The two lines correspond to the *e* and *f* substates of Λ doublet in the $^2\Pi_{1/2}$ magnetic electronic sub-state of R branch of NO [24]. For the present EC-QCL system, while scanning across the R(12.5) rotational lines of NO, a typical detection limit $\alpha_{min}= 4.75\times10^{-9}$ cm^{-1} has been achieved. This value was calculated using the empty cavity ring-down time (RDT) of 5.61 μs and standard deviation (1σ) of 0.08% with averaging of 6 RDT determinations. Using the value of α_{min} the minimum detection limit $[X]_{min}= 1.056\times10^9$ molecules cm^{-3} has been obtained when the measurements are performed under the Doppler-broadened limiting condition. The air-tight syringes (QUINTRON) were utilized to draw the breath sample from the reservoir bags through a T-connector fitted onto the bag and injected into the optical cavity at a pressure of 5 Torr insde it. The high-resolution NO spectra in exhaled breath were recorded by automated scanning of the laser over ~0.1 cm^{-1}. The absorption lines were then fitted with Gaussian line shape function and the integrated areas' under the curve were utilized to measure the NO concentration in exhaled breath. The change in NO concentration with time after the ingestion of the substrate have been monitored and denoted by ΔNO which is represented as follows

$$[\Delta NO\ (ppb)]_{t=t\ min}=[NO\ concentration\ (ppb)]_{t=t\ min}- [NO\ concentration\ (ppb)]_{t=0\ min}$$

Where, [NO concentration (ppb)]$_{t=0\ min}$ is the baseline NO concentration in exhaled breath before the ingestion of the substrates.

2.3 Statistical Method

For statistical analysis of the experimental data Origin Pro 8.0 software (Origin Lab Corporation, USA) and Analyse-it Method Evaluation software (Analyse-it Software Ltd, UK, version 2.30) were utilized in this thesis. Normality test was performed to verify the experimental data whether it was normally distributed or not. The one-way analysis if variance, abbreviated as one–way ANNOVA test, was applied for parametric distributed data and Mann-Whitney test for non-parametric data. To get the statistical significance of the experimental data, a two-sided p value of < 0.05 was considered. Box-Whisker plots were utilized to demonstrate the statistical distribution of data. To get the optimal diagnostic cut-off value for clinical validity of the data, a receiver operating characteristic (ROC) curve was utilized [26, 27]. The ROC curve was drawn by plotting the sensitivity against (1-specificity) with respect to the gold-standard method. The optimal cut-off value corresponds to the maximum sensitivity and specificity.

2.4 References

[1] O'Keefe A, Integrated cavity output analysis of ultra-weak absorption. *Chem. Phys. Lett.* **29,** 331-336 (1998).

[2] O'Keefe A, Scherer J J and Paul J B, cw Integrated cavity output spectroscopy. *Chem. Phys. Lett.* **307,** 343-349 (1999).

[3] Mazurenka M *et al.*, Cavity ring-down and cavity enhanced spectroscopy using diode lasers. *Annu. Rep. Prog. Chem., Sect. C* **101,** 100-142 (2005).

[4] Hodgkinson J and Tatam R P, Optical gas sensing: a review. *Meas. Sci. Technol.* **24,** 012004 (2013).

[5] McCurdy M R *et al.*, Recent advances of laser-spectroscopy based techniques for applications in breath analysis. *J. Breath Res.***1,** 014001 (2007).

[6] Berden G and Engeln R, Cavity Ring-Down Spectroscopy: Techniques and Applications. Wiley (2009). DOI: 10.1002/9781444308259

[7] Wojtas, J, Application of cavity enhanced absorption spectroscopy to the detection of nitric oxide, carbonyl sulphide and ethane-breath biomarkers of serious diseases. *Sensors* **15,** 14356-14369 (2015).

[8] Maddaloni P *et al.*, Off-axis integrated-cavity-output spectroscopy for trace-gas concentration measurements: modeling and performance. *J. Opt. Soc. Am. B* **23,** 1938-1945 (2006).

[9] Kosterev A *et al.*, Application of quantum cascade lasers to trace gas analysis. *Appl. Phys. B* **90,** 165-176 (2008).

[10] Parameswaran K R *et al.*, Off-axis integrated cavity output spectroscopy with a mid-infrared interband cascade laser for real-time breath ethane measurements. *Appl. Opt.* **48,** 73-79 (2009).

[11] Arslanov D D *et al.*, Real-time, subsecond, multicomponent breath analysis by optical parametric oscillator based off-axis integrated cavity output spectroscopy. *Opt. Exp.* **19,** 24078-24089 (2011).

[12] Bakhirkin Y A *et al.*, Mid-infrared quantum cascade laser based off-axis integrated cavity output spectroscopy for biogenic nitric oxide detection. *Appl. Opt.* **43,** 2257-2266 (2004).

[13] Crosson E R *et al.*, Stable isotope ratios using cavity ring-down spectroscopy: determination of $^{13}C/^{12}C$ for carbon dioxide in human breath *Anal. Chem.* **74,** 2003-2007 (2002).

[14] Zare R N *et al.*, High-precision optical measurements of $^{13}C/^{12}C$ isotope ratios in organic compounds at natural abundance. *Proc. Natl. Acad. Sci. USA.* **106,** 10928-10932 (2007).

[15] Zanasi R, Determination of $^{13}C/^{12}C$ carbon isotope ratio. *Anal. Chem.* **78,** 3080-3083 (2006).

[16] Maity A *et al.*,Oxygen-18 stable isotope of exhaled breath CO_2 as a non-invasive marker of *Helicobacter pylori* infection. *J. Anal. At. Spectrom.* **29**, 2251-2255 (2014).

[17] Som S *et al.*,Mechanisms linking metabolism of *Helicobacter pylori* to ^{18}O and ^{13}C-isotopes of human breath CO_2. *Sci. Rep.* **5,** 10936 (2015).

[18] Berden G, Peeters R and Meijer G, Cavity ring-down spectroscopy: Experimental schemes and applications, *Int. Rev. Phys. Chem.* **19,** 565-607 (2000).

[20] Lehmann K K and Romanini D, The superposition principle and cavity ring-down spectroscopy. *J. Chem. Phys.* **105,** 1026 (1996).

[21] Romanini D, CW cavity ring down spectroscopy. *Chem. Phys. Lett.* **264,** 316-322 (1997).

[22] Zailcki P and Zare R N, Cavity ring-down spectroscopy for quantitative absorption measurements. *J. Chem. Phys.* **102,** 2708 (1995).

[23] Calabrese V *et al.*, Nitric oxide in the central nervous system: neuroprotection versus neurotoxicity. *Nature Rev. Neurosci.* **8,** 766-775 (2007).

[24] De A *et al.*, Continuous wave external-cavity quantum cascade laser-based high-resolution cavity ring-down spectrometer for ultrasensitive trace gas detection. *Opt. Lett.* **41,** 1949-1952 (2016).

[25] Banik G D *et al.*, An EC-QCL based N_2O sensor at 5.2 μm using cavity ring-down spectroscopy for environmental applications. *Anal. Methods* **9,** 2315-2320, (2017).

[26] Tilaki K H, Receiver operating characteristic (ROC) curve analysis for medical diagnostic test evaluation. *Caspian J. Intern. Med.* **4,** 627-635 (2013).

[27] Weiss H L *et al.*, Receiver operating characteristic (ROC) to determine cut-off points of biomarkers in lung cancer patients. *Dis. Markers* **19,** 273-278 (2003).

Chapter 3

^{13}C-urea breath test and exploration of percentage-dose-recovery for non-invasive accurate diagnosis of *Helicobacter pylori* infection in human stomach

3.1 Introduction

Helicobacter pylori (*H. pylori*) infection is the primary cause of gastritis and peptic ulcer diseases, and has been linked to the onset of various critical diseases such as stomach cancer, gastric lymphoma and adenocarcinoma [1, 2]. It is estimated that more than half of the world's populations harbour *H. pylori* infection, with a prevalence of 80% or more in the Indian subcontinent [3, 4]. The infection is usually acquired early in life and may remain in the stomach for the rest of the person's life if it is not properly treated [5, 6]. Most individuals harbouring *H. pylori,* however, are usually asymptomatic and hence they remain undiagnosed. Therefore, an accurate and early detection of *H. pylori* infection is vital for initiation of proper treatment.

Currently, the ^{13}C-urea breath test (^{13}C-UBT) is considered to be an effective non-invasive method for detecting *H. pylori* infection by contrast with the direct invasive "gold standard" endoscopy and biopsy-based rapid urease test (RUT) [7, 8]. The ^{13}C-UBT is usually performed by ingestion of a test meal containing 75 mg ^{13}C-enrihced urea with 4 gm citric acid dissolved in 200 mL water. Initially, a baseline breath (fasting breath) sample is collected and subsequently a further breath sample is collected at 30 min following administration of the substrate. The $^{13}CO_2$ isotopic enrichments in breath samples are usually measured with a high-precision gas-chromatography coupled with an isotope ratio mass spectrometer (GC-IRMS). However, the ^{13}C-UBT exploits the large amount of urease enzyme, secreted by *H. pylori* in the stomach, to hydrolyze the orally administered ^{13}C-labelled urea into ammonia and ^{13}C-labelled carbon dioxide. The ^{13}C-urea derived $^{13}CO_2$ is then transported to the lungs through the bloodstream and is exhaled as $^{13}CO_2$ in the breath samples. The difference of $^{13}CO_2$ concentrations before and after ingestion of the labelled urea, which is reported as the delta-over-baseline (DOB) relative to a

standard in per mil (‰), i.e.$\delta_{DOB}{}^{13}C‰$ [$\delta_{DOB}{}^{13}C‰ = (\delta^{13}C‰)_{t=t\,\min} - (\delta^{13}C‰)_{t=0\,\min}$], will be exploited to detect the presence of *H. pylori* infection. Therefore, *H. pylori* infected individuals will exhibit an increase of $^{13}CO_2$ in their breath after certain time following ingestion of ^{13}C-enriched urea. However, to our knowledge, the time-dependent excretion patterns of the ^{13}C-UBT and the percentage dose of ^{13}C recovered per hour i.e. ^{13}C-PDR (%/hr) along with cumulative PDR i.e. c-PDR(%) in exhaled breath samples have not been investigated in detail. The ^{13}C-PDR describes the rate of ^{13}C-enriched substrate that has been exhaled as $^{13}CO_2$ in the exhaled breath whereas the c-PDR (%) accounts for the total amount of ^{13}C-enriched substrate metabolized at any given time. A complete evaluation of the excretion kinetic profiles, ^{13}C-PDR (%/hr) and c-PDR(%) of the ^{13}C-UBT is important to understand the real emptying processes, determine the optimal sampling point, elucidate the effects of urea hydrolysis rate (UHR) and accomplish the highest diagnostic accuracy as well as the best diagnostic cut-off level for broad clinical applicability of the ^{13}C-UBT method for large-scale screening purposes.

Moreover, the effect of endogenous CO_2 production associated with basal metabolic rates (BMR) may have an influence on the diagnostic accuracy of the ^{13}C-UBT. It is expected that endogenous CO_2 production varies along with age (adults > children), weight, height and sex (male > female) [9] and consequently the DOB values are also expected to vary in accordance with these factors. Yang *et al*. [5] have recently demonstrated a significant effect of endogenous CO_2 production rates on the ^{13}C-UBT even after the application of urea hydrolysis rate (UHR) in children aged between 7 months and 18 years. However, to our knowledge, no investigations of the effect of endogenous CO_2 production on ^{13}C-UBT have been performed in adults aged 20-75 years until now.

Furthermore, the determination of a precise cut-off value for discriminating between positive and negative *H. pylori* results is still the subject of debate and subsequently a wide range of diagnostics cut-off values between 1.3 and 11‰ have been suggested in several reports [7, 8]. Sometimes it is very critical to accurately diagnose if the DOB values are very close to the selected cut-off point or at the borderline and consequently the results of ^{13}C-UBT remain questionable and affects the diagnostic accuracy. Some authors have also suggested a narrow spectrum of the DOB values

called “grey zone” (2.0 to 5.0 ‰) of the ^{13}C-UBT in which the ^{13}C-UBT results are inconclusive [8]. Therefore, a DOB value within this region should be cautiously interpreted. This grey zone containing unreliable results accounts for intuitive variations of $^{13}CO_2$ in exhaled breath samples, patient’s metabolism and the limits of the analytical precision of $^{13}CO_2$ measurements. Therefore, a comprehensive revaluation of the optimal diagnostic cut-off point is required to validate the widespread clinical implementation of the ^{13}C-UBT in the diagnosis of *H. pylori* infection.

In this chapter, we investigate the time-dependent evaluation of $\delta_{DOB}{}^{13}C‰$ and ^{13}C-PDR (%/hr) along with c-PDR in exhaled breath samples after ingestion of ^{13}C-labeled urea for the detection of *H. pylori* infection by means of an optical cavity-enhanced integrated cavity output spectroscopy (ICOS) system. We have employed the cavity-enhanced optical spectroscopy method in the present study because of its fast analysis time (about 30 sec) compared to the MS-based method (typically 2 min) [10]. We also investigated the influences of endogenous CO_2 production and urea hydrolysis rate on the diagnostic accuracy of ^{13}C-UBT. Finally, we determined statistically sound several diagnostic parameters such as the optimal diagnostic cut-off value, sensitivity, specificity, accuracy, the risk of false-positive and false-negative results of the ^{13}C-UBT using ICOS system against the defined gold standard endoscopic biopsy tests.

3.2 Materials and Methods

3.2.1 Subjects

Eighty three subjects (61 male, 22 female, age: 21-72 yrs with mean age: 38.33± 11.69 yr) with a variety of gastrointestinal disorders such as chronic gastritis, duodenal and gastric ulcer and non-ulcer dyspepsia were included in the present study. On the basis of gold standard reports, such as gastrointestinal endoscopy and biopsy-based rapid urease tests (RUTs), subjects were classified into two different groups, as either *H. pylori* positive or *H. pylori* negative. For this purpose thirty four (34) controls with *H. pylori* negative and forty nine (49) patients with *H. pylori* positive were considered for the ^{13}C-UBTs. Subjects who had taken antibiotics, proto pump inhibitors or bismuth containing compound prior to four weeks of study and

subjects having previous gastric surgery were excluded from the study. The current protocol was approved by the Ethics Committee Review Board of AMRI Hospital, Salt Lake, India (Study No: AMRI/ETHICS/2013/1). Informed consent was obtained from each patient prior to enrolment in the study

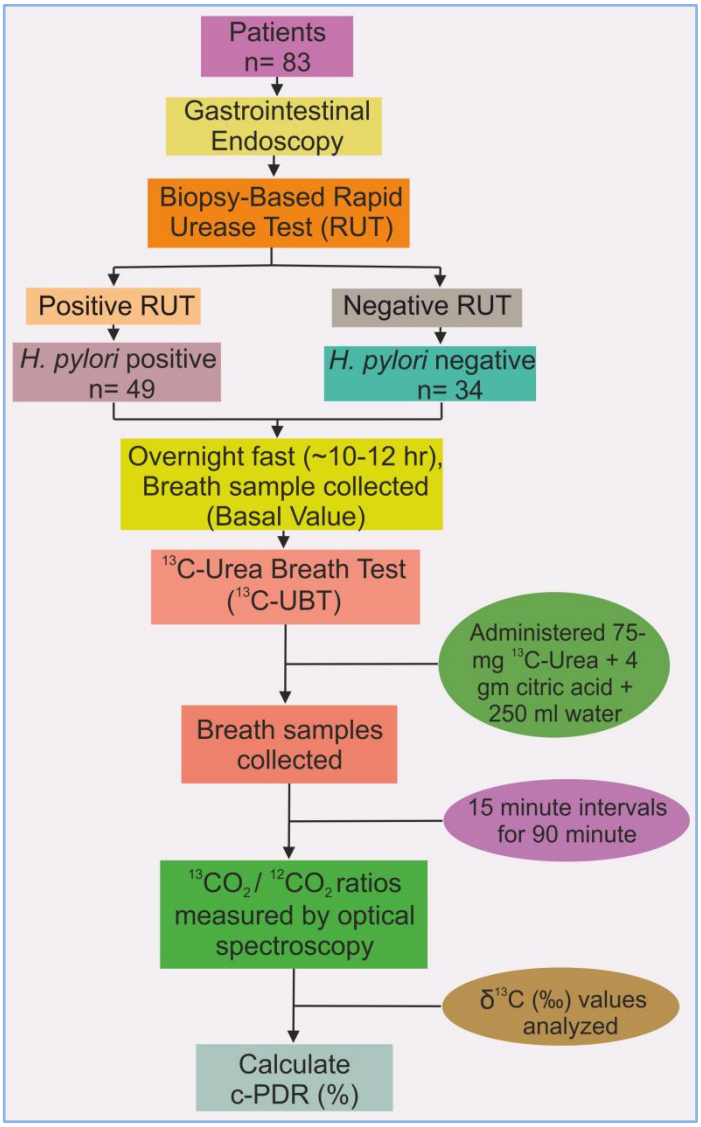

Figure 1. *Flow diagram of the methodology used in this study*

3.2.2 Breath Sample Collection and ^{13}C-UBT

After an overnight fast, subjects performed the ^{13}C-UBT within 1-2 days after endoscopy according to the standard procedure as previously mentioned in several articles [5, 7, 8, 11]. A baseline breath sample was collected in a 750 ml breath collection bag (QT00892, QuinTron Instrument Co. USA). Subjects were first

instructed to ingest 200 ml citric acid solution (4.0 gm citric acid in 200 ml water) and then a drink containing 75 mg ^{13}C-labelled Urea (CLM-311-GMP, Cambridge Isotope Laboratories, Inc. USA) dissolved in 50 ml water was orally administered as per the standard procedure. Post dose breath samples were collected subsequently at 15 min intervals up to 90 min. During breath sample collection, subjects were instructed to hold their breath for 3 s and blow smoothly through a mouth piece directly into the breath collection bag provided. All breath samples were repeated and analyzed by laser-based ICOS system described in chapter 2. Fig. 1 depicts a diagram presenting the steps of the procedure and analytical protocol used in the study.

3.3 Results and Discussion

Fig. 2 depicts the typical excretion kinetic patterns of $\delta_{DOB}{}^{13}C‰$ values in exhaled breath samples for three *H. pylori* positive and three *H. pylori* negative individuals after ingestion of ^{13}C-enriched substrate. It was observed that in *H. pylori* positive patients, the $\delta_{DOB}{}^{13}C‰$ values in breath samples reached a maximum at around 30 min and then slowly decreased, whereas no significant differences of $\delta_{DOB}{}^{13}C‰$ values in breath samples were observed for the *H. pylori* negative individuals.

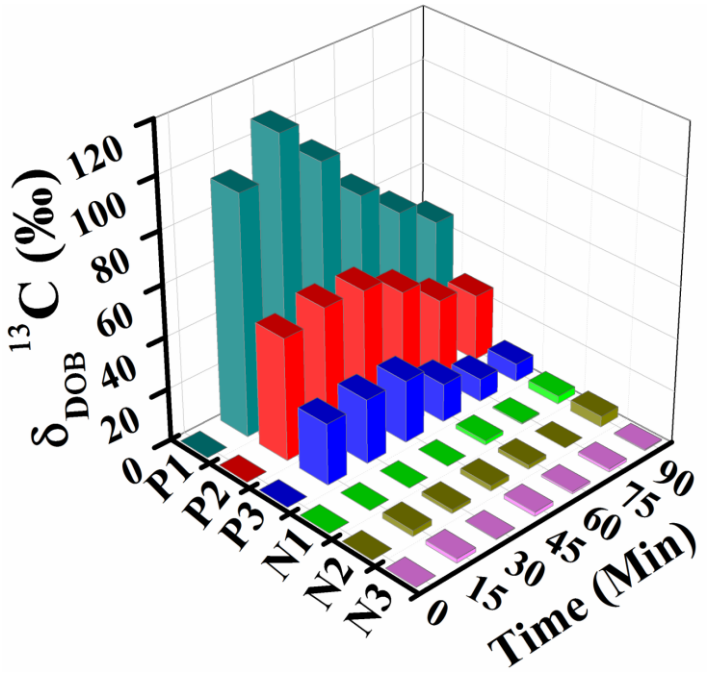

Figure 2. *Typical excretion kinetic profiles of $\delta^{13}{}_{DOB}C‰$ values in exhaled breath samples for three H. pylori positive (P1, P2 and P3) and three H. pylori negative (N1, N2 and N3) individuals as an illustration*

It was previously reported by in vitro biopsies analysis that the internal urease activity of *H. pylori* strongly depends on the medium pH values and the activity is maximum at low pH 3.0 and is minimum at pH 7.0 or 8.0 [12]. When ^{13}C-enriched urea is administered with citric acid, the internal urease activity is stimulated [13] at a pH of < 6.5. The activity is increased with acidifications of the medium owing to increased ^{13}C-urea permeability through the urea channel in the inner membrane of *H. pylori*, allowing a large increase in ^{13}C-urea access to intra-bacterial urease enzyme [12, 14]. It was also shown before that the major effect of acidification of the medium occurs within 30 minutes [12]. Consequently, an increase in the rate and quantity of $\delta_{DOB}{}^{13}$C‰ values in exhaled breath within 30 minutes is most likely to be the result of increased urease activity i.e. urease catalysed hydrolysis of ^{13}C-urea increases and thus results in enrichment of $^{13}CO_2$. The gradual decrease in δ_{DOB} ^{13}C‰ values in exhaled breath samples later on is a sign of lower urease activity because of alkalinisation of the bacterial environment by production of NH_3. Consequently, the large difference in the δ_{DOB} ^{13}C‰ values in breath samples demonstrated a clear distinction between *H. pylori* infected and uninfected individuals.

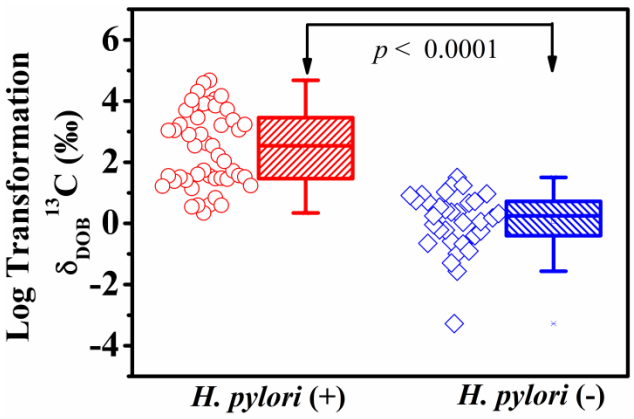

Figure 3. *Box and Whisker plot of δ_{DOB} ^{13}C‰ illustrating the statistical distribution of $^{13}CO_2$ enrichment at 30 min in H. pylori positive and H. pylori negative individuals. The scattered points represented by open-circle & open-diamond symbols correspond to experimental data points obtained by ICOS instrument*

A Box and Whisker plot of δ_{DOB} ^{13}C‰ to illustrate the distribution of $^{13}CO_2$ enrichment at 30 min in *H. pylori* positive and *H. pylori* negative individuals is shown in Fig. 3. The mean, median and inter-quartile ranges (IQRs) (i.e. mid-spread of

statistical dispersion) for positive and negative patients were 22.66‰, 12.64‰, and 4.32‰ to 31.71‰, respectively and 1.44‰, 1.24‰ and 0.56‰ to 2.06‰, respectively. It was observed that the median values of δ_{DOB} ^{13}C‰ increased significantly for the group with positive *H. pylori* individuals compared to the group with negative individuals. There was a statistically significant difference between the δ_{DOB} ^{13}C‰ values ($p < 0.0001$) obtained for two different types of groups and therefore they can be distinguished.

However, to investigate the diagnostic accuracy of the present ^{13}C-UBT for distinguishing *H. pylori* positive and *H. pylori* negative individuals, a receiver operating characteristic curve (ROC) was constructed by plotting the true positive rate (sensitivity) against false positive rate i.e. (1- specificity) at 30 minute according to the standard procedure as shown in Fig. 4. The sensitivity, specificity, false-positive and false-negative results of ^{13}C-UBT were calculated at various cut-off values. An optimal cut-off point for ^{13}C-UBT was defined as the point with the highest sensitivity, specificity and diagnostic accuracy to identify individuals with and without *H. pylori* infection.

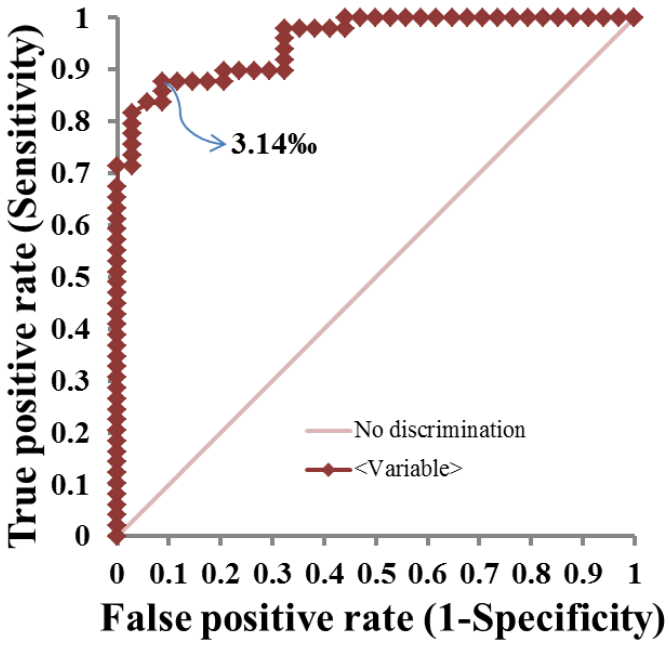

Figure 4. *Receiver operating characteristic curve (ROC) analysis for the ^{13}C-UBT. The optimal diagnostic cut-off value was determined to be δ_{DOB}^{13}C‰ = 3.14‰ at 30 minute*

The optimal diagnostic cut-off value was determined to be $\delta_{DOB}{}^{13}C‰$ (cut-off) = 3.14‰, exhibiting 87.8% sensitivity (95% confidence interval (CI) 75.2-95.4) and 91.2% specificity (95% CI 76.3-98.1) with an accuracy of 89.16%. The calculated cut-off value as determined by the ROC analysis correlated well with cut-off values of between 2-5‰ mentioned in the grey-zone [7, 8]. The area under the ROC curve referred to as AUC was also determined to be 0.95 (95% CI 91.0-99.0). At a cut-off value of 3.14‰, it was therefore, possible to correctly diagnosed 43 of 49 patients as positive (i.e. 6 false negative patient) and 31 of 34 patients as negative (i.e. 3 false positive patients). It is noted that when the DOB value is close to the cut-off point and the cut-off point is within the "grey-zone", the risk of a false-positive or false negative response of the ^{13}C-UBT is extremely high. It should be emphasized here that the "grey-zone" of the ^{13}C-UBT was not hitherto well addressed. The evaluation of the "grey-zone is very important for the early diagnosis of *H. pylori* infection because many individuals harbouring the infection fall in this region. In this study, we therefore, have explored a possible way to overcome the "grey-zone" by exploiting the time-dependent evaluation of $\delta_{DOB}{}^{13}C‰$ values in the exhaled breath samples.

However, there are several possibilities which can affect the results of ^{13}C-UBT within the "grey-zone". One such possibility is to investigate the effect of endogenous CO_2 production associated with basal metabolic rates (BMR) in individuals. To study this effect, we applied Mifflin-St Joer equations to calculate the BMR based on age, weight and height of either sex [15]. The effect of the endogenous CO_2 production rates between the two groups of *H. pylori* positive and *H. pylori* negative individuals (10.57 mmol/min vs 10.66 mmol/min) was statistically insignificant (p=0.78) (Fig. 5a). However, the effect of urea hydrolysis rate (UHR) at 30 minute on ^{13}C-UBT between *H. pylori* positive and *H. pylori* negative individuals (81.49 μg/min vs 5.30 μg/min) was statistically significant ($p < 0.0001$) which thus showed the presence of *H. pylori* infection (Fig. 5b). To study the UHR, we applied the Schofield equations [16] and used the experimentally determined $\delta_{DOB}{}^{13}C‰$ values as shown below [5]:

UHR = endogenous CO_2 production × $\delta_{DOB}{}^{13}C‰$ × 0.346294 (μg/min) (1)

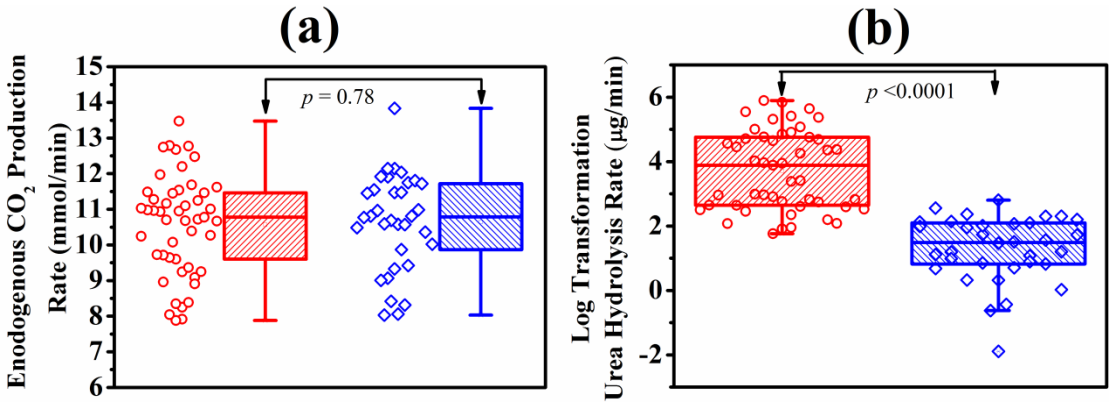

Figure 5. *The endogenous CO_2 production rates between the two groups of H. pylori positive and H. pylori negative subjects.* ***(a)*** *The difference of endogenous CO_2 production rates between these two groups was statistically insignificant with p= 0.78 (>0.05),* ***(b)*** *A statistically significant difference of urea hydrolysis rate (UHR) (p<0.0001) was observed between the two groups of H. pylori positive and H. pylori negative individuals at 30 minute*

We subsequently investigated the optimal diagnostic cut-off value of 10.48μg/min by means of UHR at 30 minute. But no significant improvement in the results of diagnostic sensitivity, specificity and accuracy was observed, demonstrating the insignificant effect of endogenous CO_2 production on ^{13}C-UBT.

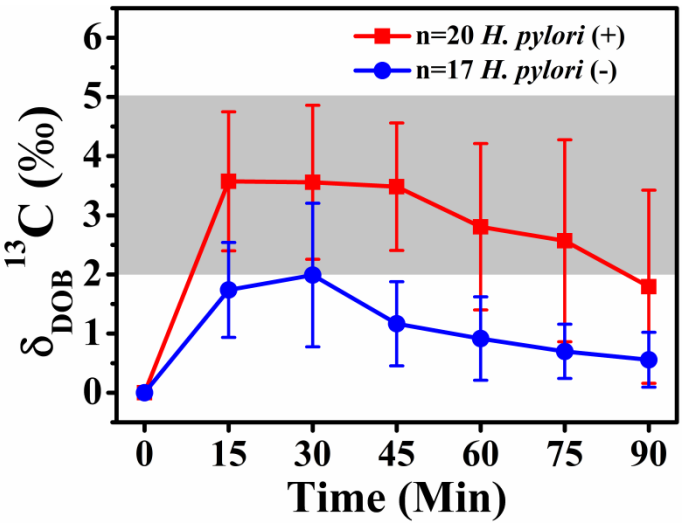

Figure 6. *The time evaluation of $\delta_{DOB}{}^{13}C$ values for the two groups of 20 H. pylori positive and 17 H. pylori negative individuals within the "grey-zone". The shaded region corresponds to 'grey-zone' and n is the number of patients*

Fig. 6 depicts the excretion patterns of $\delta_{DOB}{}^{13}C‰$ values within the "grey-zone" for the two groups (20 *H. pylori* positive & 17 *H. pylori* negative individuals) of patients. It was observed that the $\delta_{DOB}{}^{13}C‰$ values at each time point for the two groups were very close or sometimes overlaps to each other, demonstrating the accurate detection of *H. pylori* infection in the "grey-zone" is often incorrect and uncertain. We also observed that there were sudden rises or abrupt falls of $\delta_{DOB}{}^{13}C‰$ values at 30 min in the individual excretion kinetic patterns, which have essentially reflected in the outcomes of ^{13}C-UBT for producing false positive and false negative results.

Therefore to avoid the risk of diagnostic errors in the "grey-zone" and consequently to achieve the highest diagnostic accuracy of the ^{13}C-UBT, we have explored the percentage dose of ^{13}C recovered per hour i.e. ^{13}C-PDR (%/hr) and cumulative percentage dose of ^{13}C recovered i.e. c-PDR(%) in exhaled breath samples for the present ^{13}C-UBT.

To investigate the ^{13}C-PDR, we applied the following formula of Wu and colleagues [17]:

$$^{13}C - PDR\,(\%/hr) = \frac{\delta_{DOB}{}^{13}C \times R_{PDB} \times 10^{-3} \times V_{CO_2}}{\left(\frac{D}{M_t}\right) \times \left(p \times \frac{n}{100}\right)} \times 100 \qquad (2)$$

where $\delta_{DOB}{}^{13}C$ is the DOB values, R_{PDB} = 0.0112372, D is the dose of substrate administered, M_t = molecular weight of the substrate, p is ^{13}C atom % excess, n is the number of labelled carbon positions and V_{CO2} is the CO_2 production rate per hour. The c-PDR(%) values were calculated using trapezoidal rule [18] from the ^{13}C-PDR values. Fig. 7 shows the time profiles of c-PDR(%) for the two groups of patients within the "grey-zone". A clear distinction between the groups of positive and negative *H. pylori* individuals was observed after 45 min (0.75 hr) in the kinetic profiles. Thus the measurement of c-PDR(%) is more advantageous compared to a single point $\delta_{DOB}{}^{13}C$ measurement because it accounts for the cumulative effect of $\delta_{DOB}{}^{13}C‰$ at any given time.

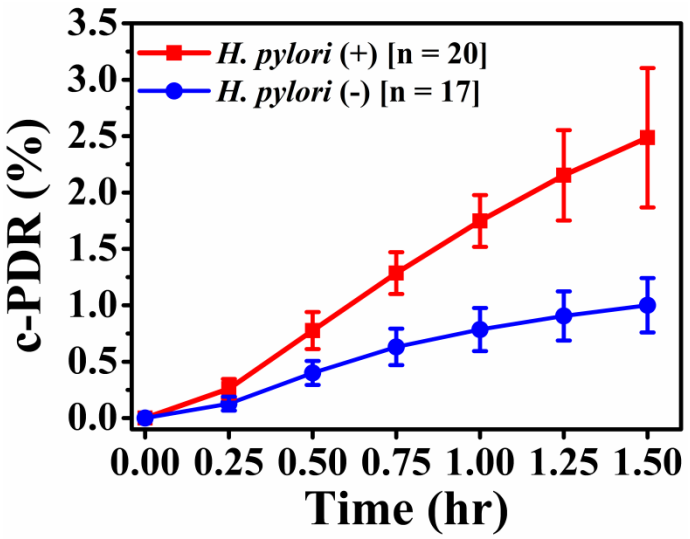

Figure 7. *Time profiles of c-PDR(%) for the two groups of 20 H. pylori positive and 17 H. pylori negative individuals within the "grey-zone"*

However, a clear disadvantage of the c-PDR (%) methodology compared to the standard single point $\delta_{DOB}{}^{13}C‰$ measurement is that at least 5-6 breath samples need to be measured. In several reports [8], many authors have also suggested that a repeat ^{13}C-UBT or invasive endoscopy and biopsy test would be an appropriate choice to have a conclusive result for the "grey-zone" patients. Nevertheless, this is much more expensive and time consuming than a single test regardless of requiring breath samples at multiple time points.

We subsequently explored the diagnostic accuracy of the ^{13}C-UBT by constructing another ROC curve using the c-PDR(%) values and Fig. 8 depicts the ROC curve. An optimal diagnostic cut-off level was estimated to be c-PDR=1.47% at 60 min, exhibiting 100% diagnostic sensitivity (95% confidence interval (CI) 92.7-100), 100% specificity (95% confidence interval (CI) 89.7-100) and 100% accuracy of the ^{13}C-UBT for the detection of *H. pylori* infection.

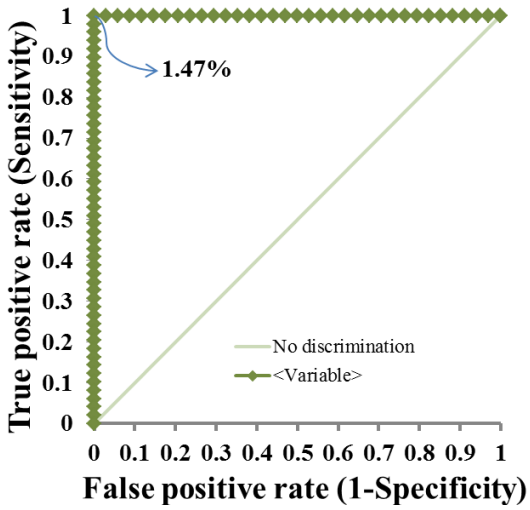

Figure 8. *Receiver operating characteristic curve (ROC) analysis for the c-PDR(%). The optimal diagnostic cut-off value was determined to be c-PDR(%) = 1.47% at 60 minute (1.0 hr)*

We also investigated whether the current c-PDR(%) methodology is statistically robust compared to the standard one for the "grey-zone" patients. Fig. 9 illustrates a simple statistical test, demonstrating that the optimal cut-off point of the standard $\delta_{DOB}{}^{13}C‰$ test i.e. 3.14‰ lies within the overlapping areas between the two groups of patients, considering only 1SD of the mean values, whereas in case of c-PDR(%) methodology, the cut-off point (1.47%) is quite far away from the overlapping areas of both types of patients even by considering 2SD. It is also noted that the cut-off value of the c-PDR(%) could be decreased to 1.29% without compromising the sensitivity and specificity of this methodology.

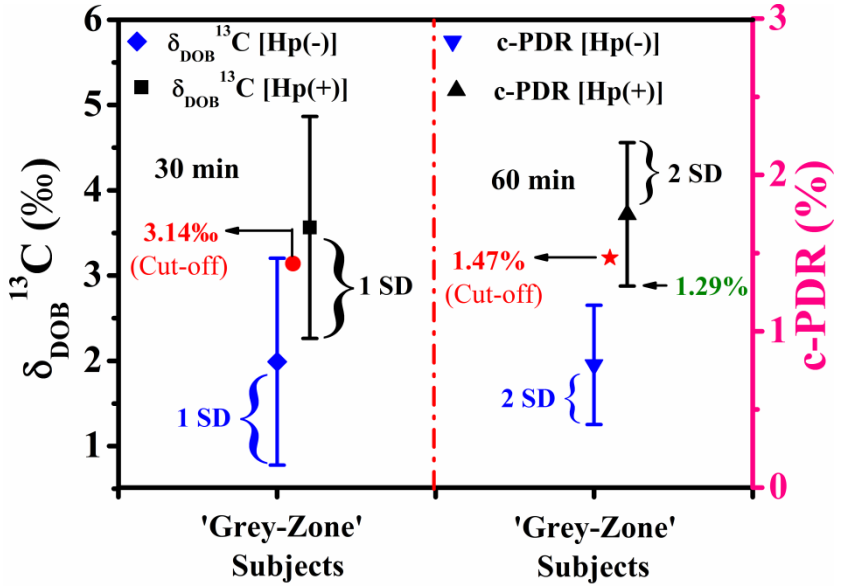

Figure 9. *A statistical comparison between single point $\delta_{DOB}{}^{13}C$‰ measurement and c-PDR (%) methodology for 'grey-zone' individuals. The error bar corresponds to 1SD and 2SD respectively for $\delta_{DOB}{}^{13}C$‰ and c-PDR (%) measurements. Hp(+) & Hp(-) stand for H. pylori positive and negative individuals respectively and SD is the standard deviation*

Thus the c-PDR(%) methodology appears to be sufficiently robust for an accurate diagnosis of *H. pylori* infection, avoiding a repeat endoscopic biopsy test as some authors have previously suggested this invasive test [8] when the DOB values are inconclusive within the "grey-zone". Moreover, we determined the positive and negative predictive values (i.e. PPV and NPV) of the present ^{13}C-UBT. The PPV and NPV essentially indicate the probabilities that the infection is truly positive and negative, respectively among the total test outcome positives and test outcome negatives, respectively [19]. The present ^{13}C-UBT demonstrated both PPV and NPV of 100%, manifesting excellent diagnostic accuracy for large scale screening purposes. Table 1 shows the comparison of various diagnostic parameters for ^{13}C-UBT in three different methodologies.

Table 1 *Comparisons of diagnostic parameters for ^{13}C-UBT in three different methodologies*

Methodology	Breath Samples Collection	Receiver Operating Characteristics (ROC) Curve Results						
		Sensitivity (%)	Specificity (%)	PPV† (%)	NPV‡ (%)	FP¥	FN§	Cut-off value
$\delta_{DOB}{}^{13}C$(‰)	Basal & 30 min	87.8	91.2	93.48	83.78	3	6	**3.14‰** (at 30 min)
UHR*(μg/min)	Basal & 30 min	87.8	91.2	93.48	83.78	3	6	**10.48μg/min** (at 30 min)
c-PDR$(%)	Basal & multiples breath samples	100	100	100	100	0	0	**1.47%** (at 60 min)

*†PPV- Positive Predictive Value; ‡NPV- Negative Predictive Value; ¥FP- False Positive; §FN- False Negative; *UHR- Urea Hydrolysis Rate; $c-PDR- Cumulative Percentage Dose Recovery.*

Finally, we have investigated the real emptying process of the present ^{13}C-UBT for *H. pylori* infected individuals. Fig. 10 illustrates the time profiles of ^{13}C-PDR (%/hr) and c-PDR(%) of *H. pylori* infected individuals. The median data for the ^{13}C-PDR(%/hr) of 49 *H. pylori* positive patients were fitted by the following mathematical formula for determination of the time of maximal empting rate [12]:

$$y = at^{b}e^{-ct} \tag{3}$$

where y is the percentage of $^{13}CO_2$ excretion per hour; t is the time and a, b, c are constants. From the fitting constants, the time of maximal emptying rate of the current ^{13}C-UBT was calculated to be t_{max}=(b/c)=0.60 hr (36 min) as shown in Fig. 10.

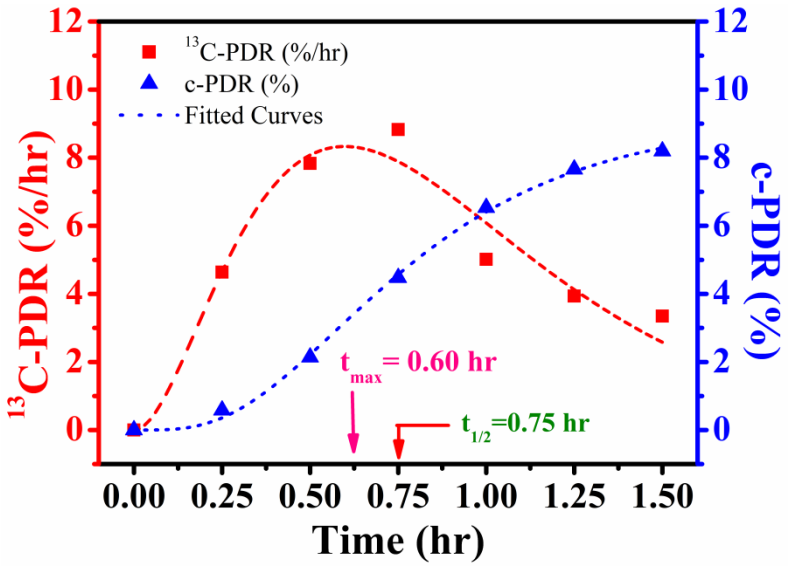

Figure 10. *Time profiles of percentage dose of ^{13}C recovered per hour, ^{13}C-PDR (%/hr) and cumulative percentage dose of ^{13}C recovered, c-PDR (%). Median values of 49 H. pylori positive patients are used to plot. Red lines are the fitted curves. t_{max} and $t_{1/2}$ indicate the time of maximal emptying rate and half emptying time, respectively*

The calculated value also supported the maximum $\delta_{DOB}{}^{13}C‰$ values at 30 min as previously observed in Fig. 2 for *H. pylori* positive patients. The c-PDR (%) data were also fitted to another three parameter model with

$$y = m\left(1 - e^{-kt}\right)^{\beta} \qquad (4)$$

where m, k and β are constants to determine the half emptying time [12] of the current protocol and it was estimated to be $t_{1/2} = (-1/k)\ln(1-2^{-1/\beta}) = 0.75hr(45\,\text{min})$. From Fig. 10 it was also observed that about 8% of total ^{13}C dose recovered over 1.5 hr which in turn exhibited the existence of *H. pylori* infection.

3.4 Conclusions

In summary, we have elucidated the time the excretion kinetic patterns of $\delta_{DOB}{}^{13}C‰$, ^{13}C-PDR (%/hr) as well as c-PDR (%) for the ^{13}C-UBT in the diagnosis of *H. pylori* infection. We subsequently investigated the effect of endogenous CO_2 production and

urea hydrolysis rates on the excretion kinetic curves. The present study clearly demonstrates how to overcome the "grey-zone" in the ^{13}C-UBT for accurate determination of the infection without any risk of diagnostic errors and consequently introduces a new diagnostic cut-off value of c-PDR(%)=1.47% at 60 min. Moreover, the current c-PDR methodology exhibited both sensitivity (true positive rates) and specificity (true negative rates) of 100% and a diagnostic accuracy of 100% compared with endoscopic biopsy tests, thus making it a sufficiently robust and novel method for an accurate and fast non-invasive diagnosis of *H. pylori* infection for large-scale screening purposes. However, it should be emphasised that although we have investigated the c-PDR (%) methodology only on limited number samples as a preliminary test, but a much larger study would be required to confirm the general rule that c-PDR (%)=1.47% at 60 min are always the best choices.

3.5 References

[1] Imrie C *et al.*, Is *Helicobacter pylori* infection in childhood a risk factor for gastric cancer? *Pediatrics* **107,** 373-380 (2001).

[2] Suzuki H, Marshall B J and Hibi T, Overview: *Helicobacter pylori* and extragastric disease. *Int. J. Hematol.* **84,** 291-300 (2006).

[3] Crowe S E, *Helicobacter infection*, chronic inflammation and the development of malignancy. *Curr. Opin. Gastroenterol.* **21,** 32-38 (2005).

[4] Thirumurthi S and Graham D Y, *Helicobacter pylori* infection in India from a western perspective. *Indian J. Med. Res.* **136,** 549-562 (2012).

[5] Yang H R, Ko J S and Seo J K, Does the diagnostic accuracy of the ^{13}C-urea breath test vary with age even after the application of urea hydrolysis rate? *Helicobacter* **13,** 239-244 (2008).

[6] Perry S, Parsonnet J and Commentry: *Helicobacter pylori* infection in early and the problem of imperfect tests. *Int. J. Epidemiol.* **34,** 1356-1358 (2005).

[7] Goddard A F and Logan R P H, Review article: urea breath tests for detecting *Helicobacter pylori*. *Aliment. Pharmacol. Ther.* **11,** 641-649 (1997).

[8] Gisbert J P and Pajares J M, Review article: ^{13}C-urea breath test in the diagnosis of *Helicobacter pylori* infection-a critical review. *Aliment. Pharmacol. Ther.* **20,** 1001-1017 (2004).

[9] Klein P D *et al.*, Normalizing results of ^{13}C-urea breath testing for CO_2 production rates in children. *J. Pediatr. Gastroenterol. Nutr.* **29,** 297-301 (1999).

[10] Savarino V, Vigneri S and Celle G, The ^{13}C-urea breath test in the diagnosis of *Helicobacter pylori* infection. *Gut* **45,** S18-122 (1999).

[11] Dominguez-Munoz J E *et al.*, A citric acid acid solution is an optimal test drink in the ^{13}C-urea breath test for the diagnosis of *Helicobacter pylori* infection. *Gut* **40,** 459-462 (1997).

[12] Pantoflickova D *et al.*, ^{13}C urea breath test (UBT) in the diagnosis of *Helicobacter pylori*; why does it work better with acid test meals? *Gut* **52,** 933-937 (2003).

[13] Scott D R *et al.*, The role of internal urease in acid resistance of *Helicobacter pylori*. *Gastroenterology* **114,** 58-70 (1998).

[14] Rektorschek M *et al.*, Influence of pH on metabolism and urease activity of *Helicobacter pylori*. *Gastroenterology* **115,** 628-641 (1998).

[15] Mifflin M D *et al.*, A new predictive equation for resting energy expenditure in healthy individuals. *Am. J. Clin. Nutr.* **51,** 241-247 (1990).

[16] Schofield W N, Predicting basal metabolic rate, new standards and review of previous work. *Hum. Nutr. Clin. Nutr.* **39,** S5-S41 (1985).

[17] Wu I C *et al.*, Metabolic analysis of ^{13}C-labeled pyruvate for noninvasive assessment of mitochondrial function. *Ann. N. Y. Acad. Sci.* **1201,** 111-120 (2010).

[18] Evenepoel P *et al.*, ^{13}C-egg white breath test: a non-invasive test of pancreatic trypsin activity in the small intestine. *Gut* **46,** 52-57 (2000).

[19] Akobeng A K, Understanding diagnostic tests 1: sensitivity, specificity and predictive values. *Acta. Paediatrica.* **96,** 338-341 (2006).

Chapter 4

Investigation of the role of carbon-13 and oxygen-18 isotopes of breath CO_2 in glucose metabolism of *Helicobacter pylori*

4.1 Introduction

Helicobacter pylori (*H. pylori*) is a micro-aerophilic pathogen, which is known to be able to colonize the mucosal surfaces of the human stomach, where it gives rise to chronic gastritis, peptic ulcers [1-3] and is closely linked to the development of certain types of gastric cancer [4]. The gastric pathogen *H. pylori* uses glucose as the primary energy substrate [5, 6], although the overall metabolism of *H. pylori* yet remains inadequately understood. Some early evidences, however, suggest that *H. pylori* has the ability to utilize glucose for metabolism through a glucokinase activity [7] and enzymes of the pentose phosphate and glycolysis pathways [8, 9]. Carbon dioxide (CO_2) is usually produced as a by-product of glucose catabolism which is then transported to the lungs through the bloodstream, and finally it is excreted in human breath. However, the precise role of glucose metabolism, especially in the pathogenesis of the *H. pylori* infection is not currently known. A new insight into the role of glucose metabolism is essential to elucidate the pathophysiology of *H. pylori* for its successful colonization of the gastrointestinal tract. However, to our knowledge, so far there have been no studies focused on glucose uptake for individuals harbouring *H. pylori* infections, exhibiting the time-dependent excretion dynamics of the metabolite CO_2 in exhaled breath. The purpose of this study was therefore, primarily to explore the potential links between breath CO_2 and *H. pylori* infections in response to unlabelled and labelled ^{13}C-enriched glucose metabolism. A complete understanding of glucose metabolism during the *H. pylori* infection could be of significance in the development of novel therapies for the micro-organism alongside new and better approaches for treating the most common human bacterial infection.

Furthermore, an earlier study revealed that the oxygen-16 (^{16}O) and the oxygen-18 (^{18}O) isotopes in $^{12}C^{16}O_2$ and water ($H_2{}^{18}O$), respectively, are rapidly interchanged during the human respiration process mediated by the metalloenzyme carbonic anhydrase (CA) [10, 11]. It is also known that *H. pylori* encodes two different forms of the metalloenzyme carbonic anhydrase (α-CA and β-CA) [12] and this gastric pathogen plays a vital role in inter-conversion of carbon dioxide and bicarbonate ($CO_2 + H_2O \leftrightarrow H^+ + HCO_3^-$), catalyzed by the CA activity [12-14]. This efficient activity suggests that investigations of breath $^{18}O/^{16}O$ isotopic fractionations of CO_2 may specifically track the gastric pathogen *H. pylori* and hence may introduce a novel non-invasive strategy in the diagnosis of *H. pylori* infections living in human stomach. As a consequence, we hypothesized that simultaneous monitoring the $^{18}O/^{16}O$ and $^{13}C/^{12}C$ stable isotope ratios of exhaled breath CO_2 associated with glucose metabolism in *H. pylori* may act as potential markers for the early detection of *H. pylori* infections or during the preclinical phase of the infections. In view of the fact that *H. pylori* is able to uptake and metabolize glucose confirmed as experimentally [15] and also by analysing the genome sequence [5] therefore, there is a pressing need to assess the clinical efficacy of the glucose utilization by *H. pylori* for large-scale screening individuals harbouring the micro-organism. In addition, unravelling the precise metabolic pathways involved in causing the isotopic fractionations of $^{12}C^{16}O^{16}O$, $^{13}C^{16}O^{16}O$ and $^{12}C^{18}O^{16}O$ in human breath during the glucose uptake by *H. pylori* remains a major challenge, whenever an individual is at-risk of developing the disease.

In this chapter, we explored the potential links of both ^{18}O and ^{13}C-stable isotopes of breath CO_2 with the gastric pathogen *H. pylori* in response to glucose ingestion. We investigated simultaneously the time-dependent excretion dynamics of the $^{12}C^{18}O^{16}O/^{12}C^{16}O^{16}O$ and $^{13}C^{16}O^{16}O/^{12}C^{16}O^{16}O$ isotope ratios of breath CO_2 from individuals with *H. pylori* positive and negative by employing a laser-based integrated cavity output spectroscopy (ICOS) method. We further explored the potential metabolic pathways underlying the glucose utilization in the pathogenesis of *H. pylori* infection and the mechanisms linking breath oxygen-18 and carbon-13 isotopic fractionations of CO_2 to the gastric pathogen *H. pylori.* Finally, we determined various diagnostic parameters such as optimal diagnostic cut-off values, diagnostic sensitivity and specificity of oxygen-18 and carbon-13 stable isotopes in breath CO_2

to gain a better insight into the diagnostic efficiency for the *non-invasive* detection of *H. pylori* infection in real-time.

4.2 Materials and Methods

4.2.1 Subjects

Two hundred and twenty four individuals (135 male and 89 female with average age of 39 ± 10 yrs (SD)) were enrolled for this study with different gastrointestinal disorders such as active peptic ulcer disease (PUD), chronic gastritis, and univestigated dyspepsia. We categorized all the human subjects in two distinct groups: infected with *H. pylori* (*H. pylori* positive patients: 124) and without the infection of *H. pylori* (*H. pylori* negative patients: 100) depending on the reports of gold standard invasive and non-invasive methods, i.e. endoscopy and biopsy based rapid urease test (RUT) and ^{13}C-urea breath test (^{13}C-UBT).The ^{13}C-UBT was considered to be indicative of *H. pylori* positive when $\delta_{DOB}{}^{13}C$ (‰) ≥ 3‰ [16-18]. There were no mismatches between the two test-reports of all the subjects enrolled in this study. Exclusion criteria included patients with previous history of diabetes and gastric surgery, taking antibiotics, proton pump inhibitors or H_2 receptor antagonists in the four week prior to endoscopy and ^{13}C-UBT. We received the Ethical approval from the Ethics Committee Review Board of AMRI Hospital, Salt Lake, Kolkata, India (Study no.: AMRI/ETHICS/2013/1). The current protocol has also been approved by the institutional administrative of S. N. Bose Centre, Kolkata, India (Ref. no.: SNB/PER-2-6001/13-14/1769) and the methods were carried out in accordance with the approved guidelines. Informed written consents were taken from all patients participating in this study.

4.2.2 Breath samples collection and measurements

All the human subjects enrolled for the study completed their endoscopic examinations and ^{13}C-UBTs, 1-2 days prior to glucose breath test (GBT). On the study day before GBT, all the patients were instructed for their mouth-washing to

prevent any kind of contact of ingested test meal with the oral cavity bacteria. After an overnight fasting (10-12 hours), an initial baseline breath sample was collected in a 750 ml breath collection bag (QUINTRON, USA, SL No.QT00892) from each subject. After that a test meal of 75mg U-$^{13}C_6$ labelled D-glucose (CIL-CLM-1396-CTM, Cambridge Isotope Laboratories, Inc. USA) or 75 mg unlabeled glucose dissolved in 50 ml water was orally administered to the patient and then subsequent breath samples were collected at 15 minute intervals up to 120 minute. The physical activities of the subjects were restricted inside a room during the test. For the measurements of $^{18}O/^{16}O$ and $^{13}C/^{12}C$ isotope ratios of exhaled breath CO_2, a laser-based high-precision ICOS system was employed.

4.3 Results and Discussion

To investigate the ^{18}O and ^{13}C isotopic fractionations of breath CO_2, we first studied the time-dependent excretion dynamics of both isotopes in exhaled breath after ingestion of an oral dose of ^{13}C-enriched glucose for *H. pylori* positive (n=72) and negative (n=55) individuals, using a laser-based high-precision cavity-enhanced integrated cavity output spectrometer (ICOS). We explored the isotopic fractionation of CO_2 by simultaneous monitoring the $^{18}O/^{16}O$ and $^{13}C/^{12}C$ stable isotope ratios in breath, expressed as delta-over-baseline (DOB) relative to the Vienna Pee Dee Belemnite standard, i.e., $\delta_{DOB}{}^{18}O‰ = [(\delta^{18}O‰)_{t=t} - (\delta^{18}O‰)_{t=basal}]$ and $\delta_{DOB}{}^{13}C‰ = [(\delta^{13}C‰)_{t=t} - (\delta^{13}C‰)_{t=basal}]$, respectively, associated with glucose metabolism.

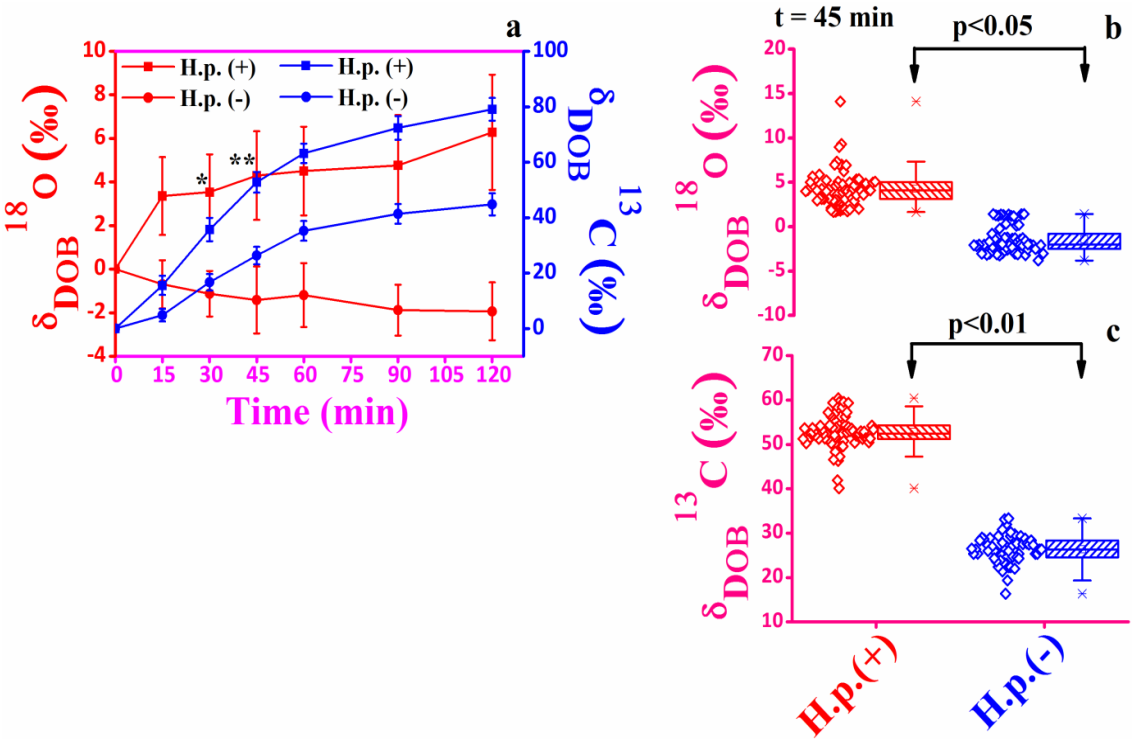

Figure 1. *Comparisons of $\delta_{DOB}{}^{18}O‰$ and $\delta_{DOB}{}^{13}C‰$ values of exhaled breath CO_2 associated with ^{13}C-labelled glucose metabolism in presence [H. p. (+)] and absence [H. p. (-)] of H. pylori infection.* ***a,*** *Excretion kinetics of $\delta_{DOB}{}^{18}O‰$ and $\delta_{DOB}{}^{13}C‰$ values for H. pylori positive [H. p. (+)] and H. pylori negative [H. p. (-)] individuals up to 120 minutes.* ***b,c,*** *The Box-Whisker plots demonstrating a statistically significant differences of $\delta_{DOB}{}^{18}O‰$ [$p< 0.05$] and $\delta_{DOB}{}^{13}C‰$ [$p<0.01$] values at 45 minutes between H. pylori positive [H. p. (+)] and H. pylori negative [H. p. (-)] individuals. *$p<0.05$ and **$p<0.01$. Data are means ± SE.*

In this investigation (Fig. 1a), individuals with *H. pylori* positive exhibited significantly higher isotopic enrichments of ^{18}O in CO_2 compared with *H. pylori* negative during the 2h-glucose metabolism, while no significant enrichments of ^{18}O in CO_2 were manifested in individuals without *H. pylori* infections. These findings suggest a potential link between *H. pylori* infections in human stomach and the ^{18}O-isotopic fractionations in exhaled breath and hence may open a new route for the non-invasive assessment of *H. pylori* infections. Carbonic anhydrase (CA) activity of *H. pylori* has previously been proposed to interchange the oxygen isotopes of CO_2 (^{16}O) and H_2O (^{18}O) efficiently [10, 11], suggesting that in our observations CA activity may play an important role in oxygen-isotope fractionations of breath CO_2 in the glucose-mediated bacterial environment. Hence a statistically significant difference in

the $\delta_{DOB}{}^{18}O‰$ values in excretion dynamics established a marked distinction (Fig. 1b) between *H. pylori* infected and non-infected individuals. Taken together, these findings indicate that the monitoring of ^{18}O-exchange between $C^{16}O_2$ and $H_2{}^{18}O$ in response to CA activity may distinctively track the development of the gastric pathogen in human stomach and might be considered as a potential biomarker for the non-invasive detection of *H. pylori* infection.

We then critically assessed the excretion dynamics of $\delta_{DOB}{}^{13}C$ (‰) (Fig. 1a) values in exhaled breath samples in response to ^{13}C-enriched glucose ingestion. The isotopic enrichments of ^{13}C in breath CO_2 were significantly higher (Fig. 1c) in individuals with *H. pylori* positive compared with individuals with *H. pylori* negative. It was noticed that for *H. pylori* positive patients the $\delta_{DOB}{}^{13}C$ (‰) values increased gradually with time at a faster rate in comparison with individuals without *H. pylori* infections. Several lines of evidence suggest that *H. pylori* can metabolize glucose in both oxidative and fermentative pathways [8, 9] and as a consequence the catabolism of glucose resulted in higher isotopic enrichments of ^{13}C in exhaled breath CO_2. Moreover, in some early evidences [9, 19], it was demonstrated the biphasic characteristics of glucose utilization by *H. pylori* with a slower initial period, followed by a second phase with a higher rate of glucose uptake. The transport and utilization of glucose was previously investigated into the intact micro-organism employing the radioactive tracer analysis. Therefore, the gradual increase of the $\delta_{DOB}{}^{13}C$ (‰) values in the time-dependent excretion dynamics is possibly attributed to the increased rate of glucose utilization through the biphasic activity of the micro-organism. Hence our results of the $\delta_{DOB}{}^{13}C$ (‰) values in exhaled breath are coincidence with the previous study [19], where the uptake of glucose into *H. pylori* cells exhibited the biphasic patterns. Our observations therefore, point to new perspectives into the physiology of *H. pylori* underlying the isotopic fractionations of ^{13}C in breath CO_2 associated with glucose metabolism.

We next explored how the time-dependent excretion dynamics of isotopic breath CO_2 changes after administration of unlabelled glucose (i.e. with no ^{13}C-enriched glucose), as the potential role of glucose metabolism in response to unlabelled glucose ingestion for individuals with *H. pylori* infection and the possible links underlying the ^{18}O and ^{13}C-isotopic fractionations of breath CO_2 remains unknown.

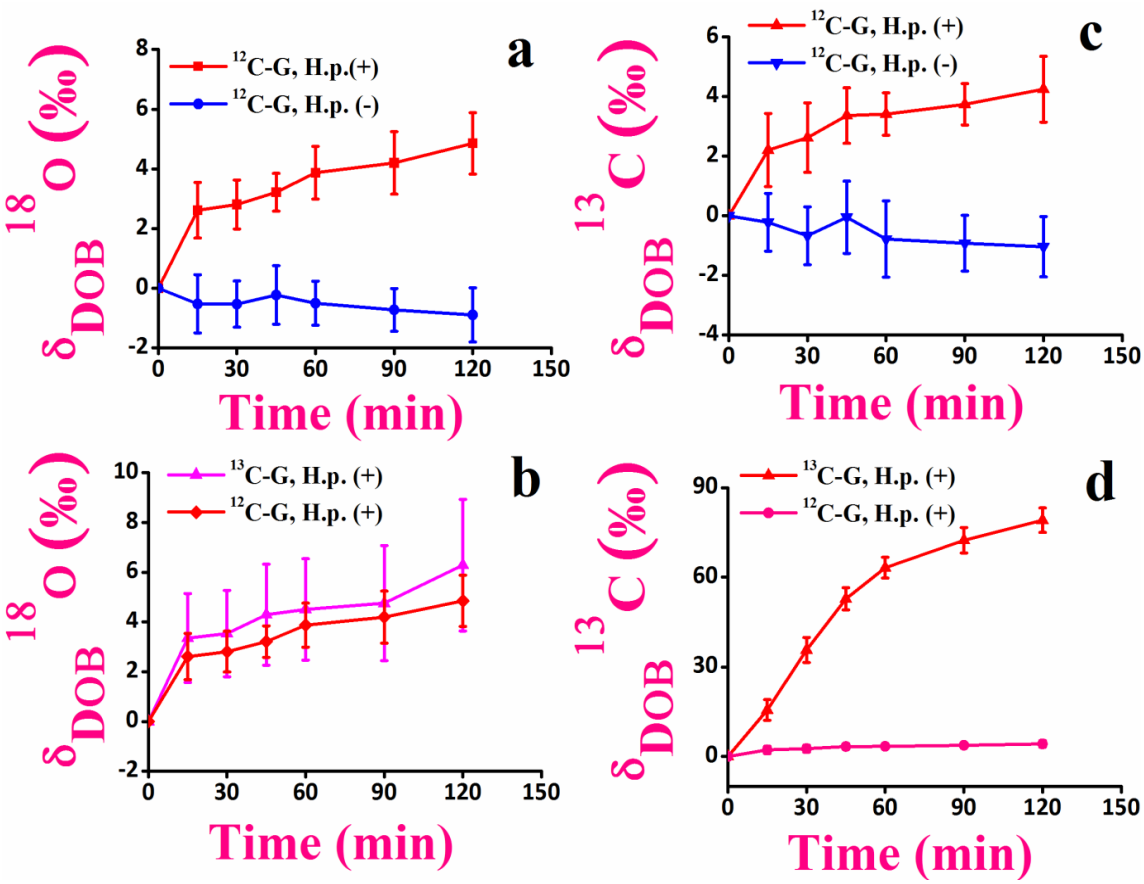

Figure 2. *Excretion kinetics of $\delta_{DOB}{}^{18}O$‰ and $\delta_{DOB}{}^{13}C$‰ values of exhaled breath CO_2 during unlabelled glucose (^{12}C-G) metabolism of H. pylori positive [H. p. (+)] and H. pylori negative [H. p. (-)] individuals.* ***a,*** *The excretion kinetics illustrating the increased $\delta_{DOB}{}^{18}O$‰ values for H. pylori positive [H. p. (+)] patients.* ***b,*** *depicts the similar excretion kinetics of $\delta_{DOB}{}^{18}O$‰ values with that of ^{13}C-enriched glucose.* ***c,d,*** *enhancement of $\delta_{DOB}{}^{13}C$‰ values for H. pylori positive [H. p. (+)] patients and comparisons with the ^{13}C-enriched glucose. Values are means ± SE.*

To investigate this, we performed the 2-h excretion kinetics of $\delta_{DOB}{}^{18}O$‰ and $\delta_{DOB}{}^{13}C$‰ values simultaneously in breath samples for a number of 52 *H. pylori* infected and 45 non-infected individuals. When the unlabelled glucose was orally administered in positive *H. pylori* patients, the post-dose $\delta_{DOB}{}^{18}O$‰ values in breath samples manifested a significant change with time and depicted the similar excretion kinetics with that of ^{13}C-enriched glucose (Fig. 2a and 2b), whereas no significant change of the post-dose $\delta_{DOB}{}^{18}O$‰ values in breath samples over time was evident for *H. pylori* negative individuals (Fig. 2a). These findings suggest that the mechanisms i.e. oxidation of glucose in the bacterial environment to form bicarbonate (HCO_3^-) and

subsequently the enzyme carbonic anhydrase-mediated rapid inter-conversion of HCO_3^- and CO_2, leading to the generation of $^{12}C^{16}O^{18}O$, exclusively depends on the substrate (glucose) regardless of its isotopic nature. Interestingly, although the isotopic nature of the substrate is vital to observe effectively the ^{13}C-isotopic enrichments of breath CO_2 (i.e. enhancement of $\delta_{DOB}{}^{13}C‰$ values), yet the enrichments of $\delta_{DOB}{}^{13}C‰$ values, due to natural abundances of ^{13}C, during glucose metabolism of *H. pylori* are significantly distinguishable for *H. pylori* positive patients (Fig. 2c and 2d), suggesting a new step towards characterizing the transport and utilization of unlabelled glucose into the human pathogen for better understanding of its physiology in the gastric niche.

Table 1 *The summary of the detailed characteristics of the study subjects for H. pylori infected and non-infected groups. UBT and GBT correspond to the urea breath test and glucose breath test respectively***.**

Parameters	***H. pylori* infected (mean ± SD)**	***H. pylori* non-infected (mean ± SD)**	**p Value**
AGE	38.91 ± 10.43	39.19 ± 9.68	0.73
HbA1c	5.13 ±0.12	5.1 ± 0.1	0.07
^{13}C-UBT (30 min)	18.12± 12.93	0.67± 0.64	< 0.001
^{13}C-GBT (45 min) $\delta_{DOB}{}^{13}C‰$	52.70 ± 3.71	26.34± 3.16	< 0.001
$\delta_{DOB}{}^{18}O‰$	4.29± 2.03	-1.41±1.53	< 0.01
^{12}C-GBT (45 min) $\delta_{DOB}{}^{13}C‰$	3.36±0.93	-0.04±1.21	<0.01
$\delta_{DOB}{}^{18}O‰$	3.11±0.63	-0.22±0.97	<0.01

In view of the breath results, we have also established the previous hypothesis [12] that the bacterium requires high CO_2 for growth and the interconversion of ^{18}O ($H_2{}^{18}O$) and ^{16}O ($C^{16}O_2$) is vital, catalyzed by the enzyme carbonic anhydrase activity (α-CA and β-CA) of *H. pylori* and thus this activity might be a contributing factor for the development of the disease in the gastric environment. The summary of the detailed results has been provided in the Table 1.

To distinctively track the *H. pylori* infection as well as for early detection prior to the onset of different gastric diseases, we subsequently determined numerous statistically sound optimal diagnostic cut-off points of $\delta_{DOB}{}^{18}O‰$ and $\delta_{DOB}{}^{13}C‰$ values in exhaled breath associated with ^{13}C-labelled and unlabelled glucose metabolism, using receiver operating characteristics curve (ROC) analysis (Fig. 3).

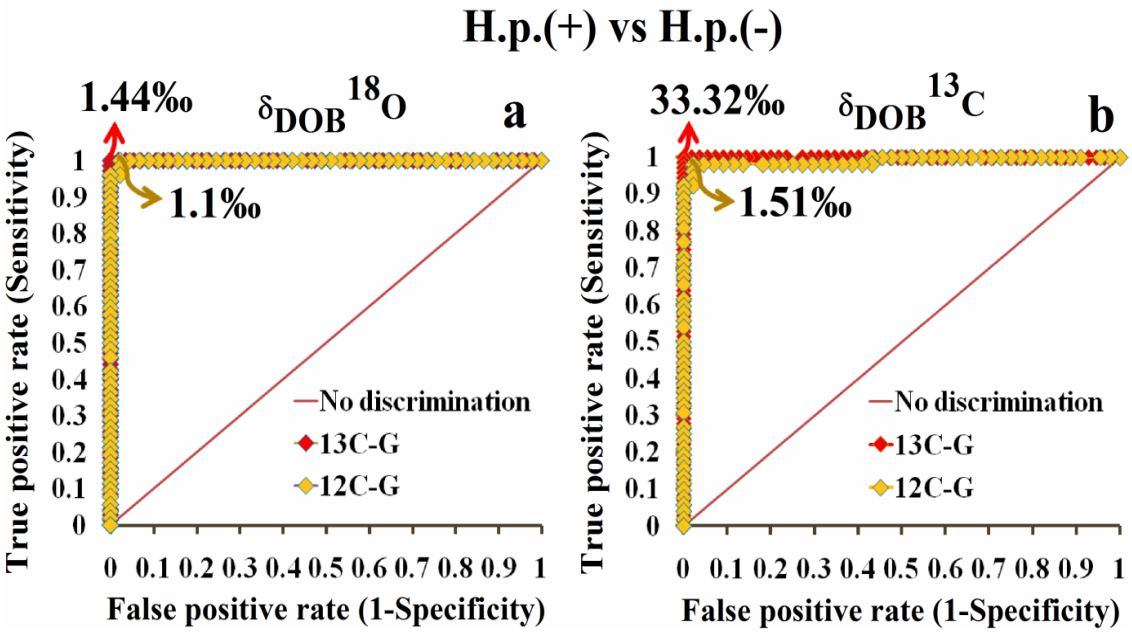

Figure 3. *Receiver operating characteristic (ROC) curves analysis for the optimal diagnostic cut-off points of H. pylori infection.* ***a,*** *$\delta_{DOB}{}^{18}O$ values ≥ 1.44‰ and 1.1‰ are indicative of the H. pylori infection associated with ^{13}C-labelled and unlabelled glucose metabolism at 45 minute, respectively, whereas* ***b,*** *$\delta_{DOB}{}^{13}C$ values ≥ 33.21‰ and 1.51‰ indicate the same for ^{13}C-labelled and unlabelled glucose metabolism, respectively.*

Individuals with $\delta_{DOB}{}^{18}O‰ \geq 1.44$ ‰ and $\delta_{DOB}{}^{18}O‰ \geq 1.1$ ‰ were considered to be *H. pylori* positive with and without ^{13}C-enriched glucose metabolism respectively, and these corresponded to the diagnostic sensitivity and specificity of 100% and ~ 98%, respectively. On the contrary, a different optimal diagnostic cut-off point of $\delta_{DOB}{}^{13}C‰ \geq 33.32‰$ between individuals with *H. pylori* positive and negative, demonstrated the sensitivity and specificity of 100% and 100%, respectively, when ^{13}C-labelled glucose is ingested, whereas without ^{13}C-labelled glucose, $\delta_{DOB}{}^{13}C‰ \geq$ 1.51‰ precisely diagnosed the infected and non-infected persons corresponding to the

similar levels of diagnostic sensitivity (100%) and specificity (98%). It is noteworthy to mention that the uncertainty of these cut-off values is associated with the less-sensitive techniques for isotope measurements and the variation of isotopic fractionations in the test meal. However, these findings suggest that the oxygen-18 and carbon-13 isotopic fractionations of the major metabolite CO_2 in human breath linked to glucose metabolism of *H. pylori* provide a new non-invasive approach to treat the world's most common chronic bacterial infection of humans and hence may have a broad clinical efficacy for precise assessment of the gastric pathogen *H. pylori.*

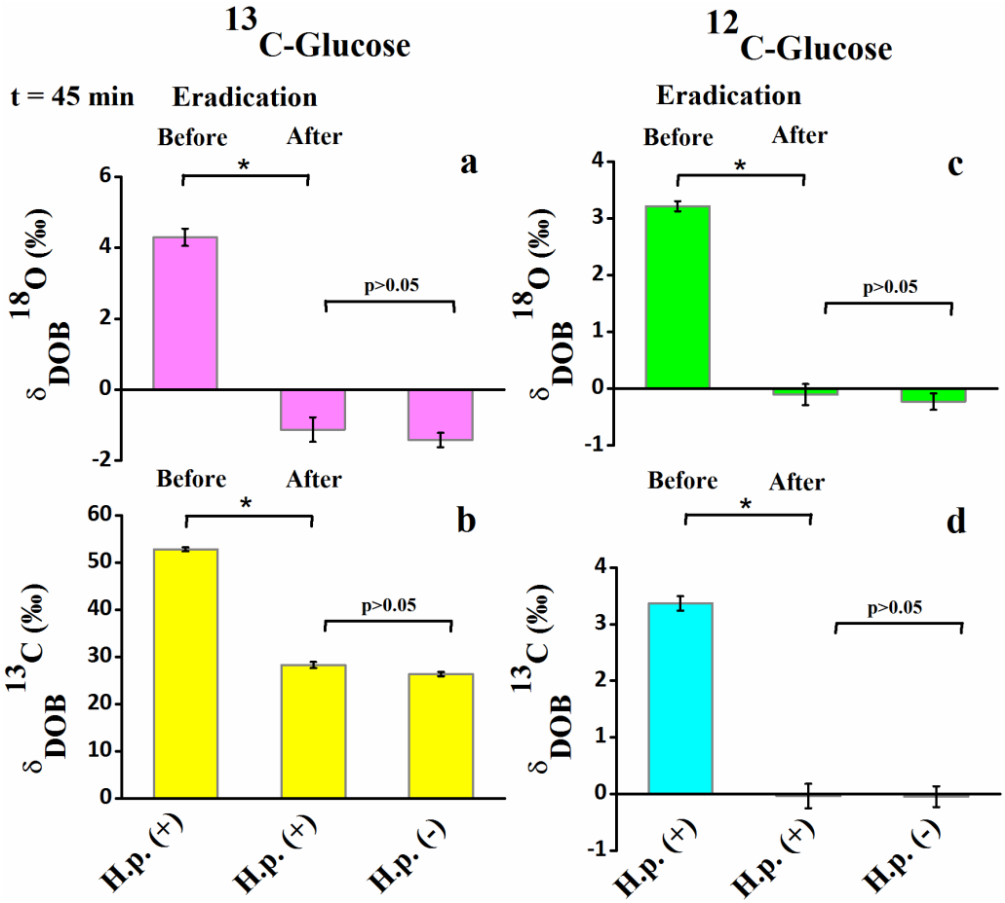

Figure 4. *Glucose breath test in response to the standard eradication therapies of the H. pylori infection.* ***a,b,c,d*** *depicted marked distinction (*p<0.01) for the* $\delta_{DOB}{}^{18}O$ *and* $\delta_{DOB}{}^{13}C$ *values at 45 minute was observed before and after the therapies in case of both* ^{13}*C-glucose and* ^{12}*C-glucose ingestion.*

We next explored the efficacy of the glucose breath test in response to the standard eradication therapies of the infection. A marked depletions of both $\delta_{DOB}{}^{18}O‰$ and $\delta_{DOB}{}^{13}C‰$ values for *H. pylori* infected patients (n=37 for ^{13}C-glucose and n=28 for

^{12}C-glucose) (Fig. 4) after complete eradication of the infection were manifested, suggesting the widespread clinical significance of the glucose breath test. Our findings associated with the glucose metabolism by *H. pylori* infections thus point towards a considerable clinical advancement in the non-invasive diagnosis of *H. pylori* infection by contrast with the currently available ^{13}C-urea breath test (^{13}C-UBT), where ^{13}C-enriched substrate (urea) is usually used. In view of this result, we therefore posit that the glucose breath test by ingestion of a natural substrate (unlabelled glucose) is a valid and potentially robust new-generation diagnostic tool and thus indicate great promise for comparatively less-expensive and non-toxic global technique, in comparison with the ^{13}C-UBT, for the non-invasive assessment i.e. early detection and follow-up of patients after eradication of *H. pylori* infection.

Finally, we elucidated the potential metabolic pathways (Fig. 5) underlying the mechanisms linking isotopic fractionations of breath CO_2 and glucose utilization by *H. pylori* infection. When a dose of glucose is orally administered to the patients, the ingested glucose disposal takes place in the cytoplasm of *H. pylori* through the HP1174 transporter (protein) [7]. After glucose enters into the cytoplasm, it is phosphorylated to produce glucose-6-phosphate which subsequently incorporated with three potential metabolic routes: glycolysis, pentose phosphate and the Entner-Doudoroff pathway [20, 21]. A part of the total glucose-6-phosphate, which goes into the pentose phosphate pathway, is predominantly oxidised into CO_2. The remaining part of glucose-6-phosphate enters into the other two metabolic pathways and may lead to the generation of pyruvate [20] and eventually gives rise to CO_2 followed by the formation of acetate as the key metabolite through the intermediary oxidative and

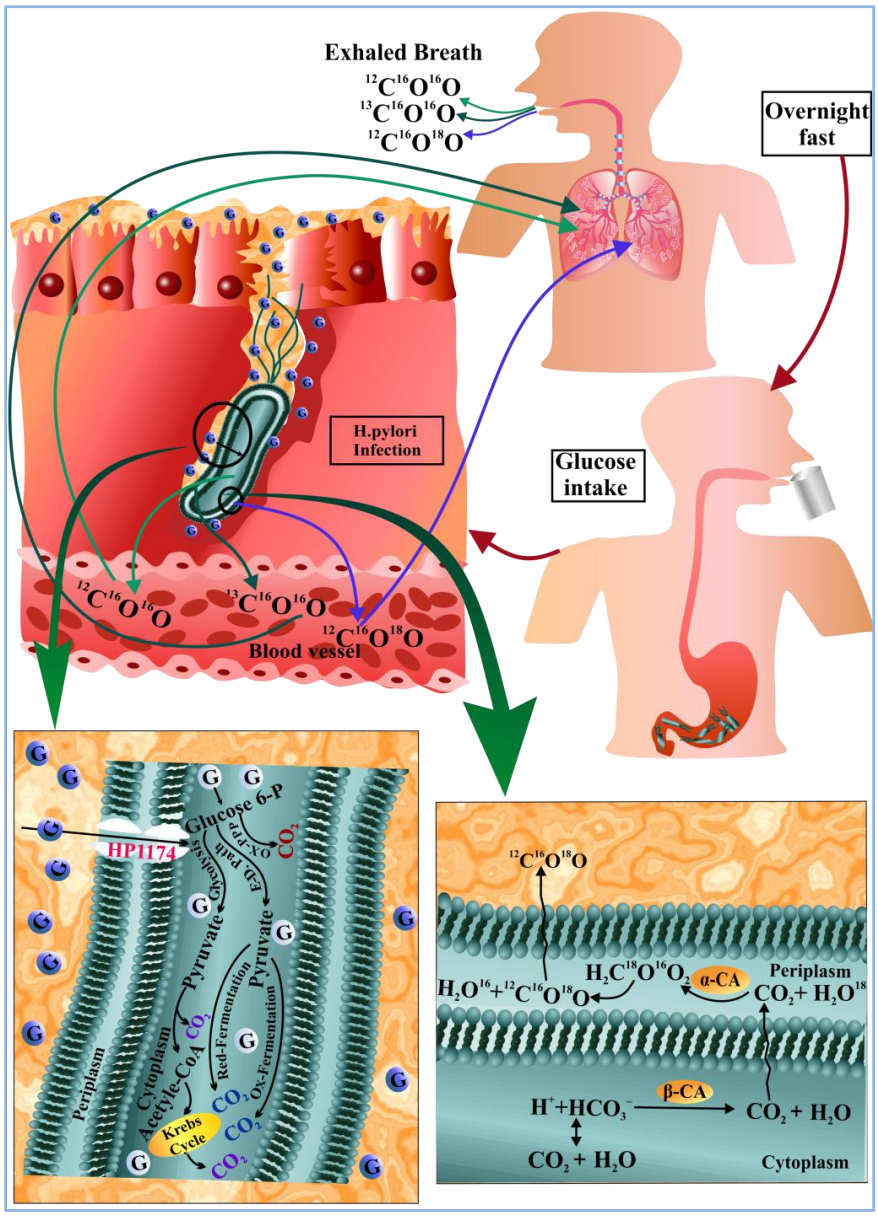

Figure 5. *Potential metabolic pathways for ^{13}C and ^{18}O-isotopic exchanges associated with glucose metabolism by H. pylori infection. The ingested glucose in the cytoplasm of H. pylori through the HP1174 transporter is phosphorylated to produce glucose-6-phosphate which subsequently incorporated with three potential metabolic routes: glycolysis, pentose phosphate and the Entner-Doudoroff pathway to finally produce major metabolite CO_2.This major metabolite CO_2 is then transported through the blood streams and eventually excreted as $^{13}C^{16}O^{16}O$ and $^{12}C^{16}O^{16}O$ in exhaled breath. Conversely, the major metabolite CO_2 diffuses rapidly through the inner member into the periplasm of H. pylori, where it forms carbonic acid (H_2CO_3), catalyzed by the α-CA. The isotopic exchange between ^{16}O of $^{12}C^{16}O_2$ and ^{18}O of $H_2{}^{18}O$ in response to periplasmic α-CA activity leads to the generation of $^{12}C^{18}O^{16}O$, which is then transported to the lungs and is excreted through exhaled breath.*

reductive fermentation pathways [9]. Another fate for pyruvate is the conversion of acetyl-CoA, which afterwards enters into the *Krebs cycle* and generates CO_2 as a by-product [21]. Therefore, the administration of ^{13}C-glucose (either from ^{13}C-enriched exogenous glucose or naturally abundant ^{13}C-glucose) facilitates the production of $^{13}CO_2$ in the by-product CO_2 in presence of *H. pylori* infection. Thereafter, the major metabolite CO_2 ($^{13}CO_2$ and $^{12}CO_2$) produced by all these metabolic processes is then transported through the blood streams and eventually excreted as $^{13}C^{16}O^{16}O$ and $^{12}C^{16}O^{16}O$ in exhaled breath. Conversely, the cytoplasmic β-carbonic anhydrase (β-CA) activity of *H. pylori* catalyzes the reversible interconversion between the major metabolite CO_2 and HCO_3^- ($CO_2 + H_2O \leftrightarrow H^+ + HCO_3^-$).Then the CO_2 diffuses rapidly through the inner member into the periplasm of *H. pylori*, where it forms carbonic acid (H_2CO_3), catalyzed by the α-CA. Because the isotopes ^{16}O of $^{12}C^{16}O_2$ and ^{18}O of $H_2{}^{18}O$ are rapidly exchanged in response to periplasmic α-CA activity, it therefore leads to the generation of $H_2C^{18}O^{16}O_2$. This carbonic acid rapidly degasses to produce $^{12}C^{18}O^{16}O$, which is then transported to the lungs and is excreted through exhaled breath. As a result, individuals with *H. pylori* infections exhibit the preferential isotopic enrichments of ^{18}O in breath CO_2, whereas no significant change of ^{18}O in CO_2 was manifested in *H. pylori*-uninfected individuals.

4.4 Conclusions

In conclusion, our new findings point to a fundamental mechanism underlying both the ^{18}O and ^{13}C stable isotopic fractionations of the major metabolite CO_2 in human breath related to glucose metabolism of *H. pylori* infection in humans. Subsequently, we have taken a step towards unravelling the potential metabolic pathways linking the ^{18}O and ^{13}C-isotopic exchange of breath CO_2 and the glucose uptake by *H. pylori*, thus suggesting that breath $^{12}C^{18}O^{16}O$ and $^{13}C^{16}O^{16}O$ in response to glucose ingestion could be used as potential molecular biomarkers to distinctively track the pathogenesis of *H. pylori* infection in a non-invasive approach. Although many imperative gaps remain in our understanding of these processes and in the pathophysiology underlying the isotopic exchange and glucose metabolism, our studies may provide new perspectives in the isotope-specific molecular diagnosis of *H. pylori* infection and hence may pave the way for broad clinical applications along

with eradication purposes following standard therapies. Furthermore, new insight into the mechanism linking the isotopic exchange in breath molecule CO_2 to glucose metabolism of *H. pylori* is fostering exploration of the molecular basis of this infection and new and better approaches together with new pharmacological targets to prevent or treat the deleterious effects of the world's most common gastric pathogen.

4.5 References

[1] Covacci A *et al.*, *Helicobacter pylori* virulence and genetic geography. *Science* **284,** 1328-1333(1999).

[2] El-omar E M *et al.,* Interleukin-1 polymorphisms associated with increased risk of gastric cancer. *Nature* **404**, 398-402 (2000).

[3] Som S *et al.,* Excretion kinetics of ^{13}C-urea breath test: influences of endogenous CO_2 production and dose recovery on the diagnostic accuracy of *Helicobacter pylori* infection. *Anal. Bioanal. Chem.* **406,** 5405-5412 (2014).

[4] Polk D B and Peek R M, *Helicobacter pylori*: gastric cancer and beyond. *Nat. Rev. Cancer* **10,** 403-414 (2010).

[5] Tomb J-F *et al*., The complete genome sequence of the gastric pathogen *Helicobacter pylori*. *Nature* **388,** 539-547 (1997).

[6] Park S A, Ko A and Lee N G, Simulation of growth of the human gastric pathogen *Helicobacter pylori* by atmospheric level of oxygen under high carbon dioxide tension. *BMC Microbiol.* **11,** 96 (2011).

[7] Psakis G *et al*., The sodium-dependent D-glucose transport protein of *Helicobacter pylori*. *Mol. Microbiol.* **71,** 391-403 (2009).

[8] Marais A *et al.*, Metabolism and genetics of *Helicobacter pylori*: the genome era. *Microbiol. Mol. Biol. R.* **63,** 642-674 (1999).

[9] Chalk P A, Roberts A D and Blows W M, Metabolism of pyruvate and glucose by intact cells of *Helicobacter pylori* studied by ^{13}C NMR spectroscopy. *Microbiology* **140,** 2085-2092 (1994).

[10] Epstein S and Zeiri L, Oxygen and carbon isotopic compositions of gases respired by humans, *Proc. Natl. Acad. Sci. USA*. **85,** 1727-1731 (1988).

[11] Ghosh C *et al.,* Oxygen-18 isotope of breath CO_2 linking to erythrocytes carbonic anhydrase activity: a biomarker for pre-diabetes and type 2 diabetes. *Sci. Rep.* **5,** 8137 (2015).

[12] Chirica L C *et al.*, Expression and localization of α- and β-carbonic anhydrase in *Helicobacter pylori*. *Biochim. Biophys. Acta*. **1601,** 192-199 (2002).

[13] Marcus E A *et al.*, The periplasmic α-carbonic anhydrase activity of *Helicobacter pylori* is essential for acid acclimation. *J. Bacteriol*. **187,** 729-738 (2005).

[14] Maity A *et al*, Oxygen-18 stable isotope of exhaled breath CO_2 as a non-invasive marker of Helicobacter pylori infection. *J. Anal. At. Spectrom.* **29,** 2251-2255 (2014).

[15] Mendz G L, Burns B P and Hazell S L, Characterisation of glucose transport in *Helicobacter pylori*. *Biochim. Biophys. Acta*. **1244,** 269-276 (1995).

[16] Goddard A F and Logan R P H, Review article: urea breath tests for detecting *Helicobacter pylori*. *Aliment. Pharmacol. Ther.* **11,** 641-649 (1997).

[17] Gisbert J P and Pajares J M, Review article: ^{13}C-urea breath test in the diagnosis of *Helicobacter pylori* infection-a critical review. *Aliment. Pharmacol. Ther.* **20,** 1001-1017 (2004).

[18] Maity A *et al.*, Residual gas analyzer mass spectrometry for human breath analysis: a new tool for the non-invasive diagnosis of *Helicobacter pylori* infection. *J. Breath Res.* **8,** 016005 (2014).

[19] Mendz G L, Hazell S L and Burns B P, Glucose utilization and lactate production by *Helicobacter Pylori. J. Gen. Microbiol*. **139,** 3023-3028 (1993).

[20] Mendz G L, Hazell S L and Burns B P, The Entner-Doudoroff pathway in *Helicobacter pylori*. *Arch. Biochem. Biophys*. **312**, 349-356 (1994).

[21] Pitson S M *et al.*, The tricarboxylic acid cycle of *Helicobacter Pylori. Eur. J. Biochem*. **260,** 258-267 (1999).

Chapter 5

Investigation of ^{13}C and ^{18}O isotopic fractionation of breath CO_2: Potential markers for simultaneous diagnosis of *Helicobacter pylori* infection and type 2 diabetes

5.1 Introduction

As described in chapter 4, that *Helicobacter pylori*, the most common bacterial pathogen in human stomach, causes a wide variety of gastrointestinal disorders including gastritis, peptic ulcer disease, non-ulcer dyspepsia, gastric cancer and mucosa-associated lymphoid tissue lymphoma [1-3]. Over the past decade, several lines of evidence suggested that the effects of *H. pylori* infection may not only be confined to the gastrointestinal tract but can also be associated with several other extragastric diseases such as idiopathic thrombocytophenic purpurae (ITP), cardiovascular disease, anemia, diabetes mellitus and insulin resistance [4-6]. Early studies demonstrated that the prevalence of *H. pylori* infection is much higher in type 2 diabetes (T2D) patients compared to non-diabetic controls, where T2D is the most common metabolic disorder that is characterized by high levels of blood glucose resulting from insulin resistance and pancreatic β-cell dysfunction [7, 8]. However, in contrast, some epidemiological studies also implicated that individuals with T2D have higher risk of developing *H. pylori* infection [9, 10]. Therefore, a growing body of evidence suggests that there is a potential link between *H. pylori* infection and T2D but it still remains controversial [6, 11] and the underlying mechanism in the pathogenesis of *H. pylori* infection in subjects with T2D is still unclear.

However, genome-wide sequence data suggest that *H. pylori* utilize glucose as the primary energy source and metabolize it both in oxidative and fermentative pathways [12]. Carbon dioxide (CO_2) is produced as a major by-product of glucose catabolism, which is then transported through the bloodstream to the lungs, and afterwards it is excreted in exhaled breath. Accumulating evidences indicate that during colonization *H. pylori* plays a vital role in glucose homeostasis through regulation of gastric

hormones and has ability to alter the glucose metabolism by inducing chronic inflammation, which further leads to the development of T2D [6, 13]. However, to our knowledge, no studies have focused till date on glucose metabolism for the assessment of potential relationship between *H. pylori* and T2D. Therefore, the primary aim of the present study was to unravel such relationship by monitoring isotopic breath $^{13}CO_2$ in response to ^{13}C-enriched glucose metabolism, which may directly contribute for the early detection of *H. pylori* infection and its complicacies prior to the onset of T2D.

Furthermore, recent evidences suggest that oxygen-18 (^{18}O) isotopes of body water ($H_2{}^{18}O$) and oxygen-16 (^{16}O) isotopes of $^{12}C^{16}O_2$ are rapidly interchanged during the respiration process catalyzed by the enzymatic activity of carbonic anhydrase (CA), a ubiquitous metalloenzyme present in human body as well as in *H. pylori* [14]. It is also noteworthy that alteration of glucose metabolism is strongly associated with changes of CA activity in patients with T2D [15-17]. All these activities therefore suggest that simultaneous monitoring of $^{18}O/^{16}O$ and $^{13}C/^{12}C$ isotope ratios of breath CO_2 associated with glucose metabolism may potentially be linked with *H. pylori* infection and T2D and thus might act as potential markers for non-invasive assessment of *H. pylori* infection in complication with T2D without any endoscopic biopsy tests and blood sample measurements. However, there have been so far no direct experimental evidences to support this concept and therefore it still remains a tantalizing but unproven hypothesis. Therefore, another aim of the present study was therefore to explore a new non-invasive methodology, which can precisely diagnose the *H. pylori* infection in subjects with T2D. This may have a huge impact not only in early diagnosis of *H. pylori*-induced T2D patients, but also the precise transition from non-diabetic controls to T2D subjects infected with this gastric pathogen.

In this chapter, we investigated the potential link between *H. pylori* infection and type 2 diabetes by exploiting isotopic fractionations of carbon-13 (^{13}C) and oxygen-18 (^{18}O) in human breath in response to ^{13}C-enriched glucose metabolism. Using a laser-based high-precision integrated cavity output spectroscopy (ICOS) technique, we have investigated the excretion kinetics of ^{18}O and ^{13}C isotopes of breath CO_2 in individuals with T2D or non-diabetic controls harbouring *H. pylori* infection. Finally, we determined numerous diagnostic parameters such as optical diagnostic cut-off

values of breath $^{12}C^{18}O^{16}O$ and $^{13}C^{16}O^{16}O$, diagnostic sensitivity and specificity levels to gain a better insight into the diagnostic efficacy of the present methodology.

5.2 Material and Methods

5.2.1 Subjects

In the present study, we enrolled 131 individuals [n= 73 male and n= 58 female, average age: 48±15 yrs] with different gastrointestinal disorders such as chronic gastritis, dyspepsia, peptic ulcer disease. The subjects were classified into three distinct groups: *H. pylori* positive with type 2 diabetes [Hp(+)T2D(+), n=37], *H. pylori* positive without type 2 diabetes [Hp(+)T2D(-), n=51] and *H. pylori* negative without type 2 diabetes [Hp(-)T2D(-), n=43] depending on both gold standard invasive and non-invasive methods i.e. endoscopy, biopsy-based rapid urease test (RUT) and ^{13}C-urea breath test (^{13}C-UBT). The ^{13}C-UBT indicates individuals with positive *H. pylori* infection with $\delta_{DOB}{}^{13}C$ (‰) ≥ 3‰ at 30 min [3]. Moreover, we also categorized diabetic and non-diabetic subjects in accordance to the standard outlines of American Diabetic Association (ADA) [18]. Individuals with T2D were determined with gycosylated hemoglobin (HbA1C%) ≥ 6.5% and 2h-oral glucose tolerance test (2h-OGTT) ≥ 200 $mgdL^{-1}$, whereas individuals with HbA1C% < 5.7% and 2h-OGTT < 140 $mgdL^{-1}$ were considered as non-diabetic controls. All the clinical parameters deipted in the following Table 1.

Table 1*: Clinical characteristics of the subjects (data expressed as mean ± SD). p< 0.05 indicates a statistically significant difference.*

Parameter	Hp(-)T2D(-)	Hp(+)T2D(-)	Hp(+)T2D(+)	*p* value
No. of Subjects	43	51	37	
Age (years)	47±10	46±7	50±9.5	>0.05
Weight	61±7.6	62±7.1	65±8.3	>0.05
Fasting blood glucose ($mgdL^{-1}$)	97±10.1	101±6.4	159±11.4	<0.05
2h-post dose blood glucose ($mgdL^{-1}$)	117±14.1	120±10.7	211±31.3	<0.05
HbA1C(%)	5.24±0.14	5.31±0.28	10.7±1.1	<0.05

Subjects were excluded from the study if they had any previous history of gastric surgery, hypertension, asthma, anemia, smoking and alcohol consumption. Moreover, subjects taking any medication that may alter the glucose metabolism, proton pump inhibitors or H_2 receptor antagonists in four week prior to endoscopy and ^{13}C-UBT were also excluded from the present study. Current study was performed in accordance with approved guidelines by the Ethical Committee Review Board of AMRI Hospital, Salt Lake, Kolkata, India (Study no.: AMRI/ETHICS/2013/1). The study was also approved by the administration of S. N. National Centre, Kolkata, India (Ref. no.: SNB/PER-2-6001/13-14/1769). Informed written consents were taken from all the subjects prior to breath test.

5.2.2 Breath Sample Collection

All the subjects completed their endoscopic examination and ^{13}C-UBT, 1-2 days prior to glucose breath test (GBT). All the subjects were instructed to wash their mouth before the GBT to prevent any kind of contact from orally administered test meal with oral cavity bacteria and also restricted their physical movement during the experiment period. After an overnight fasting (~10-12 h) baseline breath sample was collected in a breath collection bag (QUINTRON, USA, SL No.QT00892). Then a test meal containing 75 mg U-$^{13}C_6$ labelled D-glucose (CIL-CLM-1396-CTM, Cambridge Isotope Laboratories, Inc. USA) with 75 gm normal glucose dissolved in 250 ml water was given to the subject for oral administration and subsequently breath samples were collected in 30 min intervals upto 180 min. The $^{13}C/^{12}C$ and $^{18}O/^{16}O$ isotope ratios of CO_2 in breath samples were measured using a laser-based high-resolution integrated cavity output spectroscopy (ICOS).

5.3 Results and Discussion

Here, we first explored the potential role of the major metabolite, CO_2 and its three most abundant stable isotopic species in the pathogenesis of *H. pylori*-induced type 2 diabetes and a possible relationship between the gastric pathogen and diabetes mellitus. To investigate this, we studied the time-dependent excretion kinetics of both ^{13}C and ^{18}O isotopic fractionations of exhaled breath CO_2 using ICOS method

(Fig.1a) after ingestion of an oral dose of ^{13}C-enriched glucose in three different group of patients with Hp(+)T2D(+), Hp(+)T2D(-) and Hp(-)T2D(-). It was observed that the subjects with Hp(+)T2D(-) group exhibited significantly higher isotopic enrichments of $\delta_{DOB}{}^{13}C(‰)$ values in exhaled breath with time compared to both groups of patients with Hp(-)T2D(-) and Hp(+)T2D(+) during the 3h glucose metabolism.

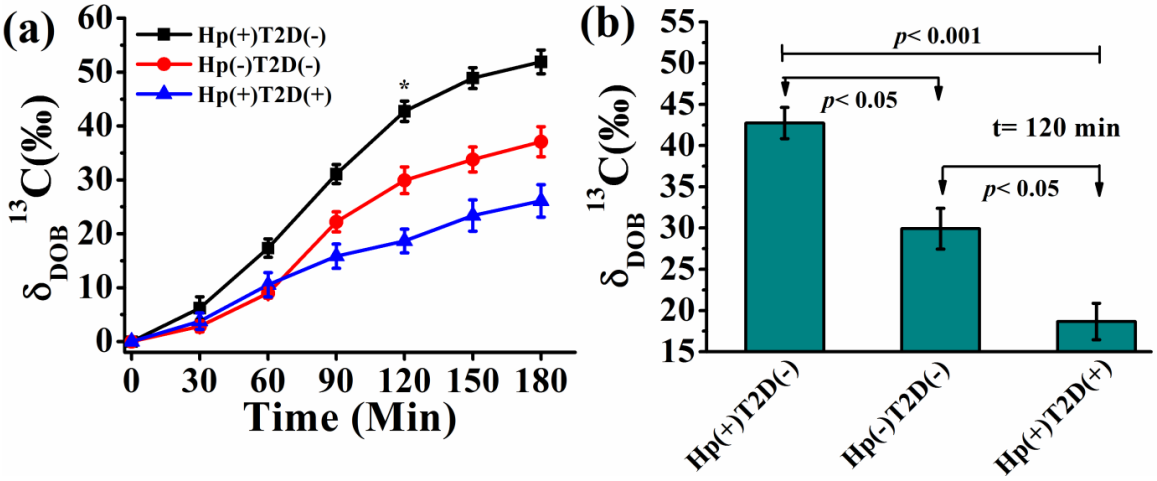

Figure 1. *Comparisons of excretion kinetics of $\delta_{DOB}{}^{13}C(‰)$ values among the three group of subjects i.e. H. pylori infection with/without complication of T2D in response to ^{13}C-enriched glucose metabolism. (a) Represent the significant enrichment of ^{13}C isotope in exhaled breath for subjects with Hp(+)T2D(-) group (n= 51) compared to both Hp(-)T2D(-) (n= 43) and Hp(+)T2D(+) (n= 37) group and (b) illustrate a marked statistical difference (p< 0.05) of $\delta_{DOB}{}^{13}C(‰)$ values among the three group of subjects at 120 min. * indicates p< 0.05.*

Early reports suggest that *H. pylori* can utilize glucose in both oxidative and fermentative pathways and the metabolism follows a biphasic characteristics involving an initial slow phase of metabolism followed by a rapid phase [19, 20] which is most likely to be involved in causing the significantly higher isotopic enrichments of $\delta_{DOB}{}^{13}C(‰)$ values for Hp(+)T2D(-) group compared to Hp(-)T2D(-) group of patients. But for the group of patients with Hp(+)T2D(+) there was no such significant isotopic enrichments of $\delta_{DOB}{}^{13}C(‰)$ values in response to ^{13}C-glucose

metabolism. It is quite well known that both *H. pylori* infection and T2D are inflammatory disease and produce oxidative stress [21-23] leading to β-cell dysfunction and deficits in insulin secretion, which directly affects the glucose metabolism. Recent evidences also demonstrate that patients with *H. pylori* infection accompanied with T2D exaggerate more oxidative stress and chronic inflammation than the patients with *H. pylori* infection with non-diabetic controls, [24] causing further depletion of isotopic ^{13}C in exhaled breath CO_2 for Hp(+)T2D(+) group with respect to the groups of Hp(-)T2D(-) and Hp(+)T2D(-). We also observed statistically significant differences ($p < 0.05$) of $\delta_{DOB}{}^{13}C(‰)$ values in excretion kinetics among the three distinct groups of patients (Fig.1b). Taken together, our findings suggest that isotopic fractionations of ^{13}C in exhaled breath CO_2 are strongly associated with glucose metabolism in *H. pylori*-induced T2D patients and thus establishing a strong association between *H. pylori* infection and T2D.

We next investigated the oxygen-18 (^{18}O) isotopic fractionations of breath CO_2 by studying the time-dependent excretion dynamics of $\delta_{DOB}{}^{18}O(‰)$ values in response to ^{13}C-labelled glucose and the results are depicted in Fig 2a. The ^{18}O-isotopic enrichments in exhaled breath CO_2 were significantly higher for Hp(+)T2D(+) group compared to Hp(-)T2D(-) and Hp(+)T2D(-) groups, while no such significant enrichments of $\delta_{DOB}{}^{18}O(‰)$ values in exhaled breath CO_2 for Hp(-)T2D(-) group were observed. Several lines of evidence [25, 26] suggest that *H. pylori* encodes two distinct form of carbonic anhydrase (CA) [i.e. α-CA and β-CA] which promotes a rapid exchange of ^{18}O-isotopes of body water (H_2O^{18}) with ^{16}O isotopes of $^{12}C^{16}O_2$ [27]. Moreover, CA is also present in human body and it is well documented that, the catalytic activity of CA in erythrocytes (red blood cells) is enhanced in patients with T2D [15, 16, 28]. Therefore, these activities are possibly attributed to the marked enrichment of ^{18}O-isotopic fractionations in breath CO_2 for Hp(+)T2D(+) group of patients.

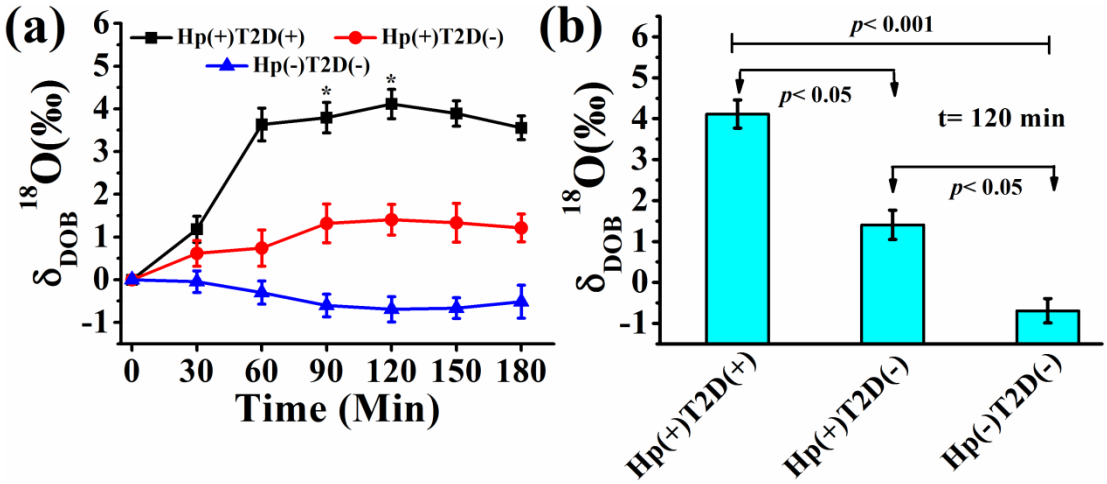

Figure 2. *Exploration of excretion kinetics plot of $\delta_{DOB}{}^{18}O$ ‰ values in response to ^{13}C-enriched glucose metabolism upto 180 min. (a) Indicates the significant enrichment of ^{18}O isotope of breath CO_2 for the HP(+)T2D(+) group (n= 37) compared to both HP(+)T2D(-) (n= 51) and HP(-)T2D(-) (n= 43) group due to the enhanced carbonic anhydrase activity. (b) Illustrates a significant differences (p< 0.05) of $\delta_{DOB}{}^{18}O$ ‰ values among the three group at 120 min (* indicates p< 0.05).*

However, due to only bacterial CA activity in the glucose-mediated bacterial environment the Hp(+)T2D(-) group exhibited comparatively higher isotopic enrichments of $\delta_{DOB}{}^{18}O(‰)$ compared to Hp(-)T2D(-) group. It is also noteworthy that erythrocytes CA activity in human body for CO_2 hydration/bicarbonate dehydration is much higher than the bacterial CA activity [29], which is likely to be the effects of the observation of comparative results of $\delta_{DOB}{}^{18}O(‰)$ for the different category of patients. In view of the above results, our findings suggest that the monitoring of ^{18}O-isotopes in breath may distinctively track the gastric pathogen *H. pylori* and T2D and thus might be considered as a potential biomarker for non-invasive detection of *H. pylori* infection in T2D patients and also unveiling a missing link between ^{18}O-isotopic exchange in breath CO_2 and the pathogenesis of *H. pylori*-induced T2D which has never been explored before.

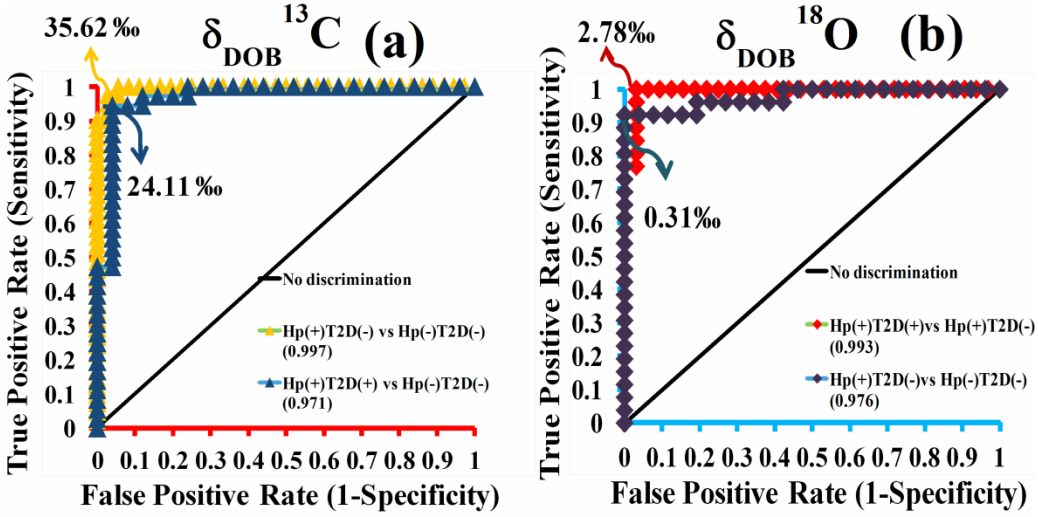

Figure 3. *Receiver operating characteristic (ROC) curve analysis for an optimal diagnostic cut-off value for simultaneous assessment of H. pylori infection and T2D at 120 min. (a) Illustrate individuals with* $\delta_{DOB}{}^{13}C$ *> 35.62 ‰ were considered as HP(+)T2D(-) group of subjects with ~ 97.6 % sensitivity and* $\delta_{DOB}{}^{13}C$ *values < 24.11 ‰ indicating the presence of HP(+)T2D(+) group of subjects with ~ 94.4 % sensitivity at 120 min. Conversely (b)* $\delta_{DOB}{}^{18}O$ *> 2.78‰ was taken account for the presence of HP(+)T2D(+) group with 100% sensitivity.*

We finally determined several optimal diagnostic cut-off points of $\delta_{DOB}{}^{13}C$(‰) and $\delta_{DOB}{}^{18}O$(‰) values in breath at 120 min associated with ^{13}C-glucose metabolism to assess the clinical validity of the present methodology and also to precisely track simultaneously the gastric pathogen and T2D in a non-invasive way. We utilized receiver operating characteristic curve (ROC) analysis by plotting true positive rate (sensitivity) against false positive rate (1-specificity) as shown in Fig 3a and 3b. Individuals with $\delta_{DOB}{}^{13}C‰ > 35.62‰$ at 120 min were considered as *H. pylori* positive without complication of T2D with sensitivity and specificity of ~97.6% and 97.2% respectively. Individuals with $\delta_{DOB}{}^{13}C‰ < 24.11‰$ were considered as *H. pylori* positive with T2D, whereas individuals were suggested to be *H. pylori* negative without T2D with $35.62‰ \leq \delta_{DOB}{}^{13}C‰ \leq 24.11‰$ and these corresponded to the similar diagnostic sensitivity and specificity. Conversely, with a different cut-off value of $\delta_{DOB}{}^{18}O‰ > 2.78‰$, the subjects were considered as positive *H. pylori* with T2D with a sensitivity of ~ 100% and specificity of ~96.9% and individuals with

$\delta_{DOB}{}^{18}O‰ < 0.31‰$ were taken into consideration of *H. pylori* negative without T2D with 92.3% sensitivity and 100% specificity (Table 2). Taken together, these findings suggest that carbon-13 and oxygen-18 isotopic fractionations of breath CO_2 in response to the glucose-metabolism are potentially linked in the pathogenesis of *H. pylori*-induced T2D and consequently suggest a broad clinical efficacy for accurate assessment of *H. pylori* infection in diabetic patients, opening a new route for treating these common diseases.

Group	Cut-off point of $\delta_{DOB}{}^{13}C‰$	Sensitivity	Specificity	PPV	NPV	Accuracy
Hp(+)T2D(-) vs Hp(-)T2D(-)	35.62‰	97.6%	97.2%	98%	97%	97.4%
Hp(-)T2D(-) vs Hp(+)T2D(+)	24.11‰	94.4%	96%	96%	94%	95.08%
	Cut-off point of $\delta_{DOB}{}^{18}O‰$					
Hp(+)T2D(+) vs Hp(+)T2D(-)	2.78‰	100%	96.9%	96%	100%	98.27%
Hp(+)T2D(-) vs Hp(-)T2D(-)	0.31‰	92.3%	100%	100%	94%	96.15%

Table 2. *Different optimal diagnostic parameters corresponding to the cut-off values of $\delta_{DOB}{}^{13}C‰$ and $\delta_{DOB}{}^{18}O‰$ for the assessment of H. pylori infection and T2D at 120 min. PPV and NPV indicates positive predictive value and negative predictive value respectively.*

5.4 Conclusions

In this chapter, we have demonstrated that analysis of oxygen-18 and carbon-13 isotopes of breath CO_2 through the excretion kinetics revealed a strong association between *H. pylori* infection and type 2 diabetes. We first established that ^{18}O and ^{13}C-isotopes in response to ^{13}C-enriched glucose ingestion may precisely track the selective evolution of *H. pylori*-induced T2D patients as well as *H. pylori*-induced non-diabetic controls and thus might be considered as potential biomarkers for non-invasive assessment of the gastric pathogen prior to the onset of T2D. While there are several important gaps in our study for understanding the molecular mechanisms

underlying the pathogenesis of the diseases that should be explored in future research, but our current results may open new perspectives into the isotope specific molecular detection of T2D associated with *H. pylori* infection.

5.5 References

[1] Polk D B and Peek Jr R M, *Helicobacter pylori*: gastric cancer and beyond. *Nat. Rev. Cancer* **10**, 403-414 (2010).

[2] El-Omar E M *et al.*, Interleukin-1 polymorphisms associated with increased risk of gastric cancer. *Nature* **404,** 398-402 (2000).

[3] Som S *et al.*, Excretion kinetics of ^{13}C-urea breath test: influences of endogenous CO_2 production and dose recovery on the diagnostic accuracy of *Helicobacter pylori* infection. *Anal. Bioanal. Chem.* **406,** 5405-5412 (2014).

[4] Franceschi F *et al.*, Extragastric diseases and *Helicobacter pylori*. *Helicobacter* **20,** 40-46 (2015).

[5] Yang Z *et al.*, Potential effect of chronic *Helicobacter pylori* infection on glucose metabolism of Mongolian gerbils. *World J. Gastroentrol.* **20,** 12593-12604 (2015).

[6] He C, Yang Z and Lu N-H, *Helicobacter pylori* infection and diabetes: is it a myth or fact? *World J. Gastroentrol.* **20,** 4607-4617 (2014).

[7] Donath M Y and Shoelson S E, Type 2 diabetes as an inflammatory disease. *Nat. Rev. Immunol.* **11,** 98-107 (2011).

[8] Donath M Y *et al.*, Mechanisms of beta-cell death in type 2 diabetes. *Diabetes,* **54,** 108-113 (2005).

[9] Devrajani B R *et al.*, Type 2 diabetes mellitus: a risk factor for *Helicobacter pylori* infection: a hospital based case-control study. *Int. J. Diabetes Dev. Ctries.* **30,** 22-26 (2010).

[10] Yang G H *et al.*, Gastric *Helicobacter pylori* infection associated with risk of diabetes mellitus, but not prediabetes. *J. Gastroenterol. Hepatol.* **29,** 1794–1799 (2014).

[11] Hsieh M C *et al.*, *Helicobacter pylori* infection associated with high HbA1c and type 2 diabetes. *Eur. J. Clin. Invest.* **43,** 949-956 (2013).

[12] Mendz G L, Hazell S L and Burns B P, Glucose utilization and lactate production by *Helicobacter pylori. J. Gen. Microbiol.* **139,** 3023-3028 (1993).

[13] Chen Y and Blaser M J, Association between gastric *Helicobacter pylori* colonization and glycated hemoglobin levels. *J. Infect. Dis.* **205,** 1195-1202 (2012).

[14] Epstein S and Zeiri L, Oxygen and carbon isotopic compositions of gases respired by humans. *Proc. Natl. Acad. Sci. USA.* **85,** 1727–1731 (1988).

[15] Ibrahim S I *et al.*, Effect of hyperglycemia on erythrocyte carbonic anhydrase and lactic acid in type II diabetic subjects. *J. Diabetes Mellitus 6*, 158-165 (2016).

[16] Ghosh C *et al.*, Oxygen-18 isotope of breath CO_2 linking to erythrocytes carbonic anhydrase activity: a biomarker for pre-diabetes and type 2 diabetes. *Sci. Rep.* **5,** 8137 (2015).

[17] Ozdemir H, Kufrevioglu O I and Cetinkaya R, Effects of glycation on erythrocyte carbonic anhydrase-I and II in patients with diabetes mellitus. *Turk. J. Med. Sci.* **30,** 135-141 (2000).

[18] American Diabetes Association. Classification and diagnosis of diabetes. *Diabetes Care* **38,** S8-S16 (2015).

[19] Som S *et al.*, Mechanisms linking metabolism of *Helicobacter pylori* to ^{18}O and ^{13}C-isotopes of human breath CO_2. *Sci. Rep.* **5,** 10936 (2015).

[20] Mendz G L, Burns B P and Hazell S L, Characterisation of glucose transport in *Helicobacter pylori. Biochim Biophys Acta.* **1244,** 269–276 (1995).

[21] Donath M Y, Targeting inflammation in the treatment of type 2 diabetes: time to start. *Nat. Rev. Drug Discov.* **13,** 465-476 (2014).

[22] Akash M S H, Rehman K and Chen S, Role of inflammatory mechanisms in pathogenesis of type 2 diabetes mellitus. *J. Cell. Biochem.* **114,** 525–531 (2013).

[23] Jeon C Y *et al.*, *Helicobacter pylori* infection is associated with an increased rate of diabetes. *Diabetes Care* **35,** 520–525 (2012).

[24] Nasif W A *et al.*, Oxidative DNA damage and oxidized low density lipoprotein in type II diabetes mellitus among patients with *Helicobacter pylori* infection. *Diabetol. Metab. Syndr.* **8,** 34 (2016).

[25] Marcus E A *et al.*, The periplasmic alpha-carbonic anhydrase activity of *Helicobacter pylori* is essential for acid acclimation. *J. Bacteriol.* **187,** 729-738 (2005).

[26] Mone S B *et al.*, Roles of alpha and beta carbonic anhydrases of *Helicobacter pylori* in the urease-dependent response to acidity and in colonization of the murine gastric mucosa. *Infect. Immun.* **76,** 497-509 (2008).

[27] Maity A *et al.*, Oxygen-18 stable isotope of exhaled breath CO_2 as a non-invasive marker of *Helicobacter pylori* infection. *J. Anal. At. Spectrom.* **29,** 2251–2255 (2014).

[28] Biswas U K and Kumar A, Study on the changes of carbonic anhydrase activity in insulin resistance and the effect of methylglyoxal. *J. Pak. Med. Assoc.* **62,** 417-421 (2012).

[29] Nishimori I *et al.*, Carbonic anhydrase inhibitors: the β-carbonic anhydrase from *Helicobacter pylori* is a new target for sulfonamide and sulfamate inhibitors. *Bioorg. Med. Chem. Lett.* **17,** 3585-3594 (2007).

Chapter 6

Role of exhaled nitric oxide (NO) as a potential marker for selective detection of peptic ulcer and non-ulcer dyspepsia associated with *Helicobacter pylori*

6.1 Introduction

H. pylori is a major causative agent for the development of chronic gastritis, non-ulcer dyspepsia, peptic-ulcer disease and mucosa associated lymphoid tissue lymphoma [1, 2]. Peptic ulcer disease (PUD) is characterized by chronic inflammatory state of stomach and upper-duodenum [3-5]. Although substantial progress has been made in the field of *H. pylori* and its associated disorders, but the early-stage detection of PUD and its management still remains limited. It is noteworthy that the underlying link between *H. pylori* and non-ulcer dyspepsia (NUD) also remains controversial [6-9]. Now-a-days, several non-invasive methods, for example, ^{13}C-urea breath test (^{13}C-UBT), serology and stool antigen test are widely available for diagnosis of *H. pylori* infection but none of the above methodologies have the ability to assess the risk of development of ulcer and non-ulcer state associated with *H. pylori* infection.

However, persistent infection caused by *H. pylori* produces chronic inflammation and induces the inflammatory cytokines in gastric mucosa. It is quite well known that molecular nitric oxide (NO) is one of the major inflammatory agents generated by the enzymatic activity of nitric oxide synthase (NOS) during the conversion of L-arginine to L-citrulline [10, 11]. NO is also a biologically active unorthodox messenger molecule that plays a pivotal role in inflammatory process in the gastric environment. Moreover, NO is strongly associated with several respiratory diseases such as asthma and chronic obstructive pulmonary disease (COPD) [12, 13]. However, among all the isoforms of NOS, inducible nitric oxide synthase (iNOS) produces the largest amount of NO in gastrointestinal tract compared to endothelial NOS (eNOS) and neuronal NOS (nNOS) [11, 14]. Several studies have also shown that during the colonization of the gastric pathogen *H. pylori*, iNOS expression is significantly up-regulated which further enhances the production of NO [15, 16]. It is also noteworthy that iNOS

activity is enhanced more than two fold higher in *H. pylori* assisted peptic-ulcer patients compared to the patients with non-ulcer dyspepsia [17]. Moreover, it was found that with eradication of ulcer the iNOS activity is also significantly reduced [11, 18]. These activities suggest that iNOS plays a significant role in the pathogenesis of gastroduodenal disorders and consequently promotes the development of peptic ulcer. Taken together, all these findings in the past suggest an unproven hypothesis about the possibility of exploiting NO levels in exhaled breath that may specifically track the actual disease state of peptic ulcer and non-ulcer dyspepsia and hence may introduce a novel non-invasive strategy for early detection and selective classification of PUD from NUD in contrast to the direct invasive endoscopy and biopsy test. It is noteworthy to mention here that Maity *et al* recently showed hydrogen level (H_2) in exhaled human breath may track the pathogenesis of PUD and NUD in a selective manner [9]. However, there is no such study, till date, to reveal any potential link between NO level in exhaled human breath and progression of PUD and NUD.

There is a growing body of evidence suggesting that bacterial lipopolysaccharide, cytokines, and several additional agents other than urease are also able to stimulate the macrophage iNOS expression [19, 20] which further enhance the NO levels. It is well known that in ^{13}C-urea breath test (^{13}C-UBT), the most common non-invasive methodology for diagnosis the *H. pylori* infection, urease secretion was stimulated by the addition of urea from the pathogen *H. pylori*. Citric acid was used as an acidifier agent in ^{13}C-UBT and which also delayed the gastric emptying procedure to enhance the urease activity. So, these enhanced urease activity elevated the NO concentration by triggering the iNOS expression. We therefore, hypothesized that enhanced NO level may contribute to the pathogenesis of the preclinical phase of peptic ulcer encompassing both gastric and duodenal ulcers. As there is no such existing non-invasive method for simultaneous detection of peptic ulcer and non-ulcerous dyspepsia, therefore the real-time assessment of NO in exhaled breath may open up an alternative approach for precise evaluation of non-ulcerous state prior to the onset of ulceration in gastric niche.

In this chapter, we explored the association between exhaled breath NO and *H. pylori* infection and how exhaled NO level is altered by the enzymatic activity of the gastric

pathogen. We have also investigated the alteration of breath NO level in individuals with *H. pylori* assisted peptic ulcer disease and non-ulcer dyspepsia in response to the ingestion of urea and glucose and subsequently elucidated the potential role of urea as an inducer of NO production. We have also investigated the role urease activity on the iNOS isoform by ingesting glucose .We have further shown that breath NO can be used as a novel diagnostic marker for early recognition of ulcer in a non-invasive manner even after the standard eradication therapies of *H. pylori* infection. Finally, we determined several diagnostic parameters to gain a better insight into the pathogenicity of *H. pylori* associated peptic ulcer disease.

6.2 Materials and Methods

6.2.1 Subjects

One hundred forty eight (n=148) number of subjects with different gastrointestinal symptoms i.e. chronic gastritis, abdominal pain, non-ulcer dyspepsia, peptic ulcer disease, were enrolled for the present study. We have selectively classified all the subjects into three discrete categories i.e. non-ulcer dyspepsia (NUD, n= 57), peptic ulcer disease (PUD, n= 51) and *H. pylori* negative controls (n= 40) depending on both gold-standard invasive and non-invasive methodologies including endoscopy and biopsy based rapid urease test (RUT) and ^{13}C-urea breath test (^{13}C-UBT). In ^{13}C-UBT, subjects were classified as *H. pylori* positive at the value of $\delta_{DOB}{}^{13}C$ (‰) $\geq$ 3 ‰ at 30 min [21]. Subjects who had any previous history of gastric surgery, diabetes, crohn's disease, ulcerative colitis, hypertension, asthma, cardiovascular disease, smoking and chronic obstructive pulmonary disease (COPD) were excluded from the present study. Subjects who have taken proton pump inhibitor or H_2-receptor antagonists four weeks prior to test were also excluded from the study.

6.2.2 Breath Sample Collections

After an overnight fasting (~10-12 h), the ^{13}C-UBT was performed within 1-2 days after the completion of endoscopy. All the subjects were instructed to wash their mouth prior to the test. On the day of the test, an oral dose of 4 gm citric acid in 200 ml water solution was given to the subjects and baseline breath samples were collected in a breath collection bag (QUINTRON, USA, SL No.QT00892) after 10

min of oral ingestion. Subsequently, an oral dose of 75 mg ^{13}C-enriched urea (CLM-311-GMP, Cambridge, Isotopic Laboratories, Inc., USA) in 50 ml water was given to the patients and post-dose breath samples were collected upto 90 min in 15 min interval and the concentration of NO in exhaled breath was measured by a high-resolution cavity ring-down spectroscopy (CRDS) technique. For glucose breath test, after the overnight fasting, baseline breath samples were collected and followed by on oral dose of 75 mg normal (unlabelled) glucose in 50 ml water and breath samples were collected in 15 min interval upto 90 min. Breath samples were analyzed by a high-precision laser based integrated cavity output spectroscopy (ICOS) technique to measure the isotope ratios of $^{13}C/^{12}C$ of exhaled breath CO_2.

6.3 Results and Discussions

To investigate the possible role of NO in the pathogenesis of PUD and NUD, we first explored the time-dependent excretion kinetics of NO [i.e. ΔNO in ppb, $[\Delta NO\ (ppb)]_{t=t\ min}$ = $[NO\ concentration\ (ppb)]_{t=t\ min}$ - $[NO\ concentration\ (ppb)]_{t=0\ min}$] in exhaled breath samples after ingestion of an oral dose of ^{13}C-enriched urea for *H. pylori* positive PUD [n= 51 (gastric and duodenal ulcer, n=22 and 29)], *H. pylori* positive NUD [n=57] and *H. pylori* negative individuals [n=40], using the laser-based high-resolution continuous-wave cavity ring-down spectroscopy (*cw*-CRDS) technique as described in chapter 2.

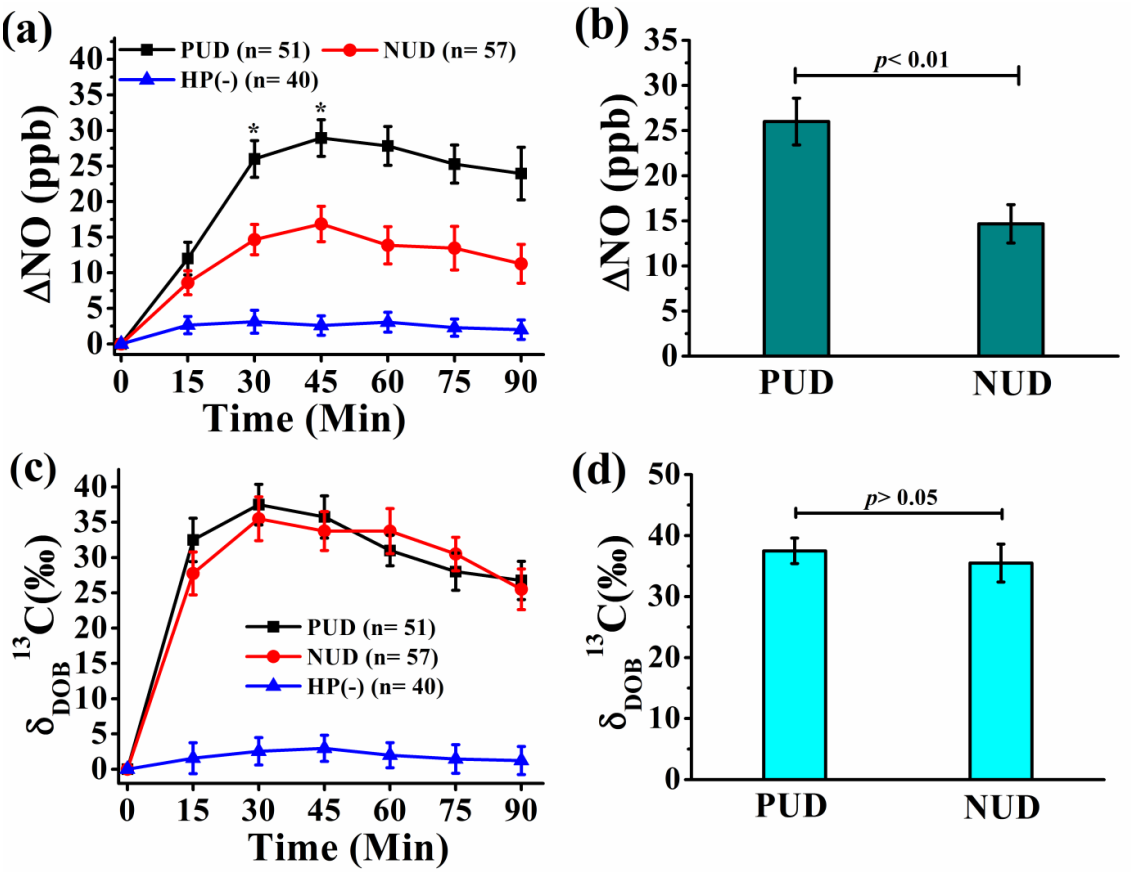

Figure 1. *Assessment of excretion kinetics of both ΔNO (ppb) and $\delta_{DOB}{}^{13}C$ (‰) values in exhaled breath associated with H. pylori infected PUD, NUD and negative individuals. (a) The excretion kinetics ΔNO illustrates the significant enrichment of ΔNO value for both PUD and NUD subjects compared to H. pylori negative subjects and thus produces (b) a marked statistical difference (p< 0.01) between PUD and NUD subjects at 30 min. (c) Indicate the excretion dynamics of $\delta_{DOB}{}^{13}C$ (‰) values for PUD, NUD and H. pylori negative subjects upto 90 minutes and revealing (d) statistically insignificant difference (p> 0.05) of $\delta_{DOB}{}^{13}C$ (‰) values between PUD and NUD subjects at 30 min.* ***** *indicates p < 0.05.*

It was observed [Fig. 1a] that subjects associated with PUD exhibited considerably higher enrichments of ΔNO in exhaled breath compared to both NUD and *H. pylori* negative individuals during the 90 min excretion dynamics, while the NUD individuals exhibited slight enrichments of ΔNO over the *H. pylori* negative subjects. Early studies revealed that in human body, NO is synthesised during the oxidative conversion of L-arginine to L-citrulline which is facilitated by the enzymatic activity

of nitric oxide synthase (NOS), specifically inducible nitric oxide synthase (iNOS). Several lines of evidence [15, 22] suggest that the iNOS gene is highly expressed in immune cells as well as in gastric epithelial cells of the stomach which is the normal site for colonization of gastric pathogen *H. pylori*. The pathogen has the potent ability to stimulate the iNOS expression during the colonization in the gastric mucosa that further assists in elevating the NO levels in the gastric environment [16, 23]. Early study [17] demonstrated that the iNOS activity in patients with peptic ulcer disease was more than two-fold higher than that of non-ulcerous patients. Therefore, in our observations the higher manifestation of breath NO levels in PUD patients compared to the patients with NUD is likely to be the effect of enhanced activity of iNOS enzyme. Several early studies [24, 25] suggest that *H. pylori*-derived urease enzyme acts as a stimulator of iNOS expression and it is over-expressed for PUD patients due to the acid acclimation process [9, 26, 27] which regulates the production of NO levels within the gastric niche. This activity may play an important role for the alteration of breath NO levels in PUD patients and as a result our findings suggest a potential link of breath NO levels with the development of *H. pylori*-associated peptic ulcer disease. Furthermore, we also observed [Fig. 1b] a statistically significant difference ($p< 0.01$) of ΔNO values between PUD and NUD patients harbouring *H. pylori* infection. Taken together, our observations indicate that monitoring of NO levels in exhaled breath may distinctively track the precise evaluation of peptic ulcer and non-ulcer in a much more profound way by means of breath test.

We next investigated how the isotopes (^{12}C and ^{13}C) of the major metabolite CO_2 in exhaled breath alter in response to the ingestion of ^{13}C-enriched urea when a person has developed ulcers or has the symptoms of non-ulcer dyspepsia. To investigate this, we explored the 90 min excretion dynamics of $^{13}C/^{12}C$ isotopic fractionation of breath CO_2, expressed as the delta-over-baseline (DOB) [i.e. $\delta_{DOB}{}^{13}C$ (‰) = $(\delta^{13}C)_{t=t\ min}$ - $(\delta^{13}C)_{t=0\ min}$], after ingestion of an oral dose of ^{13}C-urea. We observed a marked enrichment of $\delta_{DOB}{}^{13}C$ (‰) values for both *H. pylori* infected NUD and PUD patients compared to the *H. pylori* negative controls [Fig. 1c]. On the contrary, there was no significant difference of $\delta_{DOB}{}^{13}C$ (‰) values between PUD and NUD subjects [Fig. 1d], which indicates that the standard ^{13}C-UBT is still not have enough potentiality to distinguish the actual disease state, i.e. whether it is peptic ulcer or non-ulcerous state. Conversely monitoring of exhaled breath NO is capable of distinguishing *H. pylori*

infected ulcer and non-ulcer patients. Based on these results, we therefore posit that breath NO may be considered as a potential molecular biomarker or "breath-print" to selectively distinguish PUD patients from patients with NUD.

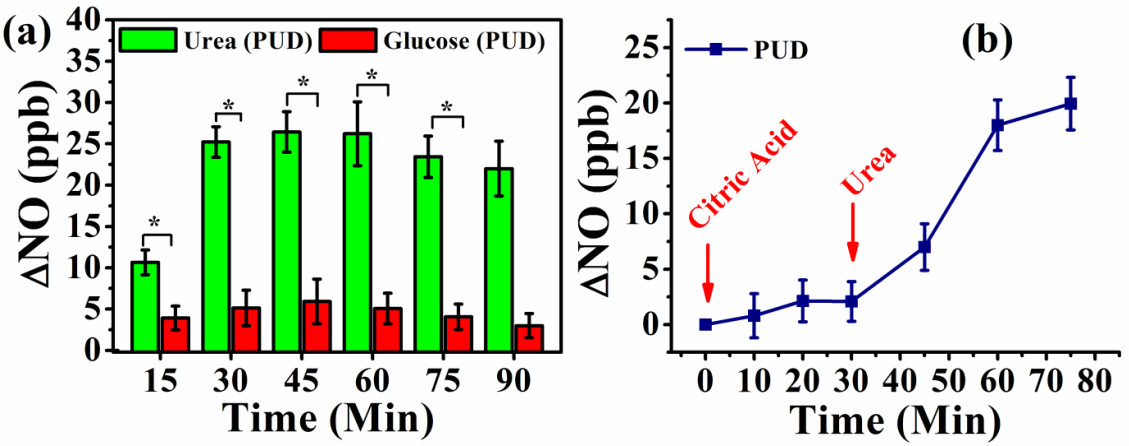

Figure 2. *Exploration of excretion kinetics of ΔNO (ppb) values for H. pylori infected PUD subjects. (a) Illustrates the excretion kinetics of ΔNO values for PUD subjects in response to unlabelled urea and glucose upto 90 min and demonstrated a significant difference (p < 0.01) of post-dose ΔNO values from 15 min (* indicates p <0 .01). (b) Elucidate the role of urea in up-regulation of ΔNO values for PUD subjects.*

However, to address the potential role of substrate dependent NO production in the pathogenesis of ulcer, we then performed the 90 min excretion kinetics of exhaled breath NO in response to unlabelled urea and glucose for a number of *H. pylori* positive PUD subjects (n= 41) [Fig. 2a]. When the unlabelled urea was orally administered for PUD subjects, the post-dose ΔNO levels exhibited a significant enrichment with time and also depicted the similar excretion kinetics patterns with the administration of ^{13}C-enriched urea. But, for unlabelled glucose no significant change of ΔNO levels was observed for PUD subjects. These findings suggest that for *H. pylori* positive PUD subjects, urease is possibly the main inducer of iNOS gene expression in human stomach [20, 25]. After oral administration of unlabelled urea with citric acid, the urease activity is stimulated due to acidification [21, 28] and the major effect of urease activation is observed around 30 minutes [21] which controls

the maximum manifestation of ΔNO levels at 30 minutes when compared with the response of unlabelled glucose. We further investigated in detail the effect of citric acid on the production of breath NO levels and the tests were performed on a group of PUD subjects (n=19). It was observed [Fig. 2b] that there was no significant change in ΔNO levels upto 30 min but a significant rise of ΔNO values was observed after administration of urea. This clearly indicates that urease plays a regulatory role in up-regulation of NO levels in exhaled breath for PUD patients. However, our results also signify that the iNOS-derived breath NO in response to urease activity may be an important parameter in the pathogenesis of *H. pylori* associated ulcer.

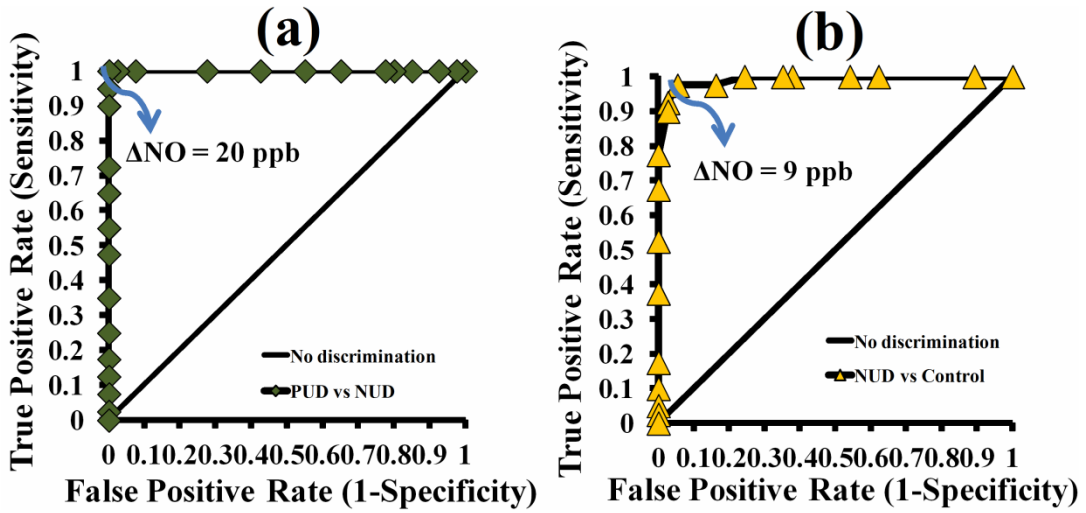

Figure 3. *Receiver operating characteristics (ROC) curve analysis for an optimal diagnostics cut-off point for PUD and NUD subjects. (a) Depict the ROC curve analysis for PUD and NUD subjects at 30 min and ΔNO ≥ 20 ppb was considered as the indication of PUD with 100 % sensitivity. (b) Indicate subjects with 9 ppb < ΔNO< 20 ppb was NUD and ΔNO ≤ 9 ppb was considered as H. pylori controls at 30 min with 97.5% sensitivity.*

To establish the clinical efficacy of breath NO for precise tracking of ulcer and non-ulcerous state linked with *H. pylori* infection, we then determined the optimal diagnostic cut-off points of ΔNO values in exhaled breath using the receiver operating characteristics (ROC) curve analysis. Individuals with ΔNO ≥ 20 ppb at 30 min were considered as *H. pylori* positive PUD subjects with 100% diagnostic sensitivity and 100% specificity [Fig. 3a]. Whereas subjects with 9 ppb < ΔNO < 20 ppb were

suggested to be *H. pylori* infected non-ulcerous state (NUD) with 97.5% diagnostic sensitivity and 94.6% specificity. Alternatively, subjects were diagnosed as *H. pylori* negative controls with $\Delta NO \leq 9$ ppb at 30 min with 97.5% sensitivity [Fig. 3b]. Taken together, our results suggest that monitoring of breath NO may have a significant impact for precise classification as well as selective detection of ulcer and non-ulcerous state associated with *H. pylori* infection.

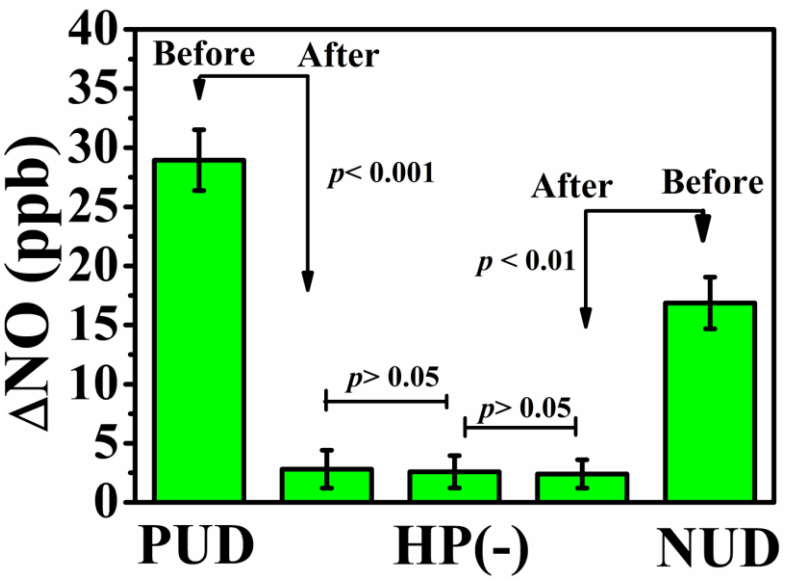

Figure 4. *Clinical validity of nitric oxide breath test. A marked depletion ($p < 0.01$) of ΔNO value was observed for both PUD and NUD subjects before and the standard eradication therapy at 30 min.*

We finally assessed the widespread clinical validity of the present method exploiting breath NO levels in response to the standard *H. pylori* eradication therapy. We performed the standard therapies on a number of individuals with PUD (n= 29) and NUD (n= 24) subjects. Figure 4 illustrates that there was a marked depletion of breath ΔNO levels following the eradication therapy and all the patients exhibited significant improvement of symptoms of peptic ulcer and non-ulcer dyspepsia after complete eradication, thus suggesting the broad clinical efficacy of NO breath test. Our observations therefore indicate that monitoring of NO levels in exhaled breath may be a new and potential strategy for early detection and follow-up of patients suffering from ulcer or non-ulcer dyspepsia.

6.4 Conclusions

In summary, we have demonstrated that a potential link between molecular NO in exhaled breath and *H. pylori* associated peptic ulcer disease (PUD) along with non-ulcerous dyspepsia (NUD). We have shown that exhaled NO is significantly altered when a person has developed ulcer or has the symptoms of NUD, thus providing the new insights into the pathogenesis of ulceration. Our results also demonstrate that breath NO may be considered as a potential biomarker for accurate detection and selective classification of PUD and NUD. It could be used as a screening tool for early detection and follow-up of patients even after standard eradication therapy. Finally, we hope that our new results linking breath NO with *H. pylori* associated peptic ulcer disease dealing with both the gastric and duodenal ulcers may open new perspectives into the pathogenecity of ulceration or ulcer-related complications.

6.5 References

[1] Covacci A *et al.*, *Helicobacter pylori* virulence and genetic geography. *Science* **284,** 1328-1333 (1999).

[2] Kusters J G, van Vliet A H M and Kuipers E J, Pathogenesis of *Helicobacter pylori* infection. *Clin. Microbiol. Rev.* **19,** 449-490 (2006).

[3] Malfertheiner P, Chan F K L and McColl K E L, Peptic ulcer disease. *Lancet* **374,** 1149-1461 (2009).

[4] Peterson W L, *Helicobacter pylori* and peptic ulcer disease. *N. Engl. J. Med.* **324,** 1043-1048 (1991).

[5] Polk D B and Peek R M, *Helicobacter pylori*: gastric cancer and beyond. *Nat. Rev. Cancer* **10,** 403-414 (2010).

[6] Blum A L *et al*, Lack of effect of treating *Helicobacter pylori* infection in patients with nonulcer dyspepsia. *N. Engl. J. Med.* **339,** 1875-1881 (1998).

[7] Talley N J and Hunt R H, What role does *Helicobacter pylori* play in dyspepsia and nonulcer dyspepsia? Arguments for and against *H. pylori* being associated with dyspeptic symptoms. *Gastroenterology* **113,** 567-577 (1997).

[8] Bernersen B, Johnsen R and Straume B, Non-ulcer dyspepsia and peptic ulcer: the distribution in a population and their relation to risk factors. *Gut* **38,** 822-825 (1996).

[9] Maity A *et al.*, Molecular hydrogen in human breath: a new strategy for selectively diagnosing peptic ulcer disease, non-ulcerous dyspepsia and *Helicobacter pylori* infection. *J. Breath Res.* **10,** 036007 (2016).

[10] Förstermann U and Sessa W C, Nitric oxide synthases: regulation and function. *Eur. Heart J.* **33,** 829-837 (2012).

[11] Cole S P, Kharitonov V F and Guiney D G, Effect of nitric oxide on *Helicobacter pylori* morphology. *J. Infect. Dis.* **180,** 1713-1717 (1999).

[12] Smith A D *et al.*, Use of exhaled nitric oxide measurements to guide treatment in chronic asthma. *N. Engl. J. Med.* **352,** 2163-2173 (2005).

[13] Gelb A F *et al.*, Barnes, Review of exhaled nitric oxide in chronic obstructive pulmonary disease. *J. Breath Res.* **6,** 047101 (2012).

[14] Kim J M *et al.*, Up-regulation of inducible nitric oxide synthase and nitric oxide in *Helicobacter pylori*-infected human gastric epithelial cells: possible role of interferon-gamma in polarized nitric oxide secretion. *Helicobacter* **7,** 116-128 (2002).

[15] Wilson K T *et al.*, *Helicobacter pylori* stimulates inducible nitric oxide synthase expression and activity in a murine macrophage cell line. *Gastroenterology* **111,** 1524-1533 (1996).

[16] Rieder G *et al.*, Up-regulation of inducible nitric oxide synthase in *Helicobacter pylori*-associated gastritis may represent an increased risk factor to develop gastric carcinoma of the intestinal type. *Int. J. Med. Microbiol.* **293,** 403-412 (2003).

[17] Rachmilewitz D *et al.*, Enhanced gastric nitric oxide synthase activity in duodenal ulcer patients. *Gut* **35,** 1394-1397 (1994).

[18] Antos D *et al.*, Inducible nitric oxide synthase expression before and after eradication of *Helicobacter pylori* in different forms of gastritis. *FEMS Immunol. Med. Microbiol.* **30,** 127-131 (2001).

[19] Lu D Y *et al.*, *Helicobacter pylori* attenuates lipopolysaccharide-induced nitric oxide production by murine macrophages. *Innate Immun.* **18,** 406-417 (2012).

[20] Cherdantseva L A *et al.*, Association of *Helicobacter pylori* and iNOS production by macrophages and lymphocytes in the gastric mucosa in chronic gastritis. *J. Immunol. Res.* **2014,** 762514 (2014).

[21] Som S *et al.*, Excretion kinetics of ^{13}C-urea breath test: influences of endogenous CO_2 production and dose recovery on the diagnostic accuracy of *Helicobacter pylori* infection. *Anal. Bioanal. Chem.* **406,** 5405-5412 (2014).

[22] Gobert A P and Wilson K T, The immune battle against *Helicobacter pylori* infection: NO offense. *Trends Microbiol.* **24,** 366-376 (2016).

[23] Kasperski J *et al.*, Does *Helicobacter pylori* infection increase the levels of exhaled nitric oxide? *Eur. J. Inflamm.* **11,** 279-282 (2013).

[24] Hardbower D M *et al.*, Chronic inflammation and oxidative stress: the smoking gun for *Helicobacter pylori*-induced gastric cancer? *Gut Microbes* **4,** 475-481 (2013).

[25] Gobert A P *et al.*, Cutting edge: urease release by *Helicobacter pylori* stimulates macrophage inducible nitric oxide synthase. *J. Immunol.* **168,** 6002-6006 (2002).

[26] Mobley H L, The role of *Helicobacter pylori* urease in the pathogenesis of gastritis and peptic ulceration. *Aliment. Pharmacol. Ther.* **10,** 57-64 (1996).

[27] Kohda K *et al.*, Role of apoptosis induced by *Helicobacter pylori* infection in the development of duodenal ulcer. *Gut* **44,** 456-462 (1999).

[28] Pantoflickova D *et al.*, ^{13}C urea breath test (UBT) in the diagnosis of *Helicobacter pylori*; why does it work better with acid test meals? *Gut* **52,** 933–937 (2003).

Chapter 7

A model-based breath analysis method for the estimation of blood glucose profile

7.1 Introduction

Diabetes is the most common metabolic disease which has been considered as a worldwide epidemic and a major threat to our society. The prevalence of diabetes is increasing rapidly. According to the report of the International Diabetes Federation (IDF), the global burden of diabetes has been estimated to be 381 million and it has been predicted to be almost double in 2030 [1]. At present, India has become the diabetic capital with a projected 101 million diabetes cases by 2030. Unfortunately, half of the diabetes individuals are undiagnosed and the early detection of diabetes is sometimes impossible due to asymptomatic nature of the disease at the preliminary stage [2, 3].

In general, diabetes is considered as a metabolic disorder in individuals with high blood glucose levels. There are two primary forms of diabetes: type 1 diabetes (T1D) and type 2 diabetes (T2D). Insulin dependent T1D occurs when insulin producing beta cells of pancreas are totally destroyed and the individuals only live on exogenous insulin. T1D has strong genetic components. In T2D, either body does not produce enough insulin than body's need or body's cells become resistant to insulin action. The occurrence of T1D is the most common at very early age. However, T1D can also develop in adults having the auto immune antibody of T1D. T2D is the most common of the diabetes cases. T2D can develop both in young and adult people. The prevalence of T2D is 85% of total diabetes cases and the numbers of affected individuals are increasing in alarming rate throughout the world. Several symptoms like polyuria, polydipsia, polyphagia are common in T2D. Early detection of T2D is very important to avoid the diabetes complications like cardiovascular disease, kidney failure and blurred vision [4].

The blood glucose measurement is necessary for diagnosis and treatment of diabetes mellitus. In case of type 1 diabetes, frequent blood glucose monitoring is desirable to adjust the exogenous insulin doses. Current techniques for blood glucose analysis are invasive. Blood sample withdrawals by these invasive methods are not only painful but also inconvenient. Generally, blood sample is collected and glucose level is estimated by glucose-oxidase method. Sometimes venous, plasma and whole body blood glucose levels are monitored in different healthcare centres. Now-a-days, less invasive capillary blood glucose monitoring meter is frequently used as a portable device operated by the patients. Patients need to prick their fingers for a drop of blood. This method suffers from several drawbacks, which limits its widespread clinical applicability for the diagnosis of pre-diabetic stage. Besides, to maintain the desired blood glucose levels, patients need to check their blood glucose levels by this method for several times per day. Blood-borne infection has been reported for the utilization of this glucose sensor [5, 6]. Further, the test strip or glucose oxidase reagent is costly enough to create an extra economical burden on the patients. Therefore, development of a point-of-care (POC) blood glucose profile monitoring methodology has become substantial interest during the last few years.

In the last few decades, several non-invasive diagnostic methods have been developed to screen the type 2 diabetes. A diagnostic agent for the detection of glucose levels in urine has been proposed to be a sound method for diagnosis of T2D [7, 8]. But correlations between the plasma and urine glucose concentrations are not sometimes good. Urine-positive results only provide an important clue, but are unable to provide sufficient basis for the diagnosis of type 2 diabetes. If the urine test result is negative, the possibility of diabetes can’t always be ruled out. Few non-invasive or minimally invasive methods have been reported to monitor the blood glucose levels. But, these methods exploit different spectroscopic techniques like infrared spectroscopy (IR), fluorescence spectroscopy, Raman spectroscopy, surface plasmon resonance (SPR) spectroscopy and spectrographic techniques. The outcomes from these techniques are limited due to signal-to-noise ratio and few common difficulties. Sometimes, calibrations are necessary to obtain the correct blood glucose levels. Few optical measurements have been further reported. But those techniques are suitable for laboratory analysis and hardly can be applied for practical clinical settings. Recently, blood glucose monitoring by exploiting human sweat has been proposed. But, the

barrier for effective use of this technique comes from the procedures for sweat collection and thereafter the level of accuracy for the test. Recently, few studies have reported the associations between the saliva and blood glucose levels. The results obtained from the saliva glucose analysis are quite satisfactory and are seemed to be reliable. The saliva glucose levels have been shown to be higher in case of diabetes than the normal healthy non-diabetic individuals. Although saliva glucose measurements methodologies are reliable, however there remain some intrinsic drawbacks. The main limitation of the saliva glucose analysis is the required measurement techniques like liquid chromatography mass spectroscopy (LC-MS) and UV-Vis spectroscopy. Therefore, this technique can hardly be applied for continuous blood glucose monitoring purposes.

The ^{13}C-glucose breath test has also been proposed to be a non-invasive diagnostic method for the detection of type 2 diabetes [8, 9]. It is based on the principle that when a dose containing ^{13}C-glucose is administered, the ^{13}C-glucose uptake is impaired for cellular glucose metabolism due to insulin resistance in T2D. Therefore it results in blunted rate of the $^{13}CO_2$ production in the exhaled breath of T2D. However, ^{13}C-glucose breath test is limited for the estimations of individual's blood glucose levels. Recently, few studies have demonstrated the association between the blood glucose levels and ^{13}C-glucose derived breath $^{13}CO_2$ isotopes [10-13]. But, no studies still now have reported any method consisting of a suitable system for the quantitative estimation of blood glucose profiles from the ^{13}C-glucose breath test in real-time.

In this chapter, we described a model-based breath analysis method, which can provide a person's blood glucose profile with time exploiting the subject's height, weight, age, sex and $^{13}C/^{12}C$ stable isotopes ratios in the exhaled breath CO_2. The model presented here exploits the physiological pathways of glucose metabolism during the standard oral glucose tolerance test (OGTT). The OGTT study is based on a method which comprises the administration of ^{13}C-labelled glucose and monitoring of $^{13}CO_2/^{12}CO_2$ isotopes ratios in pre-and post-dose exhaled breath samples. The isotopic compositions of exhaled breath CO_2 along with the patient's physical parameters need to be put into the model equations to estimate the blood glucose levels and precisely diagnosis the metabolic state of the patient.

7.2 Methods of the model

This study is consisted of a four compartmental mathematical model. Each compartment is associated with the glucose metabolism, either in insulin dependent or insulin independent pathway.

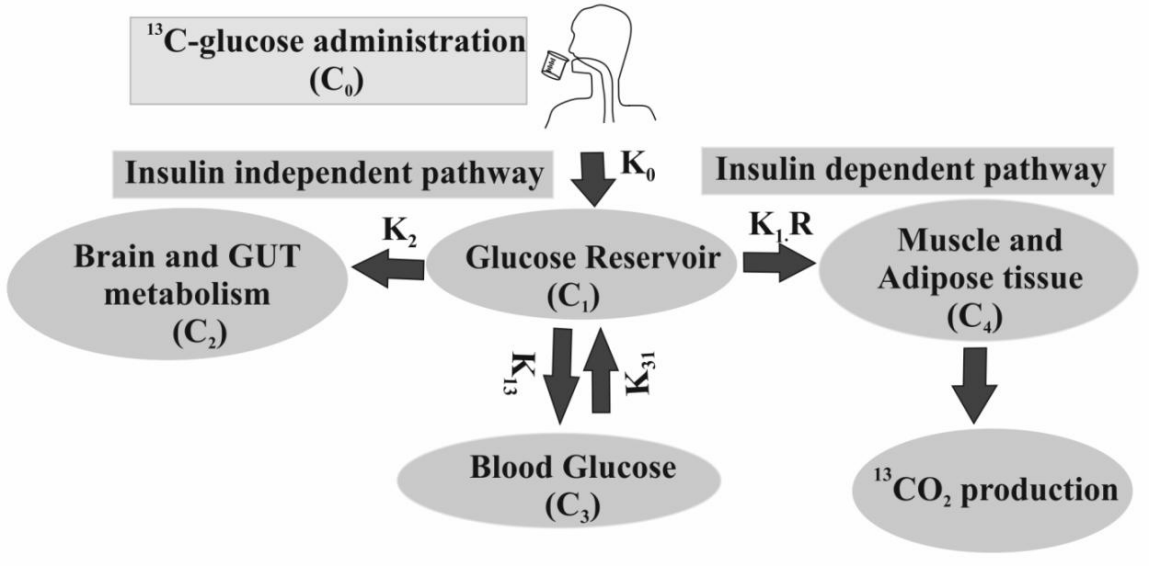

Figure 1. *Figure demonstrates a four compartmental sub-model associated with glucose metabolism after a test dose of ^{13}C-labelled glucose load. C_0 represents the concentration of ^{13}C-labelled glucose, whereas C_1, C_2, C_3, C_4 represent the concentrations of the labelled glucose in different compartments at a particular time. K_0, K_1, K_2, K_{13}, K_{31} are the transfer rate constants of the glucose among the compartments. R is the predictive insulin resistance, which is calculated from the individual's physical parameters and the exhaled breath $^{13}CO_2/^{12}CO_2$ isotopes ratios*

After the ^{13}C-enriched glucose load, the glucose metabolism depends on the cellular glucose uptake and its disposal by the tissue cells. After an overnight fasting (10-16h), when a dose consisting of ^{13}C-labelled glucose is orally administered, the majority of the glucose disposal takes place in insulin dependent peripheral tissues (especially muscle tissues). In individual with insulin resistant, the glucose uptake for cellular glucose oxidations is markedly diminished and therefore results in blunted rate of $^{13}CO_2$ production in exhaled breath from the labelled glucose metabolism.

Previous studies [6] demonstrated that the $^{13}CO_2$ excretion in exhaled breath from the ^{13}C-glucose metabolism actually reflects the insulin sensitivity of the body. Further studies [10] reported the significant correlations between the exhaled breath $^{13}CO_2$ recovery rate from labelled glucose metabolism with the insulin resistance in terms of HOMA-IR (Homeostatic model assessment) and QUICKI (Quantitative insulin sensitivity check index). Based on the previous studies [7], it can be assumed that the $^{13}CO_2$ recovery rate due to ^{13}C-labelled glucose metabolism is linearly related to insulin sensitivity (or 1/ insulin resistance):

c-PDR(%) in exhaled breath = k/insulin resistance

where, c-PDR is the cumulative percentage dose ^{13}C recovered in the exhaled breath and k is experimentally determined quantity.

We have assumed the linear relationship between c-PDR and insulin resistance due to mathematical simplicity. It is well known that QUICKI is the better predictor of insulin resistance than HOMA-IR. Therefore, we have considered QUICKI to calculate the insulin resistance for this study.

The $^{13}CO_2/^{12}CO_2$ isotope ratio is generally expressed as $\delta^{13}C$ in per mil unit (‰) which is calculated by the following equation:

$$\delta_{DOB}{}^{13}C‰ = (\delta^{13}C‰)_{t=t} - (\delta^{13}C‰)_{t=0} \quad (1)$$

DOB= delta-over-baseline

Here,

$$\delta^{13}C‰ = \left[\frac{\left(\frac{^{13}C}{^{12}C}\right)_{sample}}{\left(\frac{^{13}C}{^{12}C}\right)_{standard}} - 1 \right] \times 1000 \quad (2)$$

where, $\left(\frac{^{13}C}{^{12}C}\right)_{sample}$ and $\left(\frac{^{13}C}{^{12}C}\right)_{standard}$ are $^{13}CO_2/^{12}CO_2$ isotope ratios in sample and standard 'Pee Dee Belemnite' (PDB) (i.e. 0.0112372), respectively. We have estimated the $^{13}CO_2$ recovery rate from the following trapezoid rule [14]:

$$^{13}C - PDR(\%/h) = \frac{\delta_{DOB}{}^{13}C \times R_{PDB} \times 10^{-3} \times V_{CO_2}}{\left(\frac{D}{M_t}\right) \times \left(p \times \frac{n}{100}\right)} \times 100$$

where, V_{CO_2} is the CO_2 production rate per hour, D= dose of substrate administered, M_t = molecular weight, p= ^{13}C atom % excess, n= number of labelled carbon positions, R_{PDB} = 0.0112372. Here, V_{CO_2} is calculated from Schofield and Mifflin–St Joer equations as functions of height, weight, age and sex [15]. The cumulative percentage of $^{13}CO_2$ recovery rate (c-PDR) is derived from summing of ^{13}C-PDR (%) at the different time periods.

We experimentally determined the optimal cut-off values of c-PDR (%) from receiver operating characteristic curve (ROC) analysis for the three classes of subjects: control, pre-diabetes and type 2 diabetes. In our study, a test meal containing ^{13}C-labelled glucose (75mg) and unlabelled glucose (75gm) was administered. We have neglected the possible contribution of unlabelled glucose to produce $^{13}CO_2$ for the following two reasons:

a) The number of ^{13}C atoms in uniformly labelled ^{13}C-glucose (all six carbons are labelled with carbon-13 isotopes) is much higher than unlabelled glucose.

b) The $^{13}CO_2$ in breath is expressed as $\delta_{DOB}{}^{13}C‰$ i.e. difference between pre-and post-dose exhaled breath samples.

In the next step, we have utilized a four compartmental model (fig.1) based on the biological pathways of glucose metabolism during the oral glucose tolerance test. The compartmental model described here consists of four differential equations, which are as follows:

$$\frac{dc_0}{dt} = -K_0.C_0(t) \quad (3)$$

$$\frac{dc_1}{dt} = K_0.C_0(t) - K_1.R.C_1(t) - K_2.C_1(t) - K_{13}.C_1(t) + K_{31}.C_3(t) \quad (4)$$

$$\frac{dc_2}{dt} = K_2.C_1(t) \quad (5)$$

$$\frac{dc_3}{dt} = K_{13}.C_1(t) - K_{31}.C_3(t) \quad (6)$$

where, C_0 is the concentration of exogenous labelled glucose; C_i (i=1, 2, 3, 4) are the concentrations of the glucose in glucose reservoir (C_1), non-insulin dependent (C_2), blood vessel (C_3) and insulin dependent (C_4) compartments; K_0, K_1, K_2, K_{13} and K_{31} are the transfer rate constants of the glucose among the compartments.

The solution of equation (3) is

$$C_0(t) = C_0(0).\, e^{-K_0 * t} \tag{7}$$

From equation (4)

$$\frac{dc_1}{dt} = K_0.\, C_0(0).\, e^{-K_0.t} - (K_1.R + K_2 + K_{13}).\, C_1(t) + K_{31}.\, C_3(t)$$

$$= L_1.\, e^{-K_0 t} - L_2.\, C_1(t) + K_{31}.\, C_3(t) \tag{8}$$

where, $C_0(t)$ is given by equation (7) and $L_1 = K_0.\, C_0(0)$ and $L_2 = K_1.R + K_2 + K_{13}$

From equation (6)

$$C_1(t) = [K_{31}.\, C_3(t) + \frac{dC_3}{dt}] \tag{9}$$

After differentiating the equation (9)

$$\frac{dc_1}{dt} = \frac{1}{K_{13}} [K_{31}.\, \frac{dC_3}{dt} + \frac{d^2C_3}{dt_2}] \tag{10}$$

After putting the value of $c_1(t)$ in equation (8) and then comparing equation (8) and (9), it can be written as:

$$\frac{d^2C_3}{dt_2} + L_3.\, \frac{dC_3}{dt} + L_4.\, C_3(t) = L_5.\, e^{-K_0 t} \tag{11}$$

where, $L_5 = L_1.\, K_{13} + L_2$, $L_3 = K_{31} + L_2$ and $L_4 = L_2.\, K_{31} - K_{31}.\, K_{13}$

The equation (11) is a homogenous second order differential equation. The equation is solved with respect to two boundary conditions: $C_3 = 0$ at t= 0 and $\frac{dC_3}{dt} = 0$ at t= 0.
The final solution of the equation (11) corresponds to:

$$C_3(t) = \frac{A}{\sqrt{L_3^2 - 4L_4}}\left(K_0 - \frac{L_3 + \sqrt{L_3^2 - 4L_4}}{2}\right) e^{\frac{-L_3 + \sqrt{L_3^2 - 4L_4}}{2}\, t} + A\left[-1 + \frac{1}{\sqrt{L_3^2 - 4L_4}}\right.$$

$$\left.\left(-K_0 + \frac{L_3 + \sqrt{L_3^2 - 4L_4}}{2}\right)\right]. \quad e^{\frac{-L_3 + \sqrt{L_3^2 - 4L_4}}{2}\, t} + A.\, e^{-K_0 t} \qquad (12)$$

where $A = \frac{L_5}{(K_0^2 + L_4 - L_3 k_0)}$

From the above equation, we can calculate the blood glucose levels at different time intervals. Now, the standard test meal for the oral glucose tolerance test (OGTT) is comprised of 75 gm glucose to diagnose pre-diabetes and type 2 diabetes. Therefore, the equation (12) is multiplied by 1000 to predict the equivalent amount of excess glucose (mg) in blood for the standard 75 gm glucose load. Now a normal human body contains 5 litres (or 50 dL) blood. Therefore final model equation becomes:

$$C_4(t) = F + C_3(t) * (1000/50) \qquad (13)$$

whereas, F is a quantity which is constant for a particular subject and is used in the model to execute the programme.

This is to note that the model output blood glucose level (C_3) actually represents the excess ^{13}C-glucose in blood after the glucose metabolism. As there is no difference in chemical properties of the labelled and unlabelled glucose, the amount of glucose into the blood after the oral glucose load must be same whether the test meal contains labelled or unlabelled glucose.

From the above model equation, we estimated the blood glucose levels at the different time periods after the oral glucose load. Here, we calculated the theoretical values of K_0, K_1, K_2, K_{31} and K_{13} from the best fitting results obtained from the experimentally determined blood glucose values.

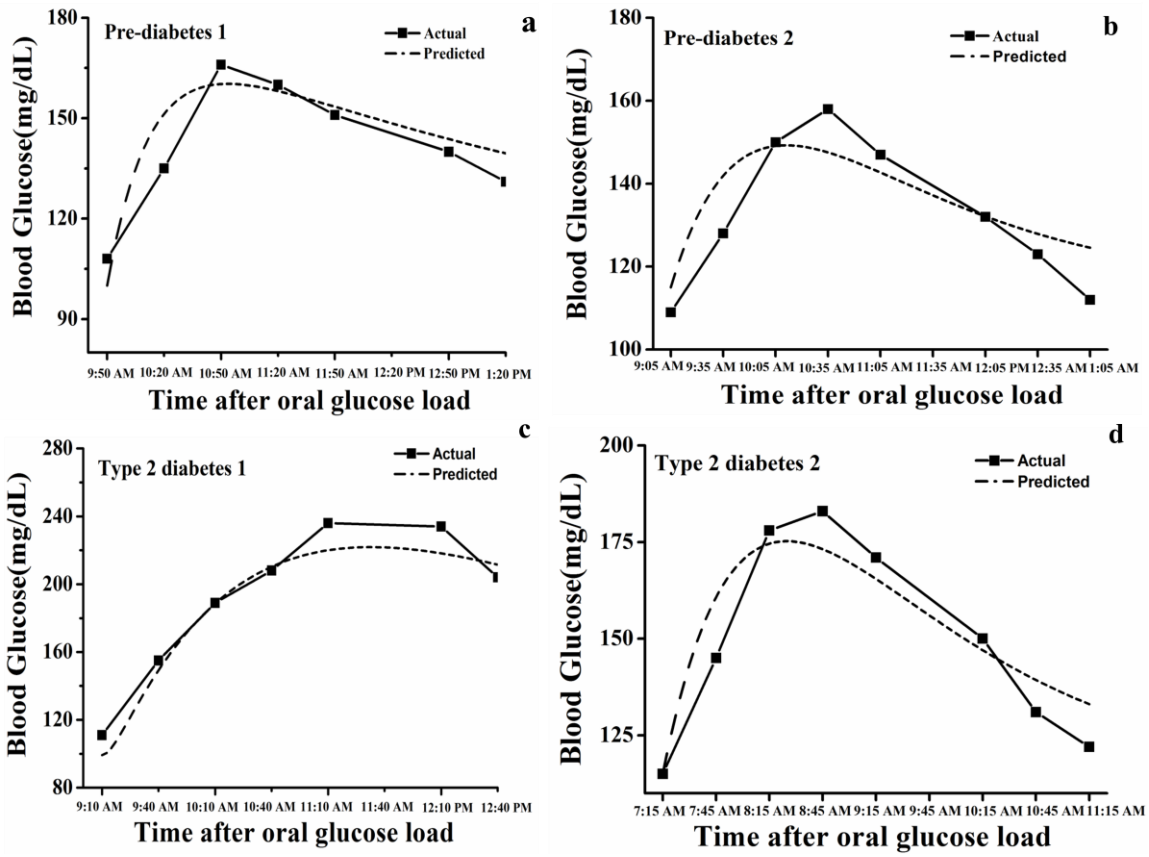

Figure 2. *Blood glucose profile of a pre-diabetes after administration of a test meal containing ^{13}C-labelled glucose. The dashed line corresponds to the model predicted blood glucose levels, whereas solid line stands for experimentally determined blood glucose levels*

We found that the estimated blood glucose levels from the model-based method are well correlated with the experimentally determined blood glucose for pre-diabetes (Fig. 2a and Fig. 2b) and type 2 diabetes (Fig. 2c and Fig. 2d). We also observed that the ^{13}C-labelled glucose can be replaced by an alternative composite test meal comprising of ^{13}C-enriched naturally abundant foods like sugarcane juice, cornflakes, baby corn etc.

Thus, this study provides a robust procedure for non-invasive diagnosis of pre-diabetes and type 2 diabetes. A Labview programme is written, which provides a person's blood glucose profile with time immediately and hence the current state of the metabolic condition of the said subject. Essentially the values of the $^{13}CO_2/^{12}CO_2$ isotopes ratios in exhaled breath are put into the model equations as input parameters

to execute the model programme. From the model equations, we can predict the individual's blood glucose profile and finally screen the most common metabolic disease in the world (fig. 3).

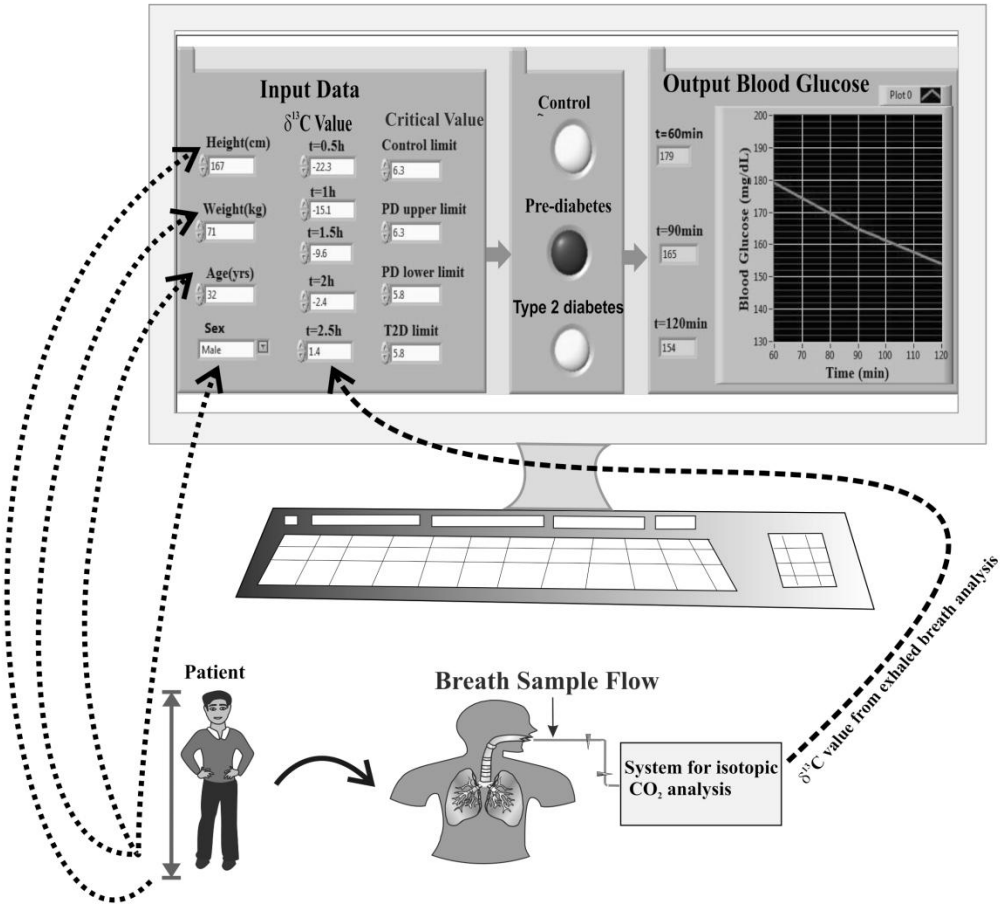

Figure 3. *A schematic representation of the model-based blood glucose monitoring method as described in present study*

7.3 Conclusion

In this chapter, we have described a model-based breath analysis for monitoring of individual's blood glucose profile. It is consisted of the utilizations of non-radioactive ^{13}C-glucose and the individual's physical parameters including age, sex, height and weight. Therefore, it enables a simple, method for the determination of the individual's blood glucose profile. The model equations are based on the different biological processes related to glucose metabolism. The biological processes are regulated by some user defined biological parameters, which are strongly associated with the model input variables. The variations of those biological parameters are

caused by the metabolic defect of the patient. The model links to the blood glucose level after a pre-determined quantity of glucose load. Therefore, it indirectly relates to the individual's glucose metabolism in real-time. Thus, the present novel method provides a new strategy for the estimation of blood glucose profile of a subject. This method not only obviates the painful invasive techniques, but also it offers a substantial improvement of the previously proposed minimally invasive blood glucose monitoring methods. When the traditional practice for the monitoring of blood glucose levels necessitates repeated blood withdrawals, this study shows a new direction for the estimation of individual's blood glucose profile from the model-based breath analysis. Finally, the study opens up a new strategy into the accurate and fast diagnosis of pre-diabetes and type 2 diabetes.

7.4 References

[1] Kondo T *et al.*, Estimation and characterization of glycosylated carbonic anhydrase I in erythrocytes from patients with diabetes mellitus. *Clin. Chim. Acta* **116,** 227-236 (1987).

[2] Zimmet P, Alberti K G M M and Shaw J, Global and societal implications of the diabetes epidemic. *Nature* **414,** 782-787 (2001).

[3] Kahn S E, Hull R L and Utzschneider K M, Mechanisms linking obesity to insulin resistance and type 2 diabetes. *Nature* **444**, 860-846 (2006).

[4] Katz A *et al.* Quantitative insulin sensitivity check index: a simple, accurate method for assessing insulin sensitivity in humans. *J. Clin. Endocrinol. Metab.* **85,** 2402-2410 (2000).

[5] Muniyappa R *et al.*, Current approaches for assessing insulin sensitivity and resistance in vivo: advantages, limitations, and appropriate usage. *Am. J. Physiol. Endocrinol. Metab.* **294,** E15-E26 (2008).

[6] Lewanczuk R Z, Paty B W and Toth E L, Comparison of the [^{13}C] glucose breath test to the hyperinsulinemic-euglycemic clamp when determining insulin resistance. *Diabetes Care* **27,** 441-447 (2004).

[7] Mizrahi M *et al.*, Assessment of insulin resistance by a ^{13}C glucose breath test: a new tool for early diagnosis and follow-up of high-risk patients. *Nutr. J.* **9,** 1-9 (2010).

[8] Qureshi K *et al.*, Comparative evaluation of whole body and hepatic insulin resistance using indices from oral glucose tolerance test in morbidly obese subjects with nonalcoholic fatty liver disease. *J. Obes.* **2010,** 1-7 (2010).

[9] Schwartz M W and Kahn S E, Diabetes: insulin resistance and obesity. *Nature* **402,** 860-861 (1999).

[10] Wallace T M, Levy J C and Matthews D R, Use and abuse of HOMA modelling. *Diabetes Care* **27,** 1487-1495 (2004).

[11] Matsuda M and Defronzo R A, Insulin sensitivity index obtained from oral glucose tolerance testing: comparison with the euglycemic insulin camp. *Diabetes Care* **22,** 1462-1470 (1999).

[12] Shapiro E T *et al.*, Insulin secretion and clearance: comparison after oral and intravenous glucose. *Diabetes* **36,** 1365-1371 (1987).

[13] Grzybowski M and Younger J G, Statistical methodology: III. receiver operating characteristic (ROC) curves. *Academic Emergency Medicine* **4,** 818-826 (1997).

[14] Wu I C *et al.*, Metabolic analysis of ^{13}C-labeled pyruvate for noninvasive assessment of mitochondrial function. *Ann. N. Y. Acad. Sci.* **1201,** 111-120 (2010).

[15] Schofield W N, Predicting basal metabolic rate, new standards and review of previous work. *Hum Nutr Clin Nutr.* **39,** S5-S41 (1985).

Chapter 8

Summary and outlooks

In this thesis, we have investigated the utilization of high-resolution laser-based integrated cavity output spectroscopy (ICOS) technique to unravel a real-life biomedical problem i.e. detection of *Helicobacter pylori* infection by means of human breath analysis. Here, we have initially elucidated the potential role of the major metabolite CO_2 with its carbon and oxygen isotopes in the pathogenesis of the gastric pathogen *H. pylori*. We have explored the ^{13}C-urea breath test (^{13}C-UBT), the gold-standard non-invasive methodology for the diagnosis of *H. pylori* infection, which is not able to precisely detect the pathogen producing several false-positive and false-negative results in the "grey-zone". Now to overcome this problem we have introduced the concept of ^{13}C-percentage dose recovery (^{13}C-PDR % / hr) and cumulative PDR (c-PDR %) methodology to accomplish the highest diagnostic accuracy in ^{13}C-UBT using the ICOS method. An optimal cut-off point of c-PDR (%) was determined using the receiver operating characteristic curve (ROC) analysis to overcome the issue of "grey-zone". We elucidated the "grey-zone" problem using the diagnostic cut-off point of c-PDR (%)= 1.47% at 60 min, which exhibited 100% diagnostic sensitivity (true positive rate) and 100% specificity (true negative rate) with an accuracy of 100% compared with the invasive endoscopy and biopsy tests. Our findings therefore suggest that the current c-PDR (%) is a valid and sufficiently robust novel approach for an accurate, specific and fast non-invasive diagnosis of *Helicobacter pylori* infection which could routinely be used for large-scale screening and diagnostic purposes.

Next, we have explored the dynamical behaviour of oxygen-18 (^{18}O) and carbon-13 (^{13}C) isotopes of breath CO_2 in response to ^{13}C-tagged glucose metabolism of *H. pylori*. Subsequently, we have explored the plausible mechanistic pathways linking to ^{18}O and ^{13}C isotopic fractionations of breath CO_2 and glucose utilization by *H. pylori*. Our findings suggest that breath $^{12}C^{18}O^{16}O$ and $^{13}C^{16}O^{16}O$ could be used as potential molecular biomarkers to distinctively track the pathogenesis of *H. pylori* infection in a non-invasive approach. We have also shown that these two major abundant isotopes

of breath CO_2 might be considered as potential markers irrespective of tagged isotopic nature of the substrate. Thus our findings may open new perspectives into the pathogen's physiology along with isotope-specific non-invasive diagnosis of the infection.

Although *H. pylori* predominantly colonize the gastrointestinal tract but it has some strong association with the most common metabolic disorder, i.e. type 2 diabetes (T2D). As the underlying relation between *H. pylori* and T2D is very complex and *H. pylori* may play an etiological factor for the development of T2D, we have therefore explored the underlying relation between *H. pylori* and T2D by exploiting the carbon-13 and oxygen-18 isotope of breath CO_2 using a high-resolution ICOS technique. We have also introduced a new methodology, i.e. glucose breath test (GBT) which has enormous potential for simultaneous assessment of *H. pylori*-induced T2D individuals as well as *H. pylori*-induced non-diabetic controls. There are several important gaps in our study for details understanding the molecular mechanisms underlying the pathogenesis of the diseases that should be explored in future research.

We have next proposed and validated that nitric oxide (NO) is a novel biomarker in exhaled breath that can precisely track the peptic ulcer disease (PUD) and non-ulcer dyspepsia (NUD). The ultra-sensitive detection of NO was performed using a laser-based high-sensitive continuous wave external cavity quantum cascade laser (*cw*-EC-QCL) based cavity ring-down spectrometer (CRDS). We have observed that level of breath NO significantly enriched in PUD subjects compared to NUD subjects thus unveiling a potential link of exhaled NO with *H. pylori* assisted ulcer and non-ulcerous state. Our results demonstrated a new alternative strategy that molecular NO in exhaled breath could be used as a potential biomarker for non-invasive diagnosis and selective classification of NUD from PUD in a more better and robust way without any endoscopic biopsy test, even after the eradication of *H. pylori* infection.

Finally we have developed a mathematical model based on biological pathways of glucose metabolism for non-invasive monitoring of blood glucose profile and subsequently the diagnosis of T2D. Our findings demonstrated that the blood glucose profiles based on the breath analysis are well correlated with the invasive blood sample measurements. Our novel methodology described in this thesis may open up a new-frontier area of non-invasive monitoring of blood glucose profile in human with

the aim to selective diagnosis of individuals with prediabetes (PD), type 2 diabetes (T2D) and non-diabetic control (NDC).

Thus the present thesis explores and exploits the optical cavity-enhanced techniques such as integrated cavity output spectroscopy (ICOS) and cavity ring-down spectroscopy (CRDS) for biomedical research and clinical diagnotics. The high-resolution ICOS and CRDS have been utilized to measure ultra-low concentration of trace species in human breath with high-precision. Thus this thesis opens up a new strategy for the diagnosis of *Helicobacter pylori* infection by means of the analysis of some unique molecular species with their isotope ratios in exhaled human breath.